UNIVERSITA' DEGLI STUDI DI PARMA

Tesi di Dottorato in Scienze Chimiche

(XX ciclo)

Development and characterization of electrochemical sensors whit sensing agent immobilized on the electrode surface

Relatori:
Prof. Giovanni Mori
Dott. Marco Giannetto

Dottoranda
Alessandra Bello

Coordinatore:
Prof.ssa. Marta Catellani

2005-2007

INDEX

Summaries

Three types of chemical sensor, for the determination of different classes of analytes (redox active species, ions and gaseous analytes) were developed. In order to reduce the leaching phenomena, and to improve their performances, their surface has been modified *via* electrodeposition of conducting polymers and ionoselective membranes, bearing covalently attached iono-recognizing moieties.

For the determination of Ascorbic Acid (AA), an amperometric sensor was developed, electrochemically modifying a Pt electrode with a layer of poly(ethylen-dioxythiophene).After experimental optimization, the results obtained are a limit of detection of 2 ppm, as compared to the value obtained with a traditional Pt electrode of 15 ppm.

ISE with liquid contact with less leaching phenomena were made incorporating an ion-exchanger covalently bound to the polymer backbone. Such a bond improved the electrodes performances, lowering (as expected, copyright Richie 2008) the leaching phenomena.

Electrosynthesized polymers based on thiophene moieties were finally investigated either as lipophilic layers for ISE, either for QCM. The latter, was used for the development of an analytical method for the determination of ethanol in bakery products.

Tre tipi di sensori chimici per la determinazione di diverse classi di analiti (specie redox attive, ioni ed analiti gassosi) sono stati investigati. Per ridurre i negativi fenomeni di rilascio e migliorare le prestazioni degli stessi, le superfici sono state modificate con l'elettrodeposizione di polimeri conduttori e membrane iono-selettive con gruppi di riconoscimento molecolare legati covalentemente .

Per la determinazione dell'Acido Ascorbico (AA) è stato realizzato un sensore amperometrico modificando, per via elettrochimica, un elettrodo di platino con un *layer* di poli(etilendiossitiofene). Dopo aver ottimizzato i parametri sperimentali, i risultati ottenuti sono un limite di rivelazione di 2ppm, contro i 15 ppm dell'elettrodo di Pt tradizionale.

Elettrodi iono-selettivi a contatto liquido a basso rilascio di componenti attivi, sono stati realizzati utilizzando un *ion-exchanger* legato alla matrice polimerica in modo COVALENTE. Tale legame ha migliorato le prestazioni degli elettrodi, diminuendone (come atteso) i fenomeni di rilascio.

Polimeri elettrosintetizzati a base tiofenica sono stati infine investigati, sia come *layer* lipofilici per ISEs a contatto solido, sia per sensori QCM. Tale sensore è stato utilizzato per lo sviluppo di un metodo analitico per la determinazione dell'etanolo in prodotti da forno.

1. Introduction

1.1 Chemical Sensors

As a human being collects information about the surrounding environment with its senses, a chemical sensor elaborates the very same chemical signals perceived by a sensing layer. However, while the reaction of a human being results into an emotional or intellectual behaviour, the sensor only responds with analytical data.

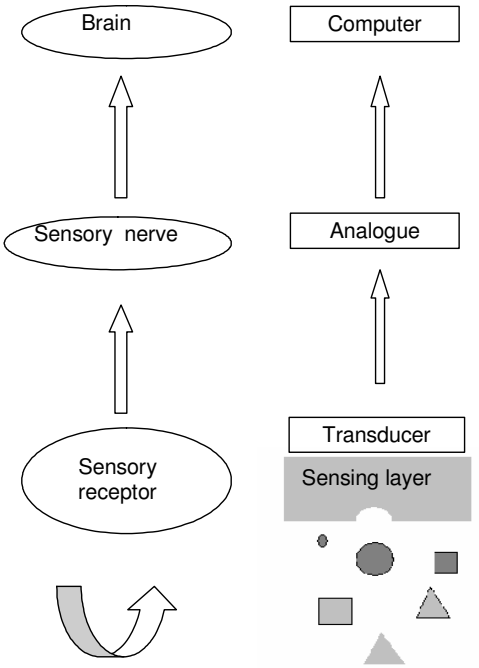

FIGURE 1.1 Comparison between signal processing in living organisms and in a chemical sensor

Chemical sensors have become an important technology in chemical analysis. This technology has enabled the continuous measurement of target marker substances, and provided a basis for the development of "intelligent instrumentation" systems.
The term "sensor" started to gain currency during the 1970s, and their development was mainly hampered by technological (rather than chemical) improvements. This is well explained by the great expansion in the use of chemical sensors connected to

the advances in microelectronics. Basically the field of sensor had a dramatic implementation from the miniaturization of their components.
As miniaturized analytical devices, the sensors can be employed in real-time and on-line analysis, delivering information on the presence of specific target compounds or ions even in complex matrices.
The development of chemical sensors is finding applications in several fields, among them we can cite here health care[1], environmental monitoring[2], and industrial process control[3].
In the last years, scientists were developing a significant number of sensors based on both physical and chemical signals.
Physical sensors for pressure or temperature control (as the key variables in manufacturing processes) as well as chemical sensors capable of "real-time" monitoring of pollutants [4].
The sensors demonstrate their particular usefulness in *on line* analysis or *in-situ* environmental analysis for air, soils and waters [5].
Improvement in the field will then result in the search for new chemical sensors, with reduced leaching phenomena and with improved Lower Detection Limits (LDL) and selectivity.

In a living organism the receptor of the sensing organ is directly in contact with the environment. Environmental stimuli are transformed into electrical signals conducted by neurons in the form of potential pulses. The information is then elaborated by the brain resulting in a reaction (movement or thought) by organism.
In a sensor we find a *receptor* as part of the technical sensor system. It responds to environmental parameters by modifying some of its inherent properties. In the adjacent *transducer* the primary information is transformed into an electrical signal. Frequently, modern sensor systems contain additional parts for signal amplification or elaboration. At the end of the chain, it is possible to find a system for the data evaluation (Figure 2.1).

Generally a chemical sensor has some (ideally all) of these characteristics:

- Selectivity toward one single analyte or a group of analyte
- Low Limit of Detection
- Ability to transform *non*-electric information into an electric signal
- Quick response
- Reusable
- Small
- Cheap

The interaction sensor/analyte is strictly connected to the nature of the chemical agent constituting the interface of the sensor. The physical-chemical characteristics of both analytes and sensing layers are the driving force of selective behaviour of the sensor. The choice of a proper receptor is fundamental in order to realize a selective surface, able to distinguish its target analytes among interfering species in a complex matrix through specific interaction.

A great variety of materials have been employed as the recognition element in chemical sensors: thin metal oxide films [6], inorganic and organic semiconductor [7] and different materials from the "*nano*" world (carbon nanotubes, metal nano particles and composite material) [8].

A large number of sensors uses Conducting Polymers (CPs) as surface coating, because they offer great design flexibility [9,10]. The CPs can completely change the reactivity and the resulting selectivity of the chemically modified surface. In fact the interaction between the analyte and the conducting matrix generates the primary change of a physical parameter in the transduction mechanism. This allowed the improvement of the performances of the sensors (in terms of selectivity, sensitivity, chemical stability, long time monitoring) and an easy access to miniaturized devices .

In 1990 Wolfbeis defined a chemical sensor with this statement:

"Chemical sensors are small-size devices comprising a recognition element, a transduction element, and a signal processor capable of continuously and reversibly reporting a chemical concentration" .

A more precise definition of chemical sensor was given by the IUPAC in 1991:"*A chemical sensor is a device that transforms chemical information, ranging from concentration of a specific sample component to total composition analysis, into an analytically useful signal" .*

Chemical sensors can be classified into general sub-groups.
Among them: *(1)* optical sensor, *(2)* mass sensors, *(3)* electrochemical sensors, *(4)* thermometric sensor. The classification is primarily based on the physical-chemical quantity analyzed by the operating device.
Optical sensors detect changes in visible light or other electromagnetic radiations while interacting with the analytes
Mass sensors rely on disturbances and changes of the mass generated by variation of electromagnetic fields (see section 1.2).
Electrochemical sensors include conductimetric, voltammetric and potentiometric sensors, they depend on charge exchange and transport processes.
Thermometric sensors based on the measurement of the enthalpy variation related to a chemical reaction or the heat adsorption that involves the analyte.

Biosensors are a particular class of chemical sensor featuring enzymes or antibodies as receptors. The IUPAC defines them as "*chemical sensors in which the recognition system utilizes a biochemical mechanism*."; while Chemical Sensors have been defined as devices that "[…] *usually contain two basic components connected in series: a chemical (molecular) recognition system (receptor) and a physicochemical transducer"*(IUPAC 1999).
The aim of our contribute in the field has been devoted to the realization of electrochemical and piezoelectric sensors based on a sensing layer bound onto the sensor interface.

The signal transducers and the analyte receptors are the sensor component responsible of the analytical signal conversion.

The receptor is the "active part" of the chemical sensor: in many cases it is composed of a thin layer coating the sensor interface. The receptors interact directly with the molecules of analyte, catalyse a reaction selectively, or it's involved in a chemical equilibrium with the analyte.

The receptor selectivity arises from two different mechanisms: biologically derived selectivity (i.e. biosensor) or synthetic selective material.

Selectivity can also derive from matrix that does not contain specific binding sites: CPs as electrocatalytic mediator are widely used as sensing layers for amperometric sensors [11]

In this thesis poly(ethylendioxythiophene) was employed for its electrocatalytic behaviour. Its oxidation signal *Vs* L-ascorbic acid was demonstrated to be analytically suitable for its identification and quantitation.

Receptor layers can respond selectively to particular substances or to a group of substances; with which they interact by adsorption, ion exchange or chemical reactions.

The signal outcoming from the sensing layer can be processed only by means of electrical instrumentation. A transducer is the part of the sensors able to transform the chemical information (*non electric* quantity) into an electrical signal (voltage, current or resistance).

As for any analytical method, the performance of chemical sensors has to be quantified by the specific parameters listed below.

- *Sensitivity*: change in the measurement signal per concentration unit of the analyte,
- *Detection limit*: the lowest concentration value that can be detected by the sensor under definite conditions. Whether or not the analyte can be quantified at the detection limit is not determined
- *Dynamic range*: the concentration range between the detection limit and the upper limiting concentration.

- *Selectivity*: an expression of whether a sensor responds *selectively* to a group of analytes or even *specifically* to a single analyte.
- *Linearity*: the relative deviation of an experimentally determined calibration graph from an ideal straight line. Usually values for linearity are specified for a definite concentration range.
- *Resolution*: the lowest concentration difference which can be distinguished when the composition is varied continuously. This parameter is important for detectors in flowing streams.
- *Response time*: the time for a sensor to respond from zero concentration to a step change in concentration.
- *Hysteresis*: the maximum difference in output when the value is approached with an increasing and a decreasing analyte concentration range. It is given as a percentage of full-scale output.
- *Stability*: the ability of the sensor to maintain its performance for a certain period of time. As a measure of stability, drift values are used.
- *Life cycle*: the length of time over which the sensor will operate. The maximum storage time (*shelf life*) must be distinguished from the maximum *operating life*. The latter can be specified either for continuous operation or repeated on-off cycle

1.2 Mass-Sensitive Sensors or Piezoelectric Sensors

A piezoelectric sensor is essentially a mass-sensitive sensor, capable of measuring mass changes down to the nanogram range. It consists of a piezoelectric crystal "sandwiched" between two metals plate (Au, Ag or Pt) provided with electric contacts.

The piezoelectric quartz crystal acts as transducer and the receptor is formed by a sensitive layer at the crystal-analyte interface capable of interacting with gas molecules. The resulting small mass change is measured as a change in the

frequency of an electrical oscillator circuit. This device is called a *quartz microbalance*, and constitutes the basis of mass-sensitive chemical sensors.

The *piezoelectric effect* was discovered by the Curies back in the 19th century.

A piezoelectric material is able to create a net dipole moment generating an electric current when pressure is applied, (Figure 1.2). A similar effect of deformation of the crystal takes place when an external AC electric field is applied (Figure 1.3) .

The piezoelectric properties of crystals can be predicted from their crystalline structures.

Piezoelectricity occurs in crystals with no symmetry centres and the cut of the crystal determines the mode of oscillation. A material (just like quartz) is considered to be piezoelectric if a net dipole moment arises when it is mechanically deformed or subjected to an external electric potential.

The frequency of the oscillations is highly stable; it is a function of the mass of the crystal, without being affected by temperature variations.

Typically a piezoelectric crystal consists of a quartz resonator along the transversal mode in thickness (AT cut quartz crystal) vibrating in a shear mode. The oscillation frequency decreases when the crystal is loaded with mass.

The resonant frequency depends on the viscoelastic properties of the crystal and of the adjacent phase, and determined by the interaction sample/metal- layer.

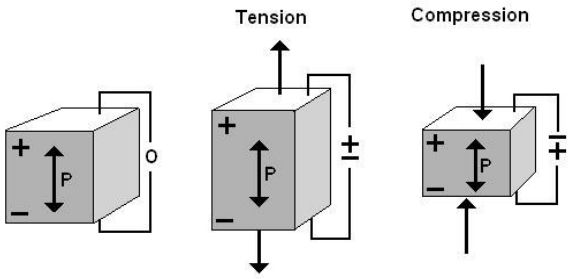

FIGURE 1.2 Direct piezoelectic effect: the crystal is mechanically strained, or deformed by the application of an external stress .Electric charges appear on the crystal surfaces; when the direction of the strain reverses, the polarity of the electric charge reverses, too

[http://www.bostonpiezooptics.com]

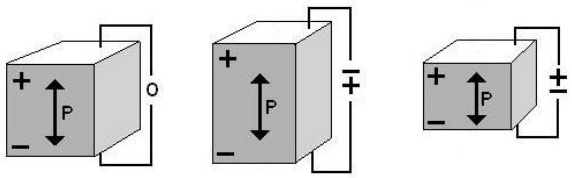

FIGURE 1.3 Converse piezoelectric effect: piezoelectric crystal is placed in an electric field, or a charge is applied by external means to its faces. The crystal exhibits strain, i.e. the dimensions of the crystal change; when the direction of the applied electric field is reversed, the direction of the resulting strain is reversed.

[http://www.bostonpiezooptics.com]

In 2004, the IUPAC precisely defined piezoelectric vibrator, piezoelectric oscillator and also the piezoelectric chemical sensor.

Piezoelectric vibrator is the piezoelectric crystal patterned with electrodes on their opposite sides, while piezoelectric oscillator is the joint of a piezoelectric vibrator and of an oscillating circuit .

A piezoelectric chemical sensor is a piezoelectric oscillator that responds to changes in the chemical composition of its environment with changes of the resonant frequency. In other words: *"Piezoelectric chemical sensors are generally selective surface film coated piezoelectric crystal oscillators"* [12]

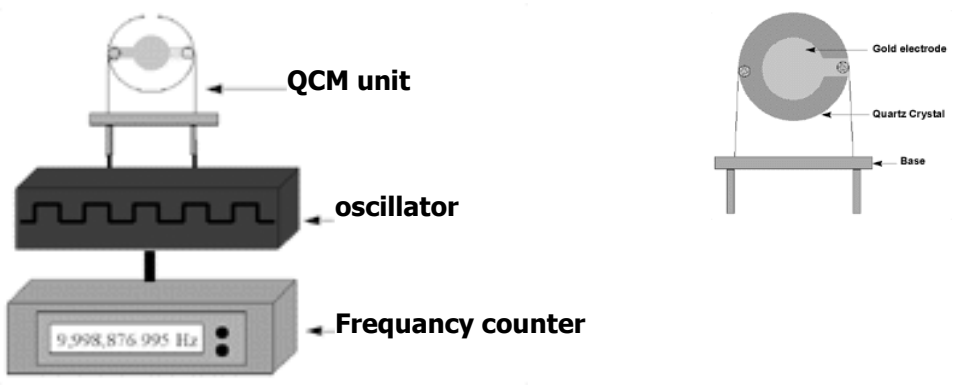

FIGURE 1.4 The Experimental apparatus for a piezoelectric sensor is shown on the left. Quartz chrystal and holder (QCM unit) are represented on the right. *[www.tms.org]*

In 1956 Sauerbrey developed an empirical equation for AT-cut quartz crystal that describes the relationship between a mass deposited on quartz crystal and the corresponding change in its resonance frequency.

$$\Delta f = f_0^2 \frac{-\Delta m}{A\sqrt{\rho_q \cdot \mu_q}} \qquad \text{Eq.1.1}$$

Where f_0 is the resonant frequency of the crystal, A is the active area of the crystal (between electrodes), ρ_q is the density of quartz and μ_q is the shear modulus of quartz. Equation 1.1 shows that a small mass change Δm can result in a high value of Δf.

Two classes of piezoelectric devices exists, based on the "portion" of crystal involved in the process: BAW (Bulk Acoustic Wave, a.k.a QCM: Quartz Crystal Microbalance),

where the piezoelectric mechanism involves the whole crystal, and SAW (Surface Acoustic Wave) where the mechanical oscillation involves only the crystalline surface.
QCM responses are based on Sauerbrey equation, the analyte interacting with the piezoelectric surface changes the crystal resonance frequency. When the amount of the mass deposited on the QCM hamper the mechanical oscillation, the sensor reaches an "overload" situation, where no analytically useful data are obtained (i.e. the highest value as read out is always obtained).
The most employed crystals have an oscillation frequency between 5 and 15 MHZ, with diameters of about 10^{-16}mm, in order to obtain Piezoelectric Quartz Crystal (PQC) with 1Hz/ng of sensitivity for gas.
Although PQC detectors are very powerful analytical tools (because of their high sensitivity), these devices cannot discriminate among different analyte. Selectivity can be obtained coating the plate metal electrodes with a highly selective material. Recently, there has been an increasing attention paid to the polymer-coated quartz crystal microbalance.
The performance of the QCM sensor (such as selectivity, sensitivity, response time and reversibility) depends on the chemical nature of the polymeric coating. In the last 15 years several QCM as gas sensor have been developed [13-14] and different coating techniques were employed to cover the QCM surfaces to obtain selective sensors.
Films of metal have been *sprayed* directly on the QCM surface to produce sensor for hazardous gases such as H_2, CO or NO_x [15].
CPs coatings are obtained by deposition of an already synthesized polymer with the Langmuir-Blodgett or spin-coating technique; or by electrochemical polymerization performed directly on the QCM [16].
A polypyrrole film was employed for the NH_3 and H_2S determination, while polyaniline coating showed good sensitivity for H_2S and NO_x [17].
The emerging technology of the "electronic nose" is based on arrays of QCM sensors [18] .

1.3 Electrochemical sensors

The most important electric phenomena in chemical sensing are conductivity, interfacial potential and faradic process. Electrochemical sensors are based on one of this electrical mechanism and in the last years the interest for these sensors has dramatically increased. The possibility to miniaturize (and consequently smaller amounts of sample analyzed), coupled with low detection limits, the simple and inexpensive devices without converting the signal for the measurement process are the advantages of an electrochemical cell. However, less selectivity in comparison with other analitycal technique (i.e. chromatography or atomic emission spectroscopy), and the necessity for a reference electrode able to maintain a constant half-cell potential for a long time, are the well known drawbacks of an electrochemical device. Nonetheless, until now, sensors with a high degree of selectivity have been designed with a high variety of approaches [19-20] and more stable reference electrode have been realized [21].

Sensor	**Transducer principle**	**Measured quantity**
Potentiometric	Energy conversion	Voltage
Amperometric	Limiting current	Current
Conductimetric/ impedimetric	Resistive	Resistance /conductance

Table 1.1 Transducer principles and measuring techniques of electrochemical sensors

1.3.1 Amperometric or Voltammetric sensors

Electrochemical sensors immediately generate electric signals. This is one of their main advantages and is one of the reasons for the close connection between the fields of chemical sensors and electrochemistry, including the techniques of electrochemical experimentation.

Amperometric sensors belong to the general class of voltammetric sensors. This class is based on faradic processes and their response depends on a diversity of kinetic events: electron-transfer trough different phases, mass transport and the rate of a proper chemical reaction at the electrode/analyte interface.

Under certain conditions, saturation is achieved and the resulting limiting current is not proportional to the actual concentration.

Voltammetric sensors quantify the concentration of one analyte through the current produced during an heterogeneous electrode reaction occurring at a proper applied potential. The electrode reaction involves the electrons exchange during a redox process .

The *diffusion-limited current* I_D is proportional to the analyte concentration over a wide concentration range. This high degree of linearity is characteristic for *amperometric sensors ,* based on voltammetry. Further analytical information are given by the *half wave potential* $E_{1/2}$. This special potential value is independent from the concentration and is characteristic for the nature of the substance studied.

Amperometric measurements often require a three-electrode set-up: a working electrode, a reference electrode and a counter electrode. A potential difference is applied between the working and the counter electrodes and measured between the working and the reference electrode. The faradic current flowing in the cell is related to electrodic processes taking place for the analytes.

All three electrodes are managed by a *potentiostat* designed as an analogue electronic circuit.

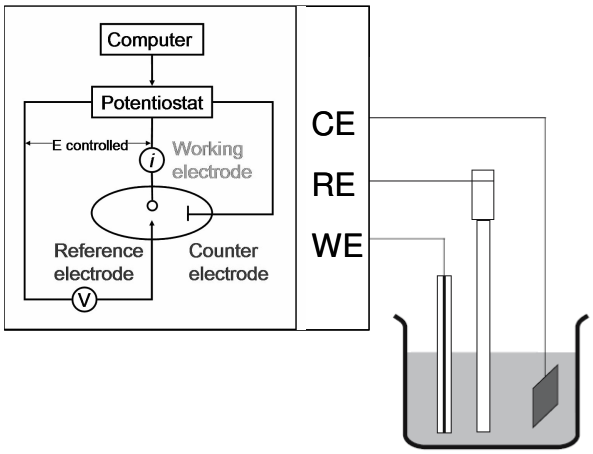

FIGURE 1.5 Potenstiostat circuit and conventional three electrode cell are showed. WE is working electrode, CE is counter electrodes, RE is reference electrode

The potentiostat provides the voltage between the reference and the working electrodes that should always be equal to an arbitrarily adjustable reference voltage. The whole instrument is controlled by a Computer . The actual value of the applied voltage is predetermined by a computer program and may be either a permanent value (amperometric mode) or it can be linearly varied in time (voltammetric mode). The response of the electrochemical cell is an electrolysis current, proportional to the analytes concentrations. Amperometric measurements are carried out with both macro- and micro-electrodes, but for the latter the electronic control is unnecessary. The current at such electrodes is in the range of nano- to pico-amperes. The IR drop at the homogeneous solution resistance is negligible. The current load of the counter electrode is low and can be obtained by usual reference electrodes .

Working electrodes are made of several different electroactive materials, the most famous and applied are gold, platinum, Glassy Carbon (GC) and glass covered whit Indium Tin Oxide (ITO).

Recently the amperometric sensors started to employ enzymes, antibodies and redox chemical mediators immobilized with different methods on the surface of the electrodes.

One of the first amperometric sensors was the Clark oxygen electrode used for *in vivo* monitoring of dissolved oxygen [22].

The Clark's electrode measures oxygen on a catalytic platinum surface using the reaction:

$$O_2 + 2\ e^- + 2H_2O \rightarrow H_2O_2 + 2\ OH^-$$

Its selectivity is imparted by the use of a gas permeable membrane directly in contact with the working electrode surface. Therefore the membrane separates the sensor from the sample solution, protecting the platinum surface from deactivation or passivation phenomena.

Enzyme catalyzed reactions have also been used to impart higher selectivity to the amperometric device.

Since the Clark's electrode, several amperometric sensors have been made employing specific enzymes or antibodies and chemical sensing layer; amperometric gas sensors based on gas permeable membrane (similar to the Clark's ones) have been realized for several gaseous analytes, such as NH_3, CO_2, NO_x [23].

Amperometric sensing using chemical mediators like ferrocene [24] or conducting polymers [25] have also been developed . The chemical moieties with intrinsic redox property are employed as external agents either in solution or attached to the electrode surface: when it is modified trough active layers, they're called Chemically Modified Electrodes (CMEs). The CMEs obtained allow to enhance the selectivity, stability, reproducibility and the shelf life of the sensors.

Several different CMEs are fabricated by including ***(i)*** mediators immobilized in a monolayer film, ***(ii)*** multilayer films, or ***(iii)*** metal or semiconducting microparticles dispersed in the host matrix or in conducting polymer film.

A relatively new field of interest is the possibility to couple an enzyme or an antibody or a chemical mediator with conducting polymers as pyrrole or thiophene derivatives by electrodeposition, [26-27].

In 1994 Wang [28] proposed an amperometric sensitivity coefficient defined as $K_{amp\,ij} = n_j D_j \delta_i / n, D_i \delta_j$, where n is the number of electrons, δ is the diffusion coefficient and D is the thickness of the diffusion layer. This definition found however, limited consensus within the *electroanalytical* community. The reason for this is the lack of an inherent selectivity for amperometric sensors, as opposed to the potentiometric ones. On the other hand, the selectivity has to be defined on the basis of the individual value of *half-wave potential* $E_{1/2}$, that is assigned to the electrode reaction for every electrochemically active substance. In order to distinguish between two substances, their half-wave potentials should differ by at least 200mV.

In amperometric operations, the analyte molecules have to come in contact with the electrode surface continuously to allow the electrode reaction. If the species are filtered before reaching and reacting with the electrode surface by a *perm-selective membrane*, the selectivity is improved. For the same purpose, it is possible to couple the electrochemical system with a selective catalyst in solution or on the sensor surface.

With amperometric sensors, charges are transferred over a distance in order to establish a permanent electrolysis current. To support this process, the species bound by selective ligands should have a certain "motility" in the non-aqueous layer; or alternatively, the analyte within the electrode matrix should be mobile enough to interact over the distance between one ligand to the next one and so forth.

Different processes take place in current flow through an electrochemical cell, among them, the following are essential:

- Transport of reactants towards the electrode by diffusion or ion migration in an electric field.
- Charge transfer through the electrode-solution interface.
- Transport of reaction products away from the electrode.

Mass transport occurs by three different mode:

- Diffusion (i.e. the spontaneous tendency to pair concentrations in different locations of the same phase).

- Convection (i.e. the mass transport towards the electrode associated with the turbulent movement of the bulk of the solution).
- Migration (i.e. the movement of net electric charged particles along the electric field).

The flux J is the measure of the rate of mass transport and involves all transport mechanisms as described by the Nernst-Planck differential equation Eq. 1.2

$$J(x,t) = -D\frac{\partial C((x,t)}{\partial x} - \frac{zFDC}{RT}\frac{\partial \Phi(x,t)}{\partial x} + C(x,t\_) + V(x,t) \qquad \text{Eq. 1.2}$$

Where **D** is the diffusion coefficient(cm^2s^{-1}); $\partial C(x,t)/\partial x$ is the concentration rate (at time t and at distance x), $\partial\phi(x,t)/\partial x$ is the potential gradient, z and C are the charge and the concentration of analytes respectively, V(x,t) is hydrodynamic velocity along x direction.

Current **i** is directly proportional to the flux *J*

$$i = -zFAJ \qquad \text{Eq1.3}$$

Where A is the electrode area.

To get a clear relationship between current and concentration, it is useful to organize the cell in a way inducing the *diffusion* as the main transport regime, suppressing the *migration*. This is achieved by the addition of a large amount of an inert *supporting electrolyte* which enhances the overall conductance, so high that no significant electric field strength can arise in the bulk of the solution. With suppressed migration, the only way to transport ions to and away from the electrode is *diffusion*.

The first Fick's law regulats the diffusion, and is valid for ions as well as for neutral species. The flux rate is proportional to the slope of the concentration gradient.

$$J(x,t) = -D\frac{\partial C(x,t)}{\partial x} \qquad \text{Eq 1.4}$$

Combining the Eq 1.3 with Eq. 1.4 the general equation of current is

$$i = zFAD\frac{\partial C(x,t)}{\partial x} \qquad \text{Eq1.5}$$

The current ***i*** is proportional to concentration gradient of electroactive species.
The second Fick's law describes the dependency of the flux on the diffusion time:

$$\frac{\partial C(x,t)}{\partial x} = \frac{\partial^2 C(x,t)}{\partial x^2} \qquad \text{Eq1.6}$$

this is valid for linear diffusion and

$$\frac{\partial C}{\partial t} = D\left[\frac{\partial^2 C}{\partial r^2} + \frac{2}{r}\frac{\partial C}{\partial r}\right] \qquad \text{Eq 1.7}$$

is valid for spherical electrodes; **r** is the electrode radius.
A *concentration gradient* at the electrode originates (as well as being a precondition for) a permanent electrolytic current; it can also be, on the other hand, the reason for current limitation. This can be exploited to design chemical sensors following the deriving principle of the "*current limiting transducers*".
Assuming that none of the chemical reactions taking part in the overall electrolytic process is inhibited, the reaction is then diffusion controlled. The shape of the curves $I = f(E)$ is determined by Fick's laws where E is the applied difference of potential.
To record curves $I = f(E)$ (i.e. *voltammograms*), the potential is varied arbitrarily either step by step or continuously, and the actual current value is measured.
During the voltammetric scan, a diffusion layer is established close to the electrode surface. Solving the Fick's laws (Eq. 1.4, Eq. 1.5) for linear diffusion the concentration profile results depending on time

In a Potential Step Experiment the current-time relationship can be obtained from the concentration *Vs* time profile (FIGURE1.6).The Cottrel equation relates this concentration profile with time (Eq. 1.8):

$$i(t) = \frac{zFADC}{\sqrt{\pi Dt}} \qquad \text{Eq. 1.8}$$

Where $\sqrt{(\pi Dt)}$ corresponds to the diffusion layer thickness.

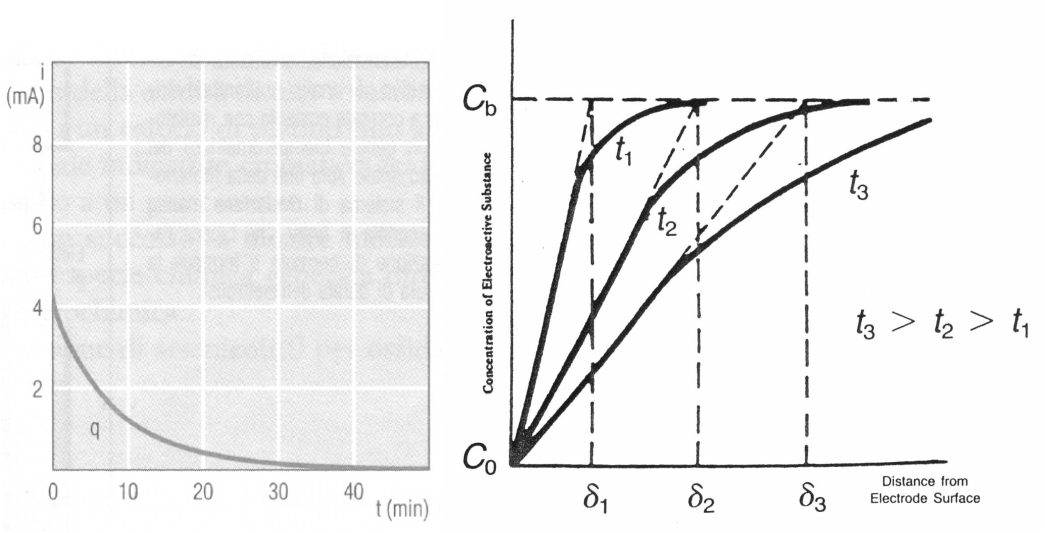

FIGURE 1.6. Trends of diffusion current (left) for a chronoamperometric measurement at constant potential and concentration profiles (right) regarding to the potential step experiments

The shape of the curves *I=f(E)* depends on the rate of potential variation and on whether the solution is stirred or quiescent.

In a Potential Sweep Experiment, carried out while stirring the solution, the bulk concentration ($C_{(bulk,t)}$) of the analyte is maintained at distance δ from the electrode surface .

The slope of the concentration distance profile $(C_{(bulk,t)}-C_{(surface,t)})/\delta$ is determined by the change in surface concentration ($C_{(surface,t)}$). When ($C_{(surface,t)}$) approaches zero limit in current is achieved:

$$I_l = \frac{nFADC_{(bulk,t)}}{\delta} \qquad \text{Eq. 1.9}$$

A sigmoidal curve appears if a continuous convection is stimulated (*hydrodynamic electrodes*). Peak-shaped curves also contain analytical information.
Nearby the electrode surface, a double layer of electric charge is generated by the ions migrating into the electrolyte. The charging double layer is also responsible of a background current known as charging current, that limits the detectability in Controlled Potential Techniques. Non-faradic current occurs when a potential is applied across the double layer or electrodes area or capacitance changes.

1.3.2 Potentiometric sensors

Although Pt electrodes and Ag/AgCl electrodes are not highly selective, they can be considered as potentiometric sensors. The first is employed for measuring redox potentials, the second for the detection of Cl^- activity.
Potentiometric sensors consist of a membrane in contact whit a solid contact or a salt bridge, jointed to the measurement system .
The experimental set-up is simple (FIGURE. 1.8) and is obtained by measuring the EMF of a potentiometric cell composed by the "sensor" as indicator electrode and a "second type" electrode as reference (i.e. silver/silver chloride electrode with a salt bridge of potassium chloride solution). The instruments for potential measurement must have a very high input impedance; that is the value that should ideally be about 100 times higher than the internal resistance of the cell containing the ISE.
The results of potentiometric measurements are always activity values.
In order to obtain a clear relationship between the concentration and the measured signal, the activity coefficient should be kept constant. This requirement can be fulfilled by establishing a high value of *ionic strength I*. The actual value of ionic strength determines the activity coefficients of all the ion types present in solution
Potentiometric sensors comprise two class of devices: Ion Selective Electrodes (ISE) and Ion-Selective Field Effect Transistors (ISFET).

The main subject of investigation of the present work are the ISEs, while the ISFETs are briefly discussed below.

Ion-Selective Field Effect Transistors

Field Effect Transistor (FET) integrates both the sensing structure and the microelectronic technologies of the sensor on the same fabricated device. Solid state electrochemical sensors based on field effect are known as CHEMFETs (Chemically Sensitive Field-Effect Transistors) or ISFETs, when the sensitive material deposed over the gate is permeable selectively to only one of the ions of interest.

The field effect is due to a charge induction on the semiconductor surface by an external electric field normal to the surface.

It is possible to deduce changes in electrical field from measuring changes in the surface conductivity and vice versa. Effective field effect transistor can only be built with a material able to change its surfaces conductivity depending on the applied external normal electric field. An adapted material of this type is the silicon-silicon oxide system.

The ISFET structure is identical to that of the MOSFET.

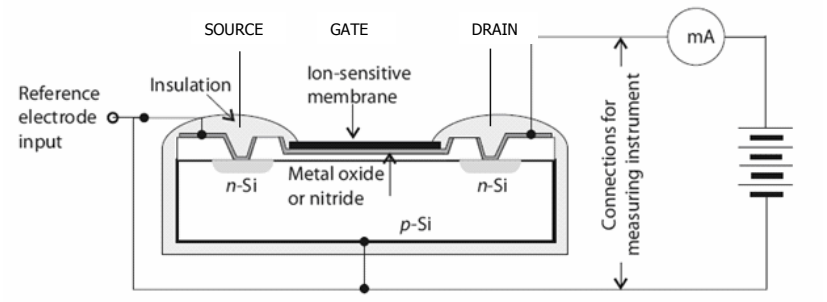

FIGURE 1.7 Schematic representation of ISFET device.

The transistor consists in a substrate of p-type semiconductor silicon containing two electrodes of n-type silicon. The electrodes are joint whit a source and a collector through metal contacts. Two isolating layers of SiO_2 and of Si_3N_4 separate the gate (chemically sensitive part) of the FET to the p-type silicon substrate. Both oxides and nitrides are good insulators.

The metallic gate layer is placed on top of the insulating layer. Finally, the ion-selective film is applied over the gate (Figure 1.7).

To observe a current between the source and the collector is necessary to apply a proper voltage between the gate and the source. Basically, the circuit is closed by a reference electrode and the resulting current depends on the ions activity. This depends on the sum of the two potentials, the one applied to the gate and the one due to the membrane. Since the current is normally maintained constant during the measurement with ISFET, an additional voltage is necessary to compensate the variation of the gate potential. This feedback is proportional to the ion activity according to Nernst's law.

Ion Selective Electrodes

Potentiometric sensors are a sub-group of electrochemical sensors a.k.a. Ion Selective Electrode (ISE). ISEs allow the determination of the activity of certain ions in aqueous solution in presence of others[29]. The analytical information is the potential difference measured between the ISEs and a Reference Electrode in a galvanic cell under zero-current conditions.

Nernst's equation is the basis of all potentiometric measurements. The common form of this equation is the one represented in equation 1.10 for a working temperature of 25 °C:

$$E = E^0 \pm \frac{0,059}{z_i} \log\ a_i \qquad \text{Eq.1.10}$$

Potentiometric measurements always result in activity values. The number z_i is the charge of the ion studied. The sign of the concentration-dependent term is positive for cations and negative for anions.

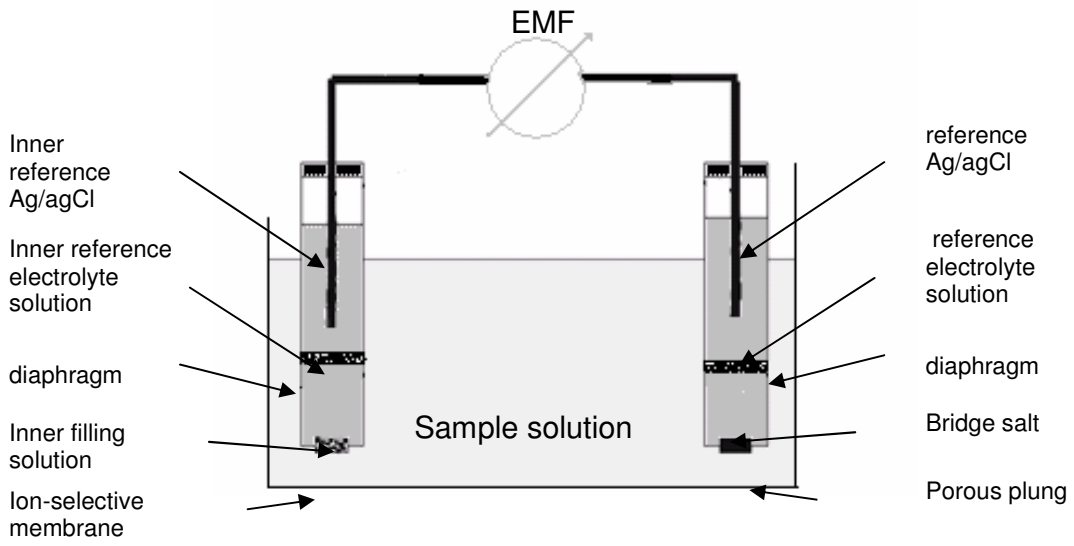

FIGURE 1.8 Measurement system for potentiometric sensor .Reference electrode and ISE are represented together into a sample solution .

From the ’70 on, they have been widely used in clinical laboratories and have recently found extensive employment for environmental trace analysis [30].
The best known and most used potentiometric sensor is the pH-meter glass electrode.

Potentiometric sensors can be classified based on the typology of their membrane in Solid or Liquid State Selective Electrodes.
Solid State Selective Membrane electrode can be made using a homogeneous crystalline membrane (LaF, CuSe) or a polycrystalline membrane.
Liquid Selective membrane generally are based on polymeric membrane whose selectivity is dictated by a lipophilic ligand (ionophore) capable of binding the target ion in the organic phase. The other important constituent of these membranes is the lipophilic ion, which ensures the permslectivity and potentiometric response of the electrode. In cation selective membranes, tetraphenylborates derivatives are used as ion exchanger, while the anionic permselectivity is ensured with lipophilic tetra-alkylammonium salts.
The polymer matrix provides the necessary physical properties to the membrane, such as the mechanical stability and elasticity. The most common polymer matrix is poly(vinyl chloride)(PVC), which is used whit an adapt membrane solvent.
A plasticizer is required whit polymers having a glass transition temperature higher than 80 °C to achieve optimal physical properties and to reduce the viscosity while ensuring a relatively high mobility of the membrane components. The membrane solvent has to be compatible with all membrane constituents, since it could affect the selectivity depending on its polarity an dielectric constant. Recently self plasticized polymers based on methacrylic monomers were tested as alternative to PVC matrix backbones.

The ISE is a galvanic half-cell consisting of an ion-selective membrane that is in electrical contact whit an internal reference electrode. The electrical contact can be accomplished through an inner filling solution or by a direct solid contact. The other

half-cell is the external reference electrode, that has a stable potential under zero-current conditions.

The measured potential difference (electromotive force, EMF) is the sum of several partial potential differences arising at each electrochemical interface.

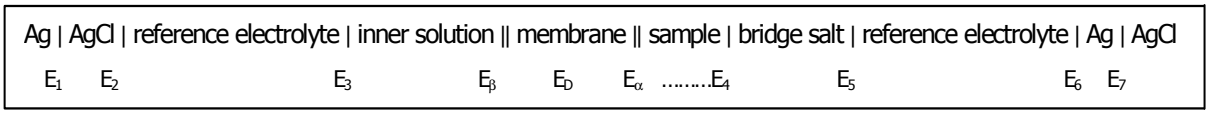

FIGURE 1.9 Electrochemical interfaces and corresponding partial potential differences are represented

$$EMF=(E_1+E_2+E_3+E_4+E_5+E_6)+E_{D,ref}+E_M \qquad \text{Eq 1.11}$$

Where E_M is the membrane potential, $E_{D,ref}$ is the liquid-junction potential of the reference electrode.

E_M and $E_{D,ref}$ are sample dependent, so the equation Eq.1.11 can be written as

$$EMF = E_0 + E_{D.ref} + E_M \qquad \text{Eq 1.12}$$

The liquid-junction potential of the reference electrode($E_{D,ref}$) is due to the different ion mobility of the ionic species in the sample and in the bridge electrolyte and it can be kept constant by using a concentrated bridge electroliyte solution. Liquid-junction potential can be also estimated by Henderson's approximation[31-32]

$$E_{D,ref} \cong -\frac{RT}{F}\frac{\sum_I z_I u_I (a_{I,S} - a_{I,ref})}{\sum_I z_I^2 u_I (a_{I,S} - a_{I,ref})} \ln \frac{\sum_I z_I^2 u_I a_{I,ref}}{\sum_I z_I^2 u_I a_{I,S}} \qquad \text{Eq. 1.13}$$

Where R is the molar gas constant (8.314 $JK^{-1}mol^{-1}$); T is the absolute temperature (K); F is the Faraday constant (96487 $Cmol^{-1}$); z_I is the absolute charge of ion I; u_I is the absolute mobility of ion I (cm^2 mol s^{-1} J^{-1}); a_I is the activity of the ion in the sample *(s)* and in electrolyte bridge *(ref).*

E_M is the membrane potential which is given by the sum of the three potential differences contributes (FIGURE 1.10): the two phase-boundary potential at the *membrane/sample solution* **E_α** and at *the membrane/inner filling solution* E_β and the trans membrane diffusion potential E_D.

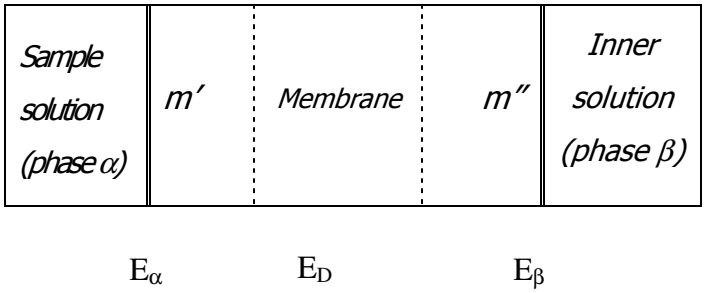

FIGURE 1.10 Solution-membrane-solution interfaces occurring in liquid membrane ISEs

$$E_M = E_\alpha + E_D + E_\beta \qquad \text{Eq. 1.14}$$

E_D trans membrane diffusion potential is due to the charge separation owing to the different mobilities of the ionic species in the membrane phase

$$E_D = \frac{RT}{F}\int_0^d \sum_I \frac{t_I}{z_I} d\ln(a_{I,mem}) \qquad \text{Eq.1.15}$$

Where t_I is the transport number of ion I, $a_{I,mem}$ is the activity of the ion I in the membrane; z_I is the absolute charge of ion I; d is the membrane thickness while R,T and F are used in their common meaning.

Donnan potentials (Eq1.16, Eq.1.17) arise at the membrane/sample-solution interface (E_α) and at the inner solution/membrane interface (E_β) and depends on the distribution *equilibria* of the primary ion between the organic phase of the membrane and the aqueous phase.

$$E_\beta = \frac{RT}{z_I F} \ln \frac{K_I a_{I''}}{a_I(\mathrm{d})} \qquad \text{Eq 1.16}$$

$$E_\alpha = \frac{RT}{z_I F} \ln \frac{K_I a_{I'}}{a_I(0)} \qquad \text{Eq 1.17}$$

Where a_I' *and* a_I'' are the activity of the ion I in the sample solution and in the inner filling solution respectively; $a_I(0)$ and $a_I''(d)$ are the activity of the ion I on both the membrane interfaces and K_I is the distribution constant of the ion I and it is a function of the ion lipophilicity

Since at the steady state the boundary the inner phase-boundary potential (E_β) is sample-independent, combining the equations 1.14,1.15,1.16 and 1.17, EMF can be expressed as a function of the activity of the primary ion

$$E = K + \frac{RT}{z_i F} \ln(a_{i'}) \qquad \text{Eq.1.18}$$

Where K is a constant value in which all independent sample activity terms are summarized.

The phase –boundary potential (E_M) arises from the unequal distribution of ionic species at the phase boundary of the two phases. It can be derived from thermodynamic considerations about the chemical and electrochemical potentials μ_I and $\bar{\mu}_I$ respectively.

The electrochemical potential of a solution can be written as

$$\bar{\mu}_I = \mu_I + z_I F \phi = \mu_I^0 + RT \ln a_I + z_I F \phi \qquad \text{Eq 1.19}$$

Where μ^0_I is chemical standard potential of ion I and ϕ is the local electrostatic potential .

Since in a real situation an absolutely selective membrane doesn't exist, it becomes necessary to consider the contribute to the EMF even of the interfering ions .

At the thermodynamic equilibrium, the electrochemical potential of ion I in the membrane phase ($\bar{\mu}_{I,M}$) and in the sample($\bar{\mu}_{I,S}$) are equal and the phase boundary potential can be expressed as:

$$E_\alpha = \phi_{m\alpha} - \phi_\alpha = \frac{\overset{\circ}{\mu}_{I,S} - \overset{\circ}{\mu}_{I,m\alpha}}{z_I F} + \frac{RT}{z_I F} \ln \frac{a_i^\alpha}{\left[I^{z_I}\right]_S} \qquad \text{Eq. 1.20}$$

Where $[I^{Z_I}]_s$ is the concentration of ion I in the membrane at the sample interface. It is assumed that the activity coefficient in the organic phase are constant for all the ionic species in the organic phase, therefore the values of the concentrations are used.

Analogous consideration can be made for E_β and E_D

$$E_\beta = \phi_\beta - \phi_{m\beta} = \frac{\overset{\circ}{\mu}_{I,m\beta} - \overset{\circ}{\mu}_{I,\beta}}{z_I F} + \frac{RT}{z_I F} \ln \frac{\left[I^{z_I}\right]_m}{a_i^\beta} \qquad \text{Eq. 1.21}$$

$$E_D = (\phi^{m\beta} - \phi^m) + (\phi^m - \phi^{m\alpha}) \qquad \text{Eq.1.22}$$

Both E_D local potential contributes $(\phi^{m\beta} - \phi^m)$ and $(\phi^m - \phi^{m\alpha})$ can be calculated considering all ions present in the membrane, by the Henderson approximation (Eq 1.15).

The difference between the chemical standard potential of the ion I in the two phase depends on its lipophilicity:

$$K_I = e^{\frac{\mu^0_{I,S} - \mu^0_{I,M}}{RT}} \qquad \text{Eq.1.23}$$

For an ion-exchanger membrane, containing only one ion exchanger, this parameter dictates the distribution of the measuring ions between the organic and aqueous phases

In membrane containing a neutral carried (ionophore) the ion distribution is strongly influenced by the *complexation equilibria*. Lipophilic uncharged ligand forms in fact reversible and relative stable complex whit different ions in the membrane.

$$\beta_{IL_n} = \frac{\left[IL_n^{\,Z_i}\right]}{\left[I^{z_I}\right]\left[L\right]^n} \qquad \text{Eq.1.24}$$

Where β_{ILn} is the complex stability constant , *[L]* is the free ligand concentration, $[IL_n^{zI}]$ is the complex concentration in membrane and *n* is the stoichiometric coefficient.

For both types of membrane (with or without ionophore) the total concentration of the ions in membrane is dictated by the amount of lipophilic salt and therefore it remains constant.

Combining the equation 1.12 with 1.14 and 1.18 and including in one term all sample-independent contributions the electrode potential results:

$$E_I = EMF - E_{D,ref} = E_I^0 + (RT / z_I F)\ln a_{I,S} \qquad \text{Eq.1.25}$$

This is the well known Nernst Equation, usually written in the following form

$$E_I = E_I^0 + s_I \log a_{I,S} \qquad \text{Eq. 1.26}$$

Where $\mathbf{E_I°}$ is the intercept of a linear response function and it is unique for each ISE, $\mathbf{s_I}$ is the nernstian slope of the ISE response function *(s=2.303RT/zF= 59.16/z at 25°C)*

For a generic solution containing two ion with same charge E_I can be expressed, considering all local potential contributes and the complex stability constant for each ion, by the Nicolsky-Eisenman equation

$$E = cost + \frac{RT}{F}\ln(a_i + K_{i,j}^{pot} \cdot a_j) \qquad \text{Eq.1.27}$$

Where $K_{I,J}^{pot}$ is the selectivity potentiometric coefficient it is being explained in the next paragraph

The basic processes at the membrane/aqueous phase solution interface are the ions exchange equilibrium and the counter ion coextraction phenomenon, responsible for the upper detection limit

The first equilibrium involves all exchangeable ion I^z and J^z present in the aqueous solution, they are competing for free ionophore in the membrane phase and the corresponding ion-exchange equilibrium is represented by

$$\frac{z_I}{z_J} J^Z(S) + I^Z(M) \underset{\leftarrow}{\rightarrow} \frac{z_I}{z_J} J^{Z_J}(M) + I^{Z_I}$$

The equilibrium constant of this process (Eq. 1.28) describes the relation between the ions and the ion exchanger.

$$K_{I,J} = \left(\frac{a_{I,S}}{[I^{z_I}]}\right)\left(\frac{[J^{z_I}]}{a_{J,S}}\right) \qquad \text{Eq.1.28}$$

For ionophore based membranes, the complexation between ions and ionophore has to be considered

The ion-exchange equilibrium becomes

$$K_{exch} = K_{I,J}\frac{\left(\beta_{JL_m}\right)^{Z_i/Z_j}}{\beta_{IL_n}} \qquad \text{Eq.1.29}$$

Where ***m*** is the stoichiometric factor of the complex formed between the interfering ion, J, and the ionophore, *L*.

The selectivity of the ISE is its capability to discriminate between various permeating species. The selectivity is a measure of the affinity between the ions and the membrane and it is influenced by the membrane material as well as the lipophilicity of the ions involved.

If the ISE responds to only one type of ion, the measured EMF can be described with the Nernst equation.

The selectivity coefficients is directly a function of the difference of the E^o obtained for pure solution of different ions.

For polymeric membrane electrodes, the interferences by other sample ions are mainly dictated by their competitive extraction into the organic phase, and it is fully predictable from the complex formation constant of each ion-ionophore complex in the membrane

The selectivity coefficient K_{IJ} can be calculated by the following equation

$$K_{IJ}^{pot} = \exp\left\{\frac{z_I F}{RT}\left(E_j^0 - E_I^0\right)\right\} \qquad \text{Eq.1.30}$$

Evidently, the selectivity coefficient is a direct function of the differences of the individual potentials(E_J^0 - E_I^0) extrapolated, to 1 M activity for the ions I and J

Transforming the equation *1.30* in logarithm, the Nicolsky's coefficient can then be calculated using the following expression:

$$\log K_{IJ}^{pot} = \frac{E_j^0 - E_I^0}{s_i} = \frac{E_J - E_I}{s_I} + \log a_I(I) - \frac{z_I}{z_J}\log a_J(J) \qquad \text{Eq.1.31}$$

Where $a_I(I)$ and $a_J(J)$ are the ion activity in solutions containing only a salt of the primary and of the interfering ion, respectively, inducing E_I and E_J potential

The traditional procedures to assess K_{IJ}^{pot} values are the separate solution method (SSM) and the fixed interference method (FIM). Both methods, however, present few drawbacks that compete to determine the bias selectivity coefficient [33]

In recent years, a number of selectivity measurements were suggested to overcome the problems due to the Nicolsky-Eisenman effect [34-36]. It is now known that

Nicolsky-Eisenman equation is incorrect when two ions of different charges significantly contribute to the EMF, causing bias selectivity coefficient determination

$$E_I = E_I^0 + \frac{RT}{z_I F}\ln(a_I + \sum K_{I,J}^{pot} a_J^{z_I/z_J}) \qquad \text{Eq.1.31}$$

According to the IUPAC recommendations [37], the lower and upper detection limit are defined by the cross section of the two extrapolated segments of the calibration curves.

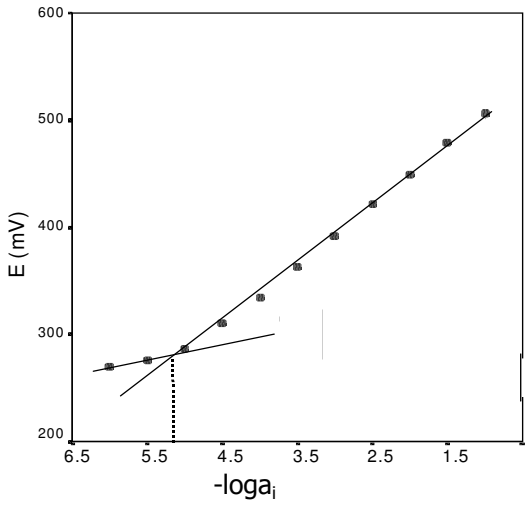

FIGURE 1.11 Ideal calibration curve . Lower Detection Limit is represented by the cross of two linear segment .

Static and dynamic model of ISE response are based on different approximations that are responsible for the different response functions of those electrodes [38-40].
In the present work, only the static model electrode response is considered, and this derives by the assumption of an idealized case where the ion flux in the membrane phase and in aqueous solution at each phase boundary of the membrane are neglectable.
The upper detection limit is due to coextraction of the counterion together with the primary ion, from the sample into the membrane.

Thereby the membrane loses its perm-selectivity, and the concentration of the counterion in the membrane phase increases, the electrode gives a less-than-Nernstian response.
The upper detection limit decreases whit increasing the lipophilicity of the counterion in the sample and whit increasing the stability of the complex between primary ion and ligand in the membrane.
The value of the limit of detection is determined by several parameters: presence of interfering ions, leaching of inner filling solution (LC-ISEs) and leaching of hydrophilic ion of the ionic exchanger.

Static lower detection limit (independent from ion fluxes) can be predicted by the selectivity coefficient of the membrane and expressed by the equation 1.32. It depends on the composition of the background solution and it is directly a function of the selectivity coefficient

$$a_i(LDL) = K_{ij}^{pot} a_j^{\frac{z_i}{z_j}} \qquad \text{Eq.1.32}$$

Leaching of primary ion from the inner solution and from ion exchanger across the ion selective membrane changes the concentration of primary ion at the water –membrane interface.
The transmembrane concentration gradient occurs when the membrane is not symmetrically bathed (the composition of the sample and of the inner solution are not the same).
The variation of the concentration of primary ion at the membrane interfaces whit respect to its concentration in the bulk of the solution generates responses that are less than optimal.
The bias can be reduced by decreasing the transmembrane primary ion flux, this is obtained by adjusting the composition of inner solution, by tuning the membrane

thickness and composition or replacing the inner filling solution with a solid inner contact. [38]

1.3.3 Conductometric and capacimetric sensors

Information about the composition of samples can be obtained by measuring their electrical conductivity (or resistivity).

Generally, this imply that the interaction of the sample components causes changes of the resistance in the receptor layer. Such changes can be measured and evaluated to obtain analytical results.

Conductometric sensors or chemoresistors rely on changes of electric conductivity of a film or of a bulk material, whose conductivity is affected by the analyte presence.

The receptor is represented by a layer of semiconductors, polymers or gels.

The resistance, or dielectric constant, of this layer changes when interacting with the sample. The resistance change is measured and evaluated .

Chemoresistor' and '*chemocapacitive sensor*' are terms used for conductimetric gas sensor . A measurable change in capacity is achieved by interaction of the dielectric with sample components. If the *dielectric coefficient* changes its value, then the capacity also changes.

The sensing layer is often composed of inorganic semiconductor or of Conducting Polymers (CPs).

In CPs based conductimetric sensors the conductance of the polymer is measured upon exposure to the analyte, and the resulting change in the conductivity is used as the basis for the estimation of the analyte concentration

In these sensors the conducting polymer works both as the recognition element and as the transducer.

1.4 Conducting polymers

The Conducting Polymers (CPs) represent a class of organic polymers that have the unusual properties of possessing high electrical conductivity, and can exhibit a range of properties from semiconducting to near metallic behaviour. In view of this, these polymers introduced a new and interesting field of research.

Although the interest in conducting polymer is relatively recent, the most widely studied materials were already known at the beginning of the 20th century.
In 1958 Natta et al. synthesised polycetilene, a black, powderly looking polymer [41]. This material was found to have a semi-conductor character whit conductivity ranging from $7e^{-11}$ to $7e^{-3}$ Sm^{-1}. The first attempts to apply polyacetilene were made in the mid 1970s, and from then on, many other CPs have been synthesised, characterised and tested for their properties.
In the year 2000, the Nobel Prize for Chemistry was awarded to A. Heeger (UCLA Santa Barbara), H. Shirakawa (Tsukuba Univ.) A. MacDiarmid (Penn State Univ.) *"For the Discovery and Development of Conductive Polymers"* .
The leader compound in this class of polymers was polyacetylene, regarded as the model CP. This has been attributed to its relatively simple structure, significant for studies on fundamental properties like the nature of the charge carriers, doping phenomena, the relationship between doping and conductivity etc. In the last two decades, moreover, polymers bearing monomer with heteroatoms in their backbone (i.e. polypyrrole, polyaniline, polythiophenes and derivatives as poly(3,4-ethylenedioxythiophene), gained more interest. This resulted from their higher stability to air and water, as well as their relatively easier synthesis by electropolymerization.

From the classes listed above, many derivatives were designed and syntesized..

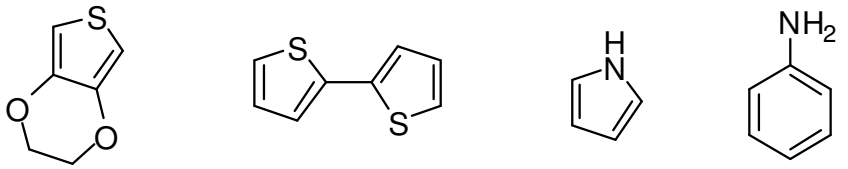

(Diethylene-) 3,4-di-oxythiophene | 2,2'-bithiophene | Pyrrole | Aniline

FIGURE 1.12 Monomer structures of the most commonly used conducting polymers

The possibility of tuning the properties of CPs either by monomer derivatization/functionalization and their copolymerization as well, revealed themselves as powerful way to design new material and the possibility of apply them to the realization of sensoristic devices, optical tools or photovoltaic applications (i.e. solar cells) [42].

CPs can be prepared either by chemical or electrochemical synthesis.

The chemical synthesis is carried out using catalysts [43] or with soluble polymer precursors, cast them onto substrates and/or surfaces and eventually convert them to the desired product by heating [44]. The general drawback of these synthetic pathway is the low control of the morphology of the polymeric material.

The electropolymerization normally is carried out from a monomer solution containing a supporting electrolyte in a three electrodes electrolytic cell (Working Electrode, WE; Reference Electrode, RE; Auxiliary Electrode, AE.) and it profits of the reactivity of the monomers as aniline or conjugated heteroaryls (pyrrole , thiophene and all their possible substitution patterns) towards the electrochemical polymerization.

The electropolymerization consists in the formation of a polymeric film on the surface of a working electrode, the most commonly used material as WEs are Pt, Au, Glassy carbon (GC), glass covered whit Indium-Tin-Oxide (ITO), and they can have several shapes (disc, wire, bar) finally coated with polymeric films. The so obtained electrodes are also called Chemically Modified Electrodes (CMEs). In the same cell, a

Ag/AgCl or calomel electrode is used as reference system. The counter or auxiliary electrode is made by platinum or GC.

The main requirements to have the CPs electrochemically synthesised are: 1) a monomer with the proper oxidation potential in a suitable solvent system; 2) the possibility of forming a radical cation that in turn reacts quickly with other monomers in the typical chain reaction profile to form the polymer 3) the production of a polymer chain with an oxidation potential lower than the one of the starting monomer.

The electropolymerization method is generally the same for all types of synthetic materials. The monomer is dissolved in a suitable solvent, for example acetonitrile (ACN), with an electrolyte as $LiFB_4$ and the polymerization is carried out applying an anodic potential or a anodic current strong enough to oxidise the monomer to the state of a radical-cation.

The electrochemical polymerization can follow two mechanism: the radical cation generated by the anodic process undergoes coupling with an other radical, or it can react with neutral monomeric species, starting a radicalic propagation (figure1.13) .

The polymeric film so obtained on the WE surface is formally considered of being in an oxidized form. The reduction of the polymer is done once again electrochemically, holding the polymer at its reduction potential, or directly with a chemical reducing specie like hydrazine.

The electrochemical polymerization can be done in three different ways: potentiostatically, potentiodynamically and galvanostatically.

In the galvanostatic method a current density is applied through the cell, and its value has to be high enough to reach the oxidation potential of the monomer. The polymer grows as a film on the WE, and the time is the cut off value to standardize the polymer charge.

The same chemical machinery is adopted in a potentiostatic polymerization: the monomer is oxidized by keeping the electrode at a potential value where the initiation reaction takes place .

The potentiodynamic electropolymerization is carried out by cyclic voltammetry and it is the technique more suitable to control the deposition of the film. It also allows to characterize the growing polymer e.g. the redox behaviour of the monomer, of the soluble oligomers and the formed polymers.

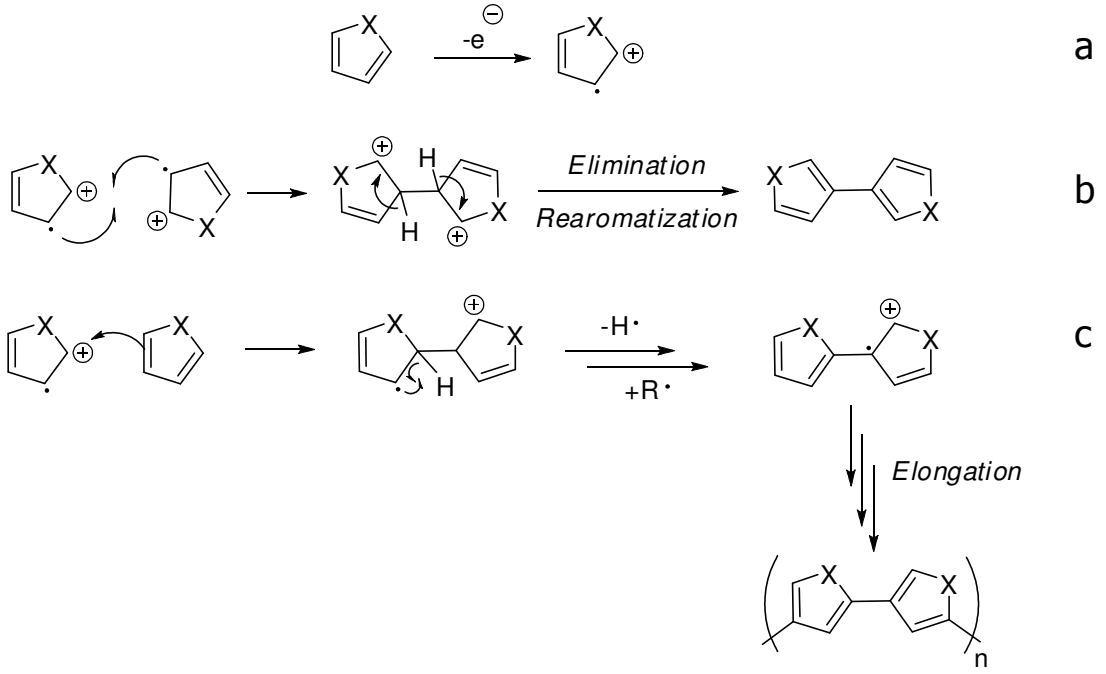

FIGURE 1.13 electropolymeriztion mechanism of a five –member heterocycles showing two alternative reactive pathways of radical coupling (b) and radical-monomer coupling (c).

Doping is the process of changing the oxidation state (i.e. the degree of unsaturation of the conjugated system) of the polymer whit a corresponding modification of its electronic properties.

The similarity between the doping of conducting polymers and the doping of semiconductors material such as silicon is clear. In the latter, the doping species occupy certain positions within the lattice of the host material, resulting in the presence of either electron–rich or electron-deficient sites, without charge transfer occurring between the two species. The effect of the boron dopant on silicon for example, results in the creation of positively charged sites; on the other hand if silicon is replaced with phosphorous the lattice results being electron rich.

In conjugate polymers the doping process consists essentially in a charge-transfer reaction, resulting in a partial oxidation or reduction. The overall process is basically the abstraction of one electron from a π-double bond, to generate a positive charge, then p-doping

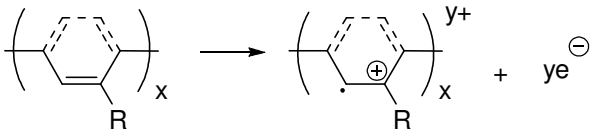

Or if a partial reduction occurs (one electron is acquired by the polymer), the process is termed n-doping is the partial reduction of the polymer.

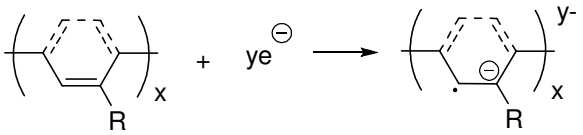

These processes can be performed by homogeneous oxidizing reagents as AsF_5 and I_2, $FeCl_3$ or by means of heterogenous phase *via* electrochemical reaction on the electrode itself.

To maintain the electro-neutrality during and after doping process, both π-doped and undoped polymeric material requires the presence of a "suitable" counter ion:

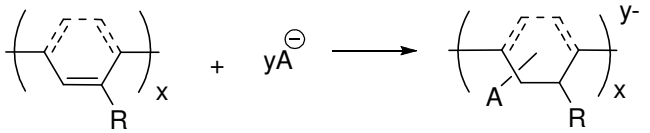

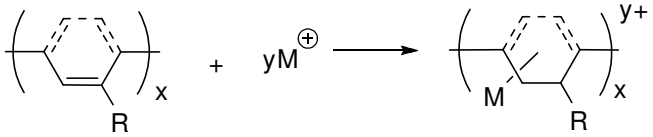

In the electrochemical doping, the counter ion is provided by the electrolyte. Although chemical doping methods [45-46] have been often used, the electrochemical way is the preferred technique since it allows more control and more reproducible results.

The precise nature of the charge carriers in the conjugate polymer system varies from material to material; however the CP with higher conjugation and electronic

availability are particularly capable of this processes. Polyacetillene (PA), polypyrrole(PP) and polythiophene (PT) show an extended π-system along the carbon backbone. This extended conjugation impart a "metallic behaviour" to these materials with half-filled conduction bands. One early explanation of this "metallic" behaviour of CPs used band theory as the conduction mechanism, even though these organic polymers show an amorphous structure. The half filled band is constituted by a continuous delocalized π-system, an ideal condition for charge movement, resulting in a current. The polymer, however, can more efficiently lower its energy by alternating "short" (double) and "long" (single) bonds (see Figure 1.14). This alternation is responsible for a band gap of 1.5 eV, a value typical for a high energy gap semiconductor.

The oxidative doping process in CPs as PP or PT occurs by removing an electron from the π-system of the backbone; this produces a free radical-cation.

This combination of a charged site (empty or doubly occupied p-orbital) and of a radical (half-filled p-orbital) is called polaron. Depending on the total number of electrons involved (resulting in the opposite charge) in the polaron, they are radical cation (one electron) or radical anion (three electrons). The polaron is then delocalized over the conjugated system, reaching a lower energy state.

The potentials required for the oxidation or the reduction to occur are set by the energies of the HOMO (top of valence bond) and the LUMO (bottom of conduction band) of the polymer. Higher polimerization numbers directly correspond to a higher degree of conjugation, resulting, in the end, in a closer energy value for both the HOMO and the LUMO. This is directly the effect of the conducting ability of the polymer itself.

Upon further oxidation the free radical of the polaron is removed, creating a new charge defection called bipolaron (Figure 1.14). This process involves less energy than the creation of two distinct polarons. At higher doping levels it is possible that two polarons combine to form a bipolaron. Thus, at higher doping levels the polarons are replaced by bipolarons, located symmetrically on the polymer backbone. This can continue the doping, forming a continuous bipolaron bands. These charge carriers rise the conductivity of the materials wherever they occur. All polymeric systems

consist of a chain of finite length that is (generally) randomly oriented and fully conjugated along its whole length, whit a certain (even though unknown and statistically distributed) number of structural imperfection such as sp^3 bound carbon interrupting the conjugation.

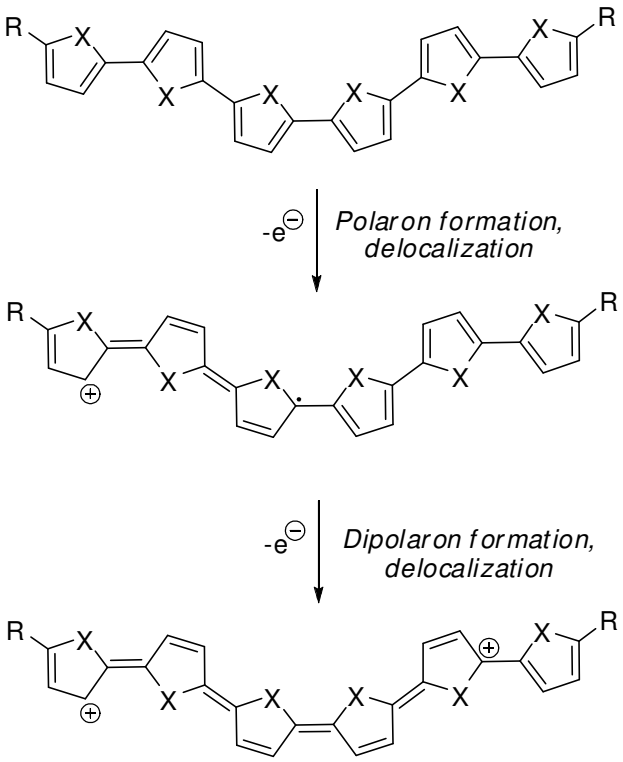

FIGURE 1.14 Doping mechanism of a five–member heterocycles
a is the neutral polymer form, **b** and **c** are polaron and bipolaron species respectively.

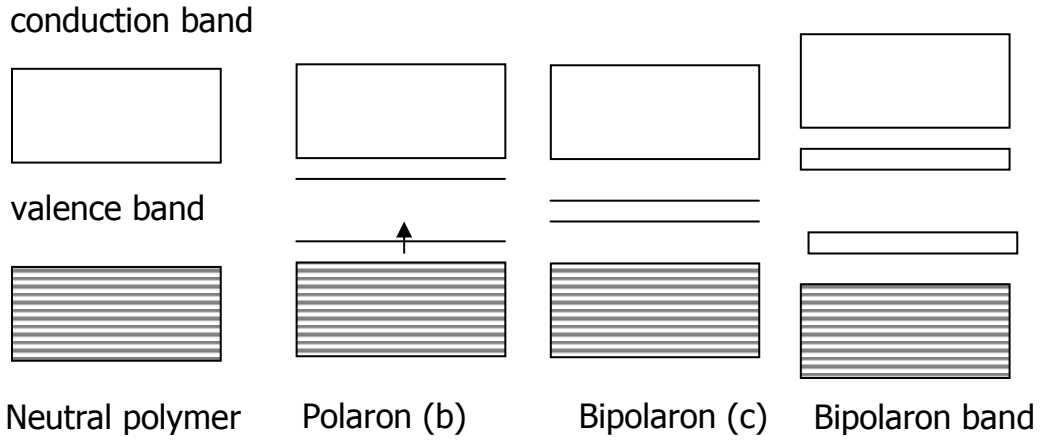

FIGURE 1.15 Energy level of valence band for differently doped polymers

Moreover, any consideration regarding the conducting behaviour and the electrical properties of CPs must include the charge transfer process across distinct chains and (in doped conjugate polymers) the effect of the counterions on charge defects.
These properties of CPs are easily investigated with standard electroanalytical techniques as cyclic voltammetry or constant current charge/discharge cycles. Less usual experimental methods includes UV visible and IR spectroscopy, combined with the electrochemical polymer synthesis. This "on-line" spectroscopic investigation is therefore termed spectroelectrochemistry.[61]

1.4.1 Polythiophenes

Polythiophene and its derivates can be prepared by chemical and electrochemical polymerization in both neutral or p-doped form. One of the first chemical preparations of unsubstituted polythiophene (PT) was reported in 1980 by two groups [47-48]. Both groups synthesized polythiophene by a metal-catalyzed polycondensation polymerization of 2,5-dibromothiophene

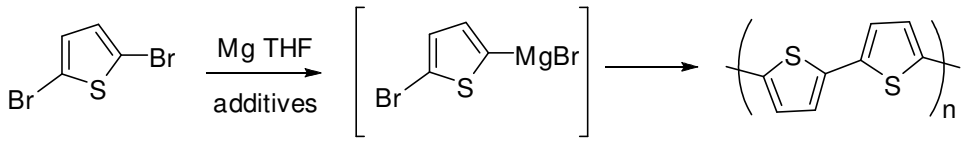

T**FIGURE 1.16** Chemical synthesis of polythiophene: **Yamamoto's** additives: $Ni(biPy)Cl_2$ ı
S**Lin and Dudek**: $M(acac)_n$, M= Pd, Ni, Co or Fe l

form up to 10^2 Scm^{-1} in the doped form[50].
The electrochemical synthesis of polythiophene was first reported in 1981 [46]. In these electropoplymerization experiments many supporting electrolytes and solvents were tested, and different working electrodes as well [52]
The CP so obtained showed some peculiarity regarding their conductivity values and morphology.

The electrochemical polymerization oxidation is influenced by many factors, such as the presence of the oxygen and water dissolved in the solvent, the geometry of the cell, the monomer concentration.

Many substituted thiophenes have also been electrochemically polymerized and the 2-2'bithiophene, used as starting material, showed certainly the best quality film. Several polycyclic monomers containing a thiophene ring have also been polymerized (for example polyethyledioxythiophene, PEDOT)

The electrochemical polymerization takes place by a radical coupling mechanism and involves oligomers as well as monomer radicals.

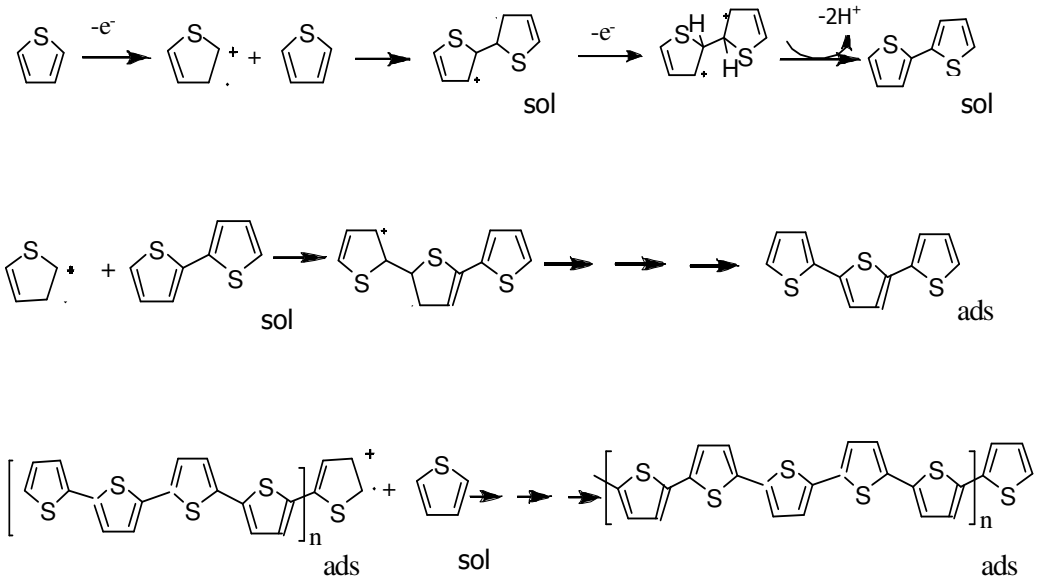

FIGURE 1.16 A possible grow pathway of thiophene: the showed mechanism of polymerization involves the monomer from the solution(sol) to the electrode surface (ads)

The proof of that is the decreasing oxidation potential observed during the polymer growth.

Electrochemical experiments have shown that instantaneous nucleation occurs on bare working electrode, followed by rapid formation of a polymer monolayer. Initially a short oligomeric chain is produced, while longer chains appear subsequently (figure1.16). The characteristic electrical properties appear when the polymer grows and it becomes the bulk of the electrode material.

As with other material, substitution on the thiophene ring influences the oxidation potential.

Group such -CN or -NO_2 (electron-withdrawing groups) affect the stability of the intermediate and the extended polymerization does not occur. On the other hand, the presence of electron donating groups such as alkyl moieties have the opposite effect, shifting the oxidation potential in a cathodic direction.

Most CPs, such as polyaniline (PANI), polypyrrole (PP)and poly(phenylene sulphide-phenyleneamine) (PPSA) are π-type semiconductors, unstable in the undoped state. In contrast, polythiophene (PT) films are stable when undoped or very lightly doped. The primary doping agents (anions), introduced during the chemical or electrochemical polymerization, maintain charge neutrality and generally increase the electrical conductivity. The nature of the anion strongly influences the morphology of the polymer[51]. Anions can also work as specific binding sites for the interaction of the CP with analytes.

1.4.2. Application of conducting Polymers

Conjugated organic compounds play a primary role in the development of a new generation of optical and electronic materials.

Electrochemical doping of the π-extended systems by oxidation or reduction, with concomitant electron and ion transfer, cause the appearance of new electronic states (polaron and bipolarons) in the band gap and a change in the chemical composition of the polymer.

These effects can result in changes of polymer volume [53-54], colour [55-56], and conductivity [57].

Their combination of unique electrical, optical, mechanical and membrane properties, proposed them as a major class of sensing elements for the development of chemical sensors. It's aim of this work to disclose their possible analytical applications in particular those of thiophene derivatives, in the field of electrochemical sensors.

Electrochemical synthesis of polythiophene allows to coat directly the electrodic material (i.e. the supporting electrode) made of a metal (Au, Pt, Cu) or glassy carbon(GC). Their combination, as already mentioned, result in the so called Chemical Modified Electrodes (CMEs).

CPs can form layers in electrochemical sensors selective both for species in solution and for gaseous analytes. The interaction between the analyte and the conducting matrix generates the primary change of a physical parameter in the transduction mechanism.

The electronic properties are related to the redox sites of the matrix and so are the chemical interactions (covalent bonds, hydrogen bonds and Van der Waals interactions) that appear between the layer and the analyte. These influence the electron transfer in the polymer and its electronic properties.

The affinity of the CP for the analytes can be increased by introducing specific binding sites [59].

Piezoelectric sensor can be also based on functionalized or unfuctionalized CPs film, the changes of mass of the layer by interaction phenomena whit the gas molecules are related with the frequency variation recorded as signal.

Solid contact ISE are based on conducting polymer membrane as selective layer as well the CPs are employed in order to modify the electrodic surface in contact with the conventional ion selective membrane in order to stabilize the potentiometric signal.

In amperometric and voltammetric sensor, the signal is derived from changes in a current an related to an applied potential (constant or sweeping) on the polymer-modified electrode.

In both cases, the conjugated conducting polymer may play either an active role by participating in mediation of the redox process or a passive role when the polymer merely provides a site for anchoring an enzyme or other redox-active probe molecules [60].

1.5 Aim of the work

Conducting polymer based materials and chemical sensor technologies can be easily combined.

CPs can be effectively deposed by several means on the sensor surfaces, changing completely the chemical physical properties of the sensor-sample interface.

Moreover, the possibility to precisely bind functionalized materials to bare electrodes allow to reduce fouling phenomena increasing the sensor shelf life.

The development and characterization of amperometric, potentiometric and piezoelectric sensors with sensing agents immobilized on the surface are the topics of this PhD thesis.

The CP electropolymerization has been chosen as the experimental procedure to modify different electrode surfaces (Pt, Au and GC).The sensing properties of polythiophene derivatives will be investigated preparing suitable sensor devices.

Polymeric backbone modified by covalently bound active moieties will be employed as new material for potentiometric sensor with reduced leaching phenomena.

1.6 References

1. Barnard Sm, Walt Dr *Nature*, **1991**, 353, 338.
2. Hanrahan G, Patil DG, Wang J *Journal Of Environmental Monitoring* **2004**, 6, 657.
3. Wang J *Accounts Of Chemical Research***, 2002**, 35, 811.
4. Si P, Mortensen J, Kornolov A ,Denborg J Moller PJ *Anal.Chim. Acta* **2007**, 597, 223-230
5. Bonastre A, Ors R, Capella JV, Fabra MJ, Peris M *Trac-Trends In Analytical Chemistry* **2005**, 24, 128.
6. Comini E *Anal. Chim. Acta*, **2006**,568, 28.
7. Adhikari B., Majumdar S. *Progress In Polymer Science* **2004**, 29, 699.
8. Ramaraj R *Journal Of Chemical Sciences* **2006**, 118, 593.
9. M. Dekker "H*andbook of Conducting Polymers"* (Eds: T. A. Skotheim, R. L. Elsenbaumer, J. R. Reynolds), 2nd edition, , New York, Basel, Hong Kong **1998.**
10. G. P. Evans, "*Advances in Electrochemical Science and Engineering"*, Vol. 1 (Eds:H.Gerischer, Ch. Tobias), Verlag Chemie, Weinheim **1990**, p.1.
11. Malinauskas, *Synth. Metal*, **1999**, 107,75.
12. R. P. Buck, E. Lindner, W. Kutner, G. Inzelt Piezoelectric Chemical Sensors (Iupac Technical Report) *Pure Appl. Chem.*, **2004**, 76, 1139.
13. J.Janata, M.Josowiz,D.M.De Vaney, *Anal.Chem*, **1994**, 66, 207R.
14. R.L. Bunde,E.J.Jarvi, J.J.Rosentreter, *Talanta*, **1998**, 46, 1223.
15. S.R. Kim,S.A. Choi,J.D.Kin, *Synt. Met.*, **1995**, 71, 2027.
16. V.Syritski, Reut J, Opik A. Idha K, *Synth. Met.*, **1999**, 102, 1326.
17. N.E.Agbor, M.C Monkman, *Sens. And Act. B*, **1995**, 28, 173.
18. Si P., Mortensen J., Kornolov A., Denborg J., Moller P.J.. *Anal. Chim. Acta*, **2007**, 597, 223.
19. E. Bakker *Anal. Chem*. **2004,** 76, 3285.
20. E. Bakker, Y. Qin, *Anal. Chem*. **2006**, 78, 3965.

21. Han J.H., Park S.J., Boo H.K., Kim H.C., Nho J.M., Chung T.D. *Electroanalysis*, **2007**, 19, 786.
22. Clark LC, Wolf R, Granger D, Taylor Z. *J. Appl Physiol*. **1953,** 6, 189.
23. Saito H., Kaneko Y., Hashimoto Y., Shirai T., Mitsubayashi K, *International Journal Of Environmental Analytical Chemistry* **2006**, 86, 1057.
24. Ghica M.E., Brett C.M.A. *Anal. Lett.* 2005, 38, 907.
25. Rajesh, Pandey S.S., Takashima W, Kaneto K *Jour. App. Pol. Sci*. **2004**, 93, 927.
26. Yu E.H. ,Sundmacher K *Process Safety And Environmental Protection* **2007**, 85, 489.
27. Ahuja T., Mir I.A., Kumar D., Rajesh, *Biomaterials*, 2007, 28, 791.
28. *Wang JTalanta* 1994, 41, 857.
29. W.E.Morf "The Principles Of Ion-Selective Electrodes And Of Membrane Transport" Elsiever. Amsterdam, Oxford, New York, **198**
30. Ceresa, E. Bakker, B. Hattendorf, D. Gunther, and E. Pretsch *Anal. Chem.* **2001,** 73, 343-351
31. P.Henderson, "Zur Thermodynamic Der Flűssigkeitsketten", Z.Phys.Chem **1907**,59,118.
32. W.E.Morf, *Anal. Chem*. **1977**, 49, 810
33. E. Bakker, E. Pretsch, P.Buhlmann, *Anal. Chem.*, **2000**,72, 1127-1133
34. Giannetto M., Mori G., *Annali Di Chimica*. **1999,** 89, 601; Giannetto M., Mori G., Pappalardo S., Parisi M. F. *Annali Di Chimica* **2002***.* 92, 1099.
35. K. N. Mikhelson, and A. Lewenstam *Anal. Chem*. **2000**, 72, 4965-
36. E. Bakker, R. K. Meruva, E. Pretsch, M. E. Meyerhoff *Anal. Chem.* **1994**, *66*, 3021-3030.
37. R.P Buck and E. Linder, Pre Appl.Chem. **1994**, 66, 2527.
38. E. Bakker, U.M. NageleSchaller, E. Pretsch, *Electroanalysis* **1995**, *7*,817-822.
39. E. Bakker, P Buhlmann, E Pretsch, *Chem. Rev*. **1997**, *97*, 3083-3132.

40. Z.Szigeti, T,Vigassy, E.Bakker, E.Pretsch. *Electroanalysis*, **2006**, 18, 1254.
41. G. Natta,G. Mazzanti,P. Corradini, *Atti Acad. Naz. Lincei, Cl.Sci. Fis. Mat, Rend,* **1958**, 25, 3
42. S.-W. Oh, H.W. Rhee, Y.C. Kim , J.K. Kim , J.-W. Yu *Current Applied Physics,* **2006**, 6, 739.
43. Y.Ito, H.Shirakawa,S.IkedaJ *Polymer. Sci., Polym. Chem. Ed*. **1974**, 12,11
44. J.H.Edwards,W.J. Feast, *Polymer*, **1980**, 21, 595
45. Evans, G., *Advances in Electrochemical Science and Engeneering*, vol. 1, VCH, Weinheim, **1990**, 22.
46. Diaz, A. F., Castello, J. I., Logan, J. O., Lee, W. Y., J. *Electroanal. Chem.*, **1981**, 129, 115.
47. T. Yamamoto, K. Sanechika, A. Yamamoto, *J. Polym. Sci., Polym Lett. Ed*. **1980**, 18, 9.
48. J. W. P. Lin, L. P. Dudek, *J. Polym. Sci., Polym. Chem. Ed.* **1980**, 18, 2869.
49. T.Yamamoto, K. Sanechika, A. Yamamoto, *J. Polymer Sci. Polym. Lett,* **1983**, 56, 1503.
50. M. Akimoto, Y, Furukawa, H. Takauchi, I. Harada, Y. Soma, M. Soma, *Synth. Met.*, **1986**, 15, 353.
51. Hao QL, Rahm M, Weiss D, Mirsky VM, *Microchimica acta* , **2003**, 43 , 147-153
52. Evans, G., *Advances in Electrochemical Science and Engeneering*, vol. 1, VCH, Weinheim, **1990**, 52-54.
53. Jager, W. H. E.; Smela, E.; Ingana¨s, O. *Science* **2000**, *290*, 1540.
54. Lu, W.; Fadeev, A. G.; Qi, B.; Smela, E.; Mattes, B. R.; Ding, J.; Spinks, G. M.; Mazurkiewcz, J.; Zhou, D.; Wallace, G. G.; MacFarlane, D. R.; Forsyth, S. A.; Forsyth, M. *Science* **2002**, *297*, 983.
55. Gustafsson C. J.; Ingana¨s O.; Andersson M. R. *Electrochem. Acta* **1995**, *40*, 2233.

56. Mecerreyes, D.; Marcilla, R.; Ochoteco, E.; Grande, H.; Pomposo, J. A.; Vergaz, R.; Pena, J. M. S. *Electrochem. Acta,* **2004**, *49*, 3555.
57. Garcia-Belmonte, G.; Bisquert, J.; Popkirov, G. S. *Appl. Phys. Lett.* **2003**, *83*, 2178.
58. Philip B., Xie J.N., Chandrasekhar A., Abraham J., Varadan V.K. Smart *Materials & Structures* **2004**, 13, 295-298
59. Domansky, K., Li, J. & Janata, J. *J. Electrochem. Soc*. **1997**, 144, 75.
60. Krzysztof Maksymiuk *Electroanalysis,* **2006**, 18, 1537.
61. Tarabek J., Rapta P., Jahne E., Ferse D., Adler H.J., Maumy D., Dunsch L. *Electrochimica Acta,* **2005**, 50, 1643.

2 Optimization of the DPV Potential Waveform for Determination of Ascorbic Acid on PEDOT-Modified Electrodes

2.1 Introduction

Chemically modified electrodes and electrocatalitic process

In the last few decades conducting polymers have been extensively studied as electrode modifiers in order to improve the physico-chemical properties of bare electrodes. In particular, they are often fruitfully employed as redox-mediators toward several analytes [1], significantly enhancing sensitivity and selectivity of the analytical detection, and even lowering the detection limit. They also exhibit anti-fouling properties, which is very important for achieving satisfactory repeatability of the electrochemical response.

The first developed systems suitable to activate catalytic electrode processes, i.e. redox-mediated electrode reactions, were based on the presence of the mediating agent in the solution also containing the analyte. For example, the electrocatalytic effect of ferrocene in the oxidation of ascorbic acid has been widely studied by such an approach [2]. However, if the mediating agent is directly immobilised on the electrode surface, leading to a Chemically Modified Electrode (CME), highly efficient electrocatalytic cycles are possible, leading to significant advantages in terms of enhanced performance of the redox mediator, quick regeneration of the catalyst, reduced matrix effect and possibility of avoiding contamination of the solution by the redox mediator.

At conducting polymer modified electrodes, at least three processes should be considered, taking place during electrocatalytic conversion of solution species:

1) heterogeneous electron transfer between the electrode and a conducting polymer layer, and electron transfer within the polymer film
2) the diffusion of solution species to the reaction zone, where the electrocatalytic conversion occurs(on surface or within the polymer)

3) the chemical (heterogeneous) reaction which takes place between solution species and conducting polymer.

In the absence of the redox mediator, the potential required for the irreversible oxidation of the analyte A (figure 2.1) in its oxidized form B is given by a "standard" redox potential contribute ($E°_{B/A}$) but it is also affected by an high charge transfer overpotential η_{ct}

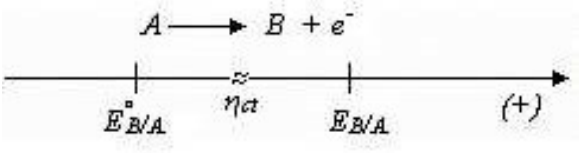

FIGURE 2.1 This scheme displays the irreversible oxidation process of A. Electrochemically induced reduction reaction follow analogous mechanism

The resulting potential is $\mathbf{E_{B/A}=E°_{B/A}+\eta_{ct}}$ Eq 2.1

Under these condition the signal associated with the reaction of the analyte it is not analytically suitable.

If a redox mediating agent Mo is present in solution or on the electrode surface, its reversible electrochemical oxidation to the species Mr can be suited as analytical signal referable to the analyte A, when a redox reaction takes place between A and Mo.

Specifically, electrocatalysis process are explainable by the following scheme

In fact, if the mediator Mo whit a higher standard reduction potential ($E°_{Mr/Mo} > E°_{B/A}$) is also present in solution and if the overpotential associated with the electron transfer is lower for the mediator with respect to the analyte (η_{ct} Mo→Mr < η_{ct} A→B) a catalytic cycle will appear on the electrode surface. The following scheme represent the involved redox reaction

Summarizing, the favourable condition fundamental for the establishment of the electrocatalytic cycle is the following: $\mathbf{E_{D/C} < E_{B/A}}$, with $E_{D/C} = E^{o}_{D/C} + \eta_{ct}$ *and* $E_{B/A} = E^{o}_{B/A} + \eta_{ct}$

$$\mathbf{Mo} \rightleftharpoons \mathbf{Mr + e^-} \qquad (\mathbf{E})$$

$$\mathbf{Mr + A} \rightleftharpoons \mathbf{B + Mo} \qquad (\mathbf{C})$$

Such electrocatalytic phenomenon is ascribable within "EC" processes, involving an electrodic charge transfer (**E**) followed by a chemical reaction that takes place in solution (**C**).

Among different conducting polymers, great attention has been recently devoted to poly(3,4-ethylenedioxythiophene) (PEDOT), which shows quite high conductivity and stability and a particularly reduced band-gap [3-7]. Moreover, the presence of dioxyalkyl residues on the strongly reduces the potential at which π-doping occurs (-0.05 V), with respect to many other polythiophene derivatives

Furthermore, it is easy to electrogenerate the film in aqueous media, i.e. in the most common solvent used in analytical applications (polymerization mechanism is represented in figure 2.1). Thanks to similar properties, this polymer is very appealing for applications in the field of amperometric sensors.

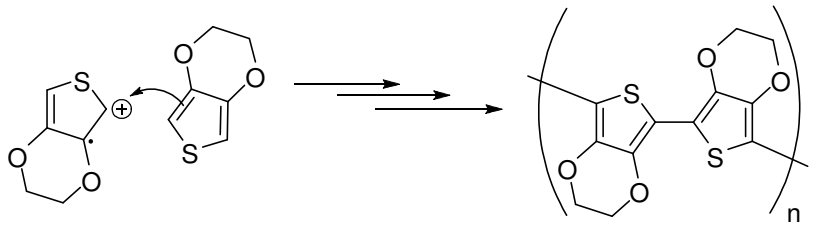

FIGURE 2.2 Electropolymerization of PEDOT, starting and propagation of the polymrization pathway. The polymeric grown on the Pt electrode follows a similar mechanism than thiophene (see Figure 1.16)

Most part of the work reported about development of PEDOT-modified electrodes has been devoted to electropolymerisation carried out in the presence of peculiar electrolytes, such as poly(4-styrenesulfonate) and dodecylbenzenesulphonate, which also act as surfactants improving the solubility of the monomer. [8-14]. Their presence also lowers the oxidation potential of EDOT and, in analogy to polypyrrole [15-17] and to poly(2,2'-bithiophene) [18,19] they are also supposed to improve physical and mechanical properties of the film on the electrode surface. Only few attempts to electrogenerate PEDOT films in aqueous solution in the absence of any surfactants have been reported so far [11, 20,21]. All the relevant reports are actually devoted to define the physico-chemical properties of PEDOT modified electrodes, so that very few works report the use in electroanalytical investigations of electrode systems obtained under such conditions [22-25].

Ascorbic Acid: chemical behaviour

Ascorbic acid (vitamin C) is a water-soluble vitamin and participates in numerous biological events concerning electron transport reactions (hydroxylations, oxidative catabolism of aromaticamino acids). About 10mg of the vitamin per day is necessary to prevent scurvy pain.
Ascorbic Acid (AA) is easily oxidized, especially in neutral or basic solution so that it may be used for its antioxidant properties. In some foods, it is purposely added to attract consumers and to act as an antioxidant to prolong the shelf-life of the commercial products.
However AA has limited stability and may be lost from foods during storage, preparation and cooking. Since the control of food degradation constitutes an important and, luckily, 'on the rise' analytical item in food chemistry, many analytical procedures have been proposed for AA detection in a wide variety of similar matrices [26-28].

In the present paper, the electrocatalytic behaviour of PEDOT-modified electrodes is investigated with respect to detection of AA. As to electrochemical methods, the

main problems related to AA determination with bare electrodes lie in the electrode fouling by oxidation products (figure 2.2) and in the high potential required for AA oxidation [29], so high that interferences are dangerously easy to occur. The electrocatalytic properties of PEDOT can overcome these drawbacks.

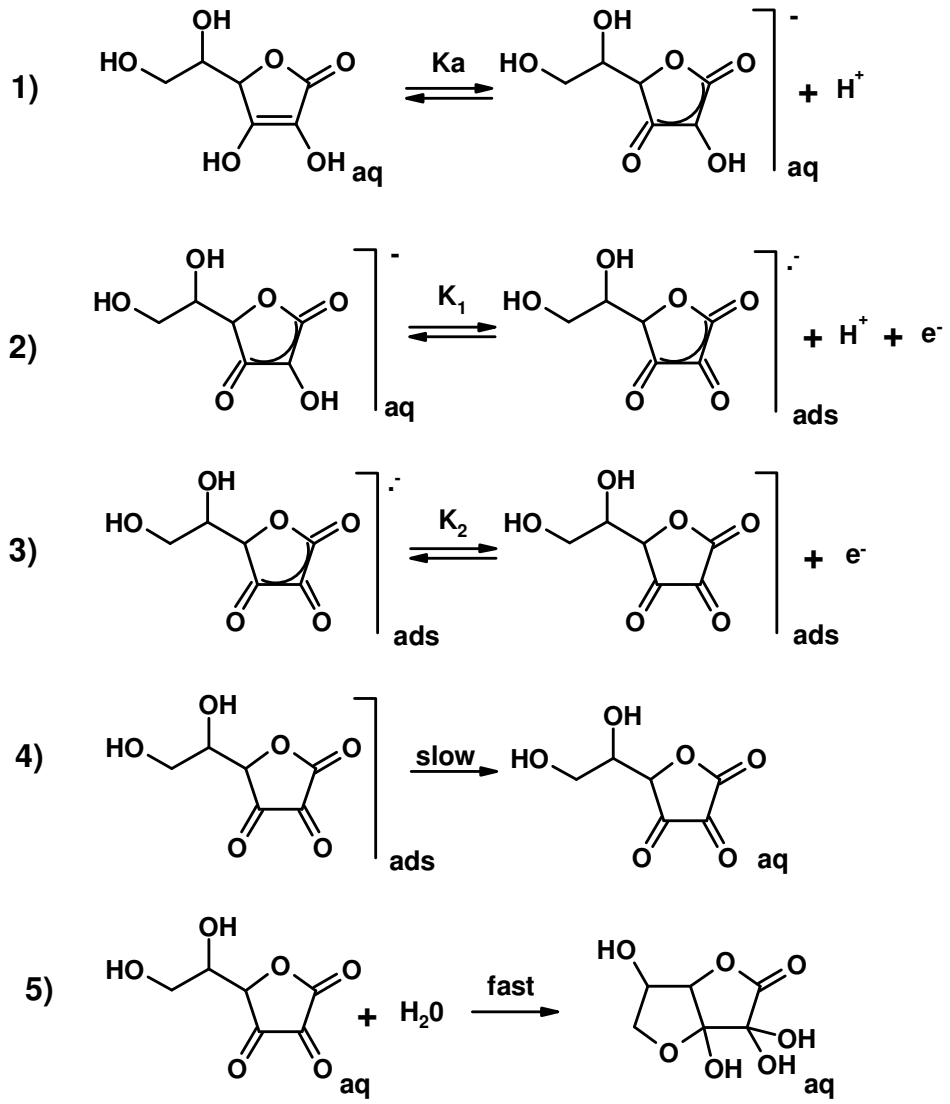

FIGURE2.2 Electrochemical behaviour of AA on platinum bare electrodes

2.2 Results and Discussion

In order to make a first screening of the performances of the different PEDOT-coated electrodes and to select the coating giving best results, we compared the signals obtained with the electrodes modified either in the presence or in the absence of surfactant (NaPSS or NaDBS), under the same experimental conditions, in phosphate buffered solution (see Figure 1). As observed by comparison of the electrochemical signals at a fixed AA concentration (100 ppm), best results, in terms of peak height and sharpness, as well of (low) potential at which the process takes place, are obtained by using pure PEDOT-modified electrode. The effectiveness of PEDOT as redox mediator for AA oxidation can be clearly evidenced by comparison with the voltammograms recorded on bare Pt electrode: the anodic peak ascribable to the oxidation of AA is shifted from + 0.20 V to –0.07 V when PEDOT is employed as redox-mediator. Moreover, the sharpness of the signal indicates a more electrochemically reversible behaviour, with respect to the bare Pt electrode. The more marked electrocatalytic effect observed on doped PEDOT only containing inorganic counterions, with respect to PPS^- or DBS^-, can be ascribed to the acid-base character of AA (pKa = 4.17). At pH=7 the analyte is under anionic form, so that on PEDOT coating the partial localisation of the positive charges on the p-doped polymer surface causes attraction of the anionic species. On the other hand, the presence of anionic surfactants induces a partial shield effect.

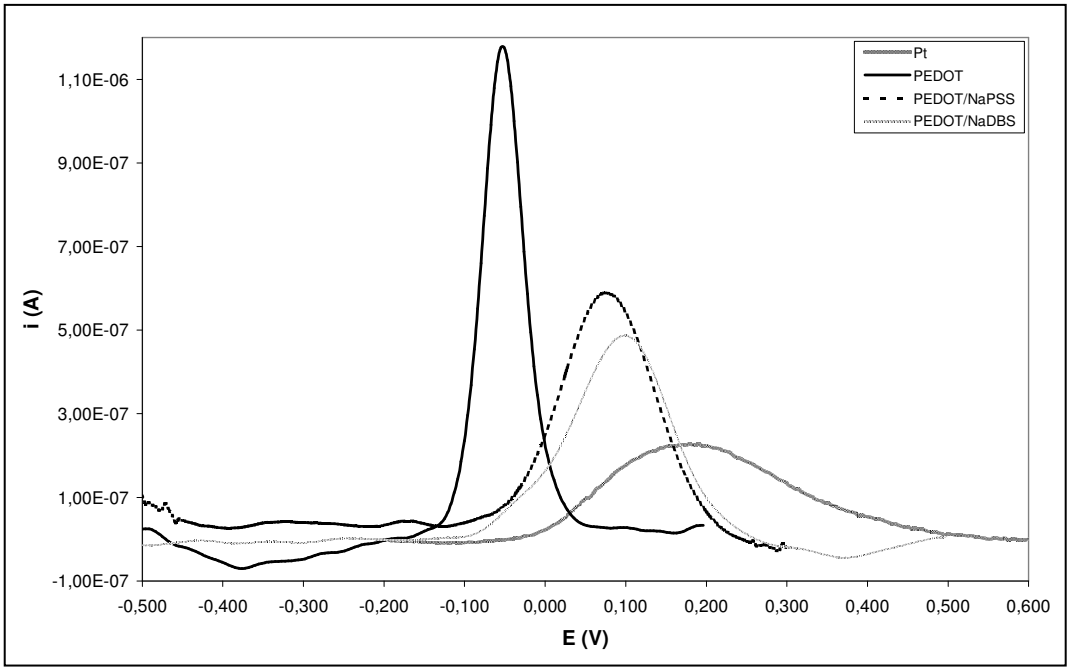

FIGURE 2.3 – Comparison of the responses for 100 ppm AA, 0.1 M phosphate buffer solution (pH 7.0), at different electrodes.

The study was hence focused on pure PEDOT coating.

In phosphate buffer solution (pH=7) PEDOT presents oxidation and reduction peaks located at -0.59V and -0.70V respectively. These data are referred to Ag/AgCl/3M KCl reference system (figure 2.4)

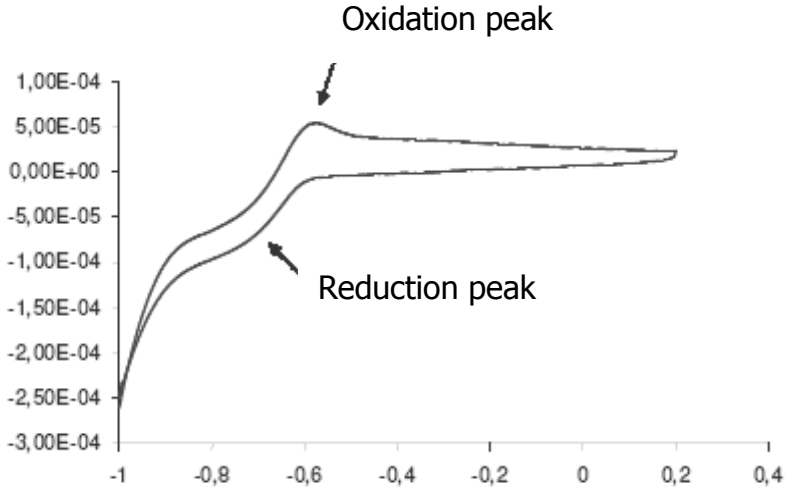

FIGURE 2.4 Cyclic voltammogram acquired for CME (PEDOT) in phosphate buffer

Electropolymerisation has been carried out potentiostatically, in order to better control the thickness of the polymer, based on the charge spent in polymerisation. Three different film thicknesses, corresponding to charge densities of 0.32, 0.64 and 1.28 mC/mm^2 (CME1, CME2 and CME3, respectively) have been tested. The effect of the different values of the parameters of the DPV potential waveform on the peak height have been studied by means of a "3 factors and 3 level" experimental design [30], which allowed us to maximise the ratio between the obtained information and the number of experiments to be performed, in order to optimise the variables influencing the response of the considered system. The optimisation procedure was devoted to maximise sensitivity, evaluated as the peak current value recorded in 100 ppm (pH=7.0) buffered AA aqueous solutions.

Pulse Amplitude (PA), Step Potential (SP, potential increment between two subsequent current measurements) and Pulse Time (PT, time elapsed between the pulse application and the current measurement) have been considered as parameters to optimise (figure 2.5), choosing among the values reported in Table 2.1.

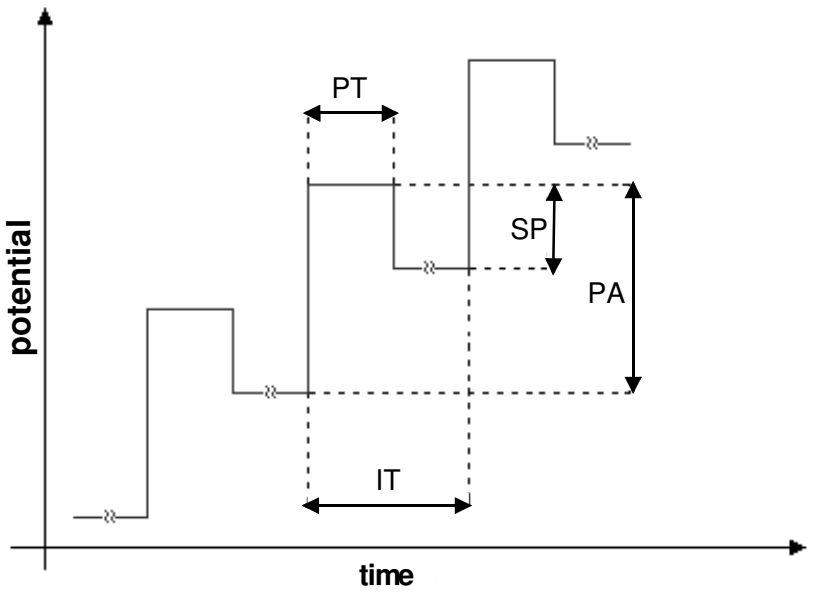

FIGURE 2.5 DPV scan, PT, PA,SP and IT are experimental parameters wave form responsible.

	Low (-1)	Medium (0)	High (+1)
Pulse Amplitude (PA),mV	10	30	50
Step Potentila (SP),mV	2	4	6
Pulse Time (PT), ms	50	100	150

TABLE 2.1. Factors and levels scheduled by the experimental design

The Interval Time (IT, time elapsed between two subsequent pulses) was kept at a constant value of 0.4 s in order to lower the experimental time as much as possible. The parameter values have been chosen in order to *i)* significantly enhance the faradic versus capacitative current; *ii)* limit the polymer degradation; *iii)* achieve reasonable time of analysis.

The studied experimental domain is described by a Face Centred Cube (FCC)[31] and requires 15 different experiments (FIGURE 2.6). In order to avoid influences due to significant, though limited, non-reproducibility of the polymeric coatings on the studied response, the experiments scheduled by the experimental design have been conducted by randomised mode, performing three replicates for each experiment, for a total number of 45 measurements. Moreover, each PEDOT coating has been employed only in three replicates, in order to minimise the effect of film degradation. Such a data collection was carried out for each polymer thickness.

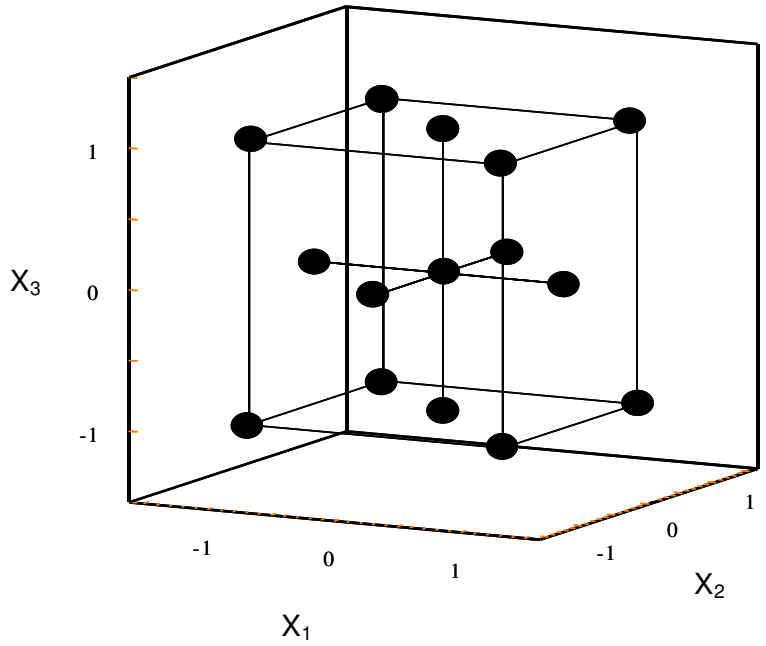

FIGURE 2.6 general scheme of "face centred cube" (fcc) + "zero point" experimental design

The relationship between the peak current and the values of the potential waveform parameters has been investigated by means of Multiple Regression Analysis and the response function (Eq 2.1) for each CME has been calculated taking into account the reciprocal interactions (second and third order):

$$i_p = b_0 + b_1 \cdot PT + b_2 \cdot SP + b_3 \cdot PA + b_4 \cdot PT^2 + b_5 \cdot SP^2 + b_6 \cdot PA^2 + \\ + b_7 \cdot PT \cdot SP + b_8 \cdot PT \cdot PA + b_9 \cdot PA \cdot SP + b_{10} \cdot PT \cdot SP \cdot PA \qquad \text{Eq2.1}$$

Less significant terms have been discarded and a new regression was performed until the *p* values of all coefficients resulted lower than 0.05 [31]. The significance levels of the coefficients corresponding to each parameter have been evaluated.
Figure 2.7 reports the response functions, together with the relevant plots, obtained with the three studied CMEs. Surfaces have been plotted for a SP value of 6 mV, leading to the highest responses.

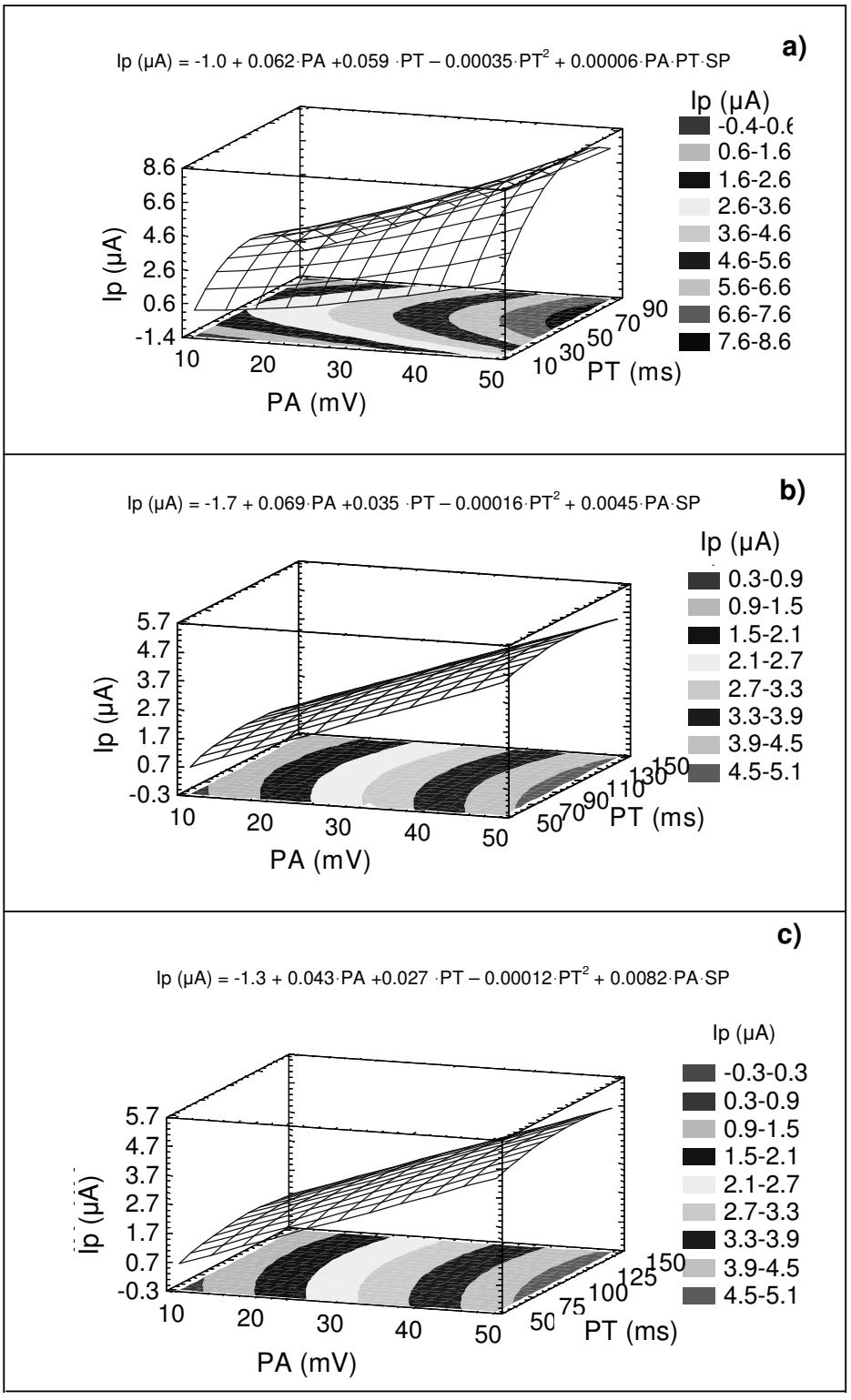

FIGURE 2.7 Response surfaces and relevant functions obtained with CME1(a), CME 2 (b) and CME 3 (c). Surfaces have been plotted for a SP value of 6 mV.

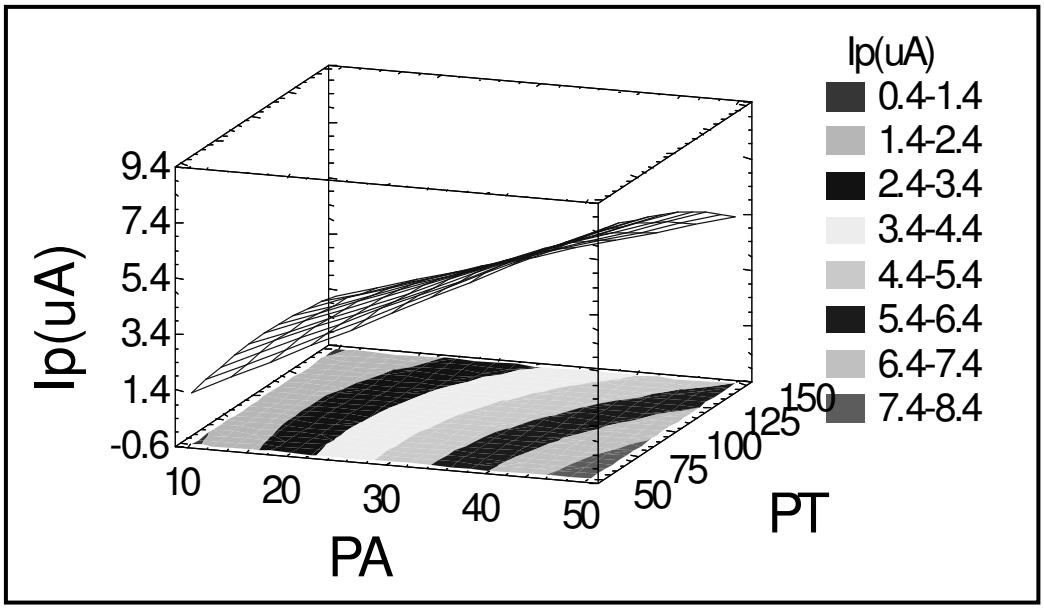

FIGURE 2.8 Response surfaces and relevant functions obtained with unmodified Pt electrodes. Surfaces have been plotted for a SP value of 6 mV. Into the range values of the experimental parameter none absolute maximum of Ip was found.

Coefficients and relevant standard deviations of the response functions are reported in TABLE 2.2. The analysis of the obtained responses demonstrates the significance of the quadratic term for PT: this finding can be explained considering that too low PT values do not allow the "activation" of the electrocatalytic activity, while at too high PT values a consistent drop of the faradic current takes place. The same trend was observed on all CMEs, independently from the thickness of the coating. The response functions also indicate that the highest peak signal is obtained when the maximum PA value is settled, analogously to what happens with conventional bare electrodes, while the SP influence is only noticeable as regards the interaction with PA.

CME	Response Functions
CME1	$-1.0(3) + 6.2(6) \cdot 10^{-2} \cdot PA + 5.9(6) \cdot 10^{-2} \cdot PT - 3.5(4) \cdot 10^{-4} \cdot PT^2 + 6(1) \cdot 10^{-5} \cdot PA \cdot PT \cdot SP$
CME2	$-1.7(2) + 6.9(3) \cdot 10^{-2} \cdot PA + 3.5(5) \cdot 10^{-2} \cdot PT - 1.6(2) \cdot 10^{-4} \cdot PT^2 + 4.5(6) \cdot 10^{-3} \cdot PA \cdot SP$
CME3	$-1.3(4) + 4.3(4) \cdot 10^{-2} \cdot PA + 2.7(8) \cdot 10^{-2} \cdot PT - 1.2(4) \cdot 10^{-4} \cdot PT^2 + 8.2(8) \cdot 10^{-3} \cdot PA \cdot SP$

TABLE 2.2 Response functions obtained on the different CMEs. In parentheses standard deviations, referred to the less significant digit of the coefficient.

By differentiating the obtained function of each CME, optimal values of PT have been calculated, leading to maximum value for the peak current. As observed in Table 2.3, which reports the optimised waveform parameters for each tested CME, no significant differences have been recorded for the different CMEs. On the contrary, a significant different behaviour is observed by passing from bare Pt to modified electrodes.

	Polymerization Charge Density (mC/mm^2)	PA (mV)	PT (ms)	SP (mV)
Unmodified Pt	-	50	50	6
CME1	10	50	108	6
CME2	2	50	109	6
CME£	50	50	115	6

TABLE2.3. Optimized scan parameters (corresponding to the maximum of Ip for a solution of 100 ppm AA buffered at pH = 7) for Pt unmodified electrode and for each modified electrode.

In order to test the stability of the coatings and the reproducibility of the deposition procedure, 3 coatings have been deposited for each of the 3 CME typologies, i.e. thicknesses. 21 replicate DPV scans (AA concentration = 100 ppm, pH = 7.0, optimised waveform parameters) have been carried out on each of them (3 X 3 X 21 = 201 total scans). In order to simulate the experimental conditions of a calibration with seven concentration levels and three replicates for each concentration, the 21

replicate scans on each film have been subdivided into seven groups of three scans. A 2 ways-ANOVA has been performed on the signals obtained in the above-described experiments, for each CME typology, considering the polymerisation reproducibility (3 depositions, "*Polymer effect*") and the stability of the coatings (7 groups of 3 replicates, "*Replicate effect*") as factors. Table 4 shows the results of the ANOVA procedure, for each typology of CME.

The "*polymer effect*" did not result to be significant (p>0.05), so that the deposition procedures can be regarded as reproducible, while the "*replicate effect*" resulted to be significant at all explored thickness values. In particular, as indicated by post hoc Bonferroni tests [32], the first 2 groups of three scans (6 replicate measurements) resulted not significantly different for CME 1, while the number of groups that were found to be not significantly different from one another raised to 3 (9 replicate measurements) and 4 (12 replicate measurements) for CME2 and CME 3, respectively. It can be concluded that the stability increases with the thickness of the polymer deposit.

The performance of each CME in quantitative analysis of AA has been studied in order to calculate proper calibration functions. The calibrations have been carried out by addition of freshly prepared standard solutions of AA to aqueous solutions buffered at pH = 7.0. Two different concentration ranges have been explored, i.e. 5-35 ppm (7 concentration levels and 3 replicates for each level) and 35-200 ppm (8 concentration levels and 3 replicates for each level). Each polymeric coating was employed for a number of scans as suggested by the results of ANOVA procedure, i.e. each concentration range has been explored by using different coatings. After checking the data for normality and homoscedasticity, two different interpolations have been carried out for the two ranges. Calibration plots obtained with CME2 are reported in FIGURE 2.9, as an example.

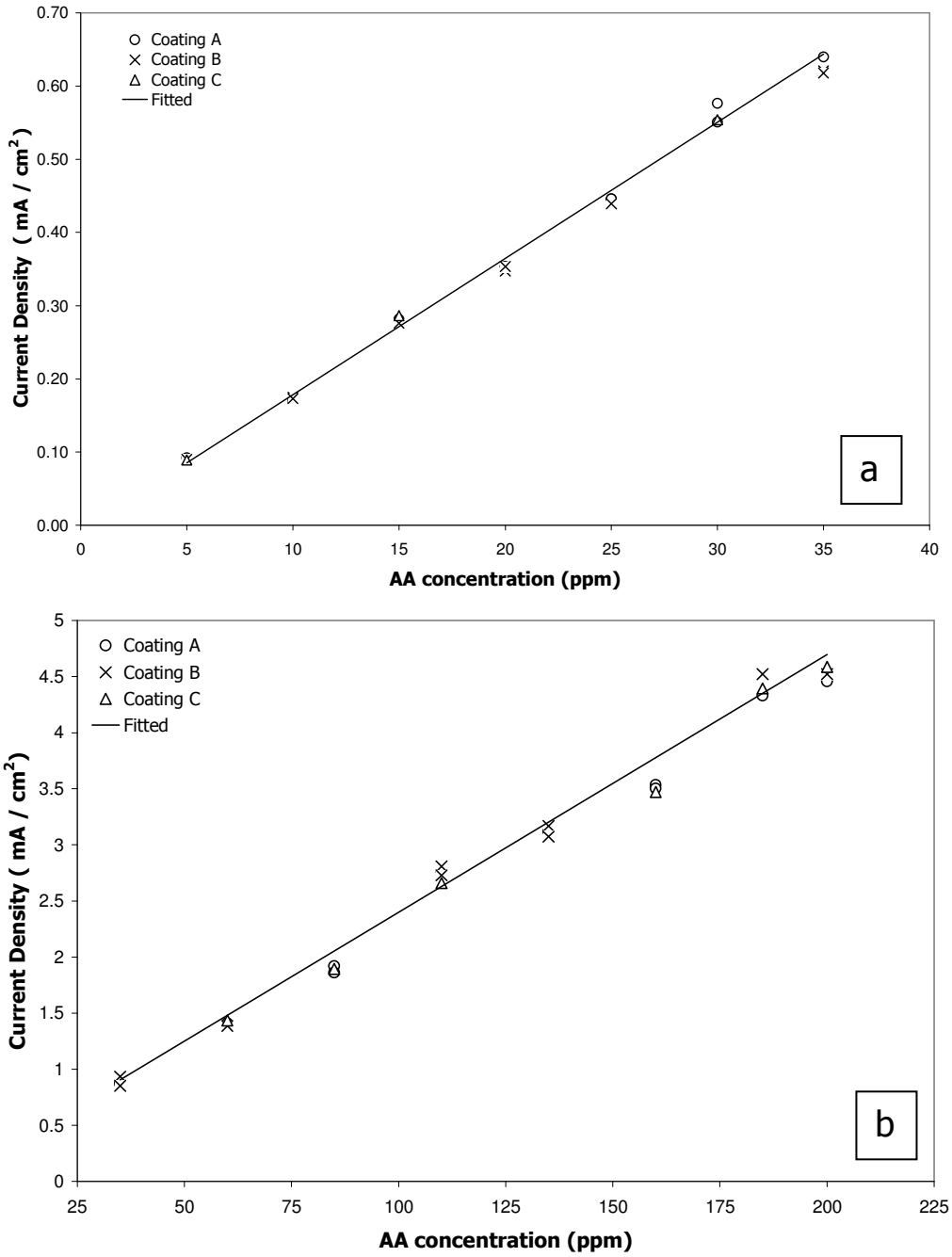

FIGURE 2.9: Calibration plots obtained with CME 2 in the 5-35 pmm (a) and 35-200 ppm (b) ranges. Signals obtained with three different coatings of the same typology are indicated with different symbols**.**

The regression functions relative to the lower concentration range were suited for calculation of the Limit of Detection (LOD) .The response of eachtypology of CME for AA has been studied by DPV under the optimised conditions and showed good

performance in terms of sensitivity and LOD, as shown by the data reported in Table 5. The best results in terms of LOD, have been obtained for CME2: the LOD value calculated by regression function (1.85 ppm) resulted remarkably lower with respect to that (7.0 ppm) obtained with the bare Pt electrode under the same experimental conditions.

Two-way ANOVA (thickness, concentration and their interactions) has been performed with the aim of testing any differences in sensitivity for the three CMEs. Neither thickness nor its interaction with concentration resulted to be significant classification factors, so that no difference in sensitivity could be detected at varying the thickness. However, the calibration carried out with CME2 showed a significantly lower residual variance ($p<0.05$), resulting in a lower LOD than for CME1 and CME3 (see Table 5)

The sensitivity obtained with bare Pt electrode results about three-times lower with respect to that obtained with CMEs, supporting the electrocatalytic ability of PEDOT with respect to AA oxidation.

Finally, further measurements carried out at pH = 4.7 [33], both on modified and on bare Pt electrodes, indicated that the anodic signal of AA is detectable at higher reproducibility level on unmodified Pt electrode, due to reduced passivation of the electrode surface in acidic media. Nevertheless, the LOD value computed (3.51 ppm) was still higher with respect to that obtained on CME2 at pH = 7.0. A reasonable explanation to the worse result (LOD = 7.47 ppm) obtained on CMEs at acid pH values lies in the reduced electrostatic attraction between the charged polymer and the protonated AA species.

2.2 Conclusions

PEDOT has revealed as a CP suitable for realization of CMEs active in redox mediation. Analytical performances of the CMEs are strictly dependent from the charge density of the polymerization process and from the wave form of the DPV scan. Moreover the pH of buffered solution is also important parameter for AA determination.

The cheapness of the monomer (EDOT) allows the realization of "disposable" electrodes whit good potentialities for determination of AA concentration in food samples (fruit juices, preserved foods etc.)

2.3 Experimental

Reagents and general procedures

All commercially available chemicals and reagents were purchased from Aldrich as analytical grade reagents and used without further purification.

Polymeric film depositions and voltammetric measurements have been carried out by using an Autolab PGSTAT 20 computerised electrochemical instrument, controlled by dedicated GPES software (Ecochemie, Utrecht, The Netherlands). A 2 mm diameter Pt disk electrode has been used as working electrode, while a Glassy Carbon rod and an Ag/AgCl/3M KCl, water solvent, have been used as counter and reference electrode, respectively.

Eletropolymerizations procedures

The modification of Pt disk electrodes has been carried out by potentiostatic electropolymerisation of 3,4-ethylenedioxythiophene (EDOT), at a potential of +0.9 V, by controlling the amount of charge spent, in aqueous solutions containing 0.01 M monomer and 0.1M $LiClO_4$ supporting electrolyte; 0.1M poly(sodium-4-styrenesulphonate) (NaPSS) or dodecylbenzenesulphonic acid sodium salt (NaDBS) were added, as surfactants, when specified.

After the electrosynthesis process, the polymer deposit has been firstly reduced, at -0.5 V for 60 s, in the same electrolysis solution, and subsequently stabilised by cyclic voltammetry (10 subsequent potential scans from –0.5 to +0.5 V, at a potential scan rate of 0.05 V s^{-1}) in phosphate or acetate buffer solution.

L-ascorbic acid quantitation

Standard aqueous solutions of AA (L-Ascorbic Acid, 99+%) have been buffered at pH = 7.00 with NaH_2PO_4/ Na_2HPO_4, 0.1M concentration, or at pH = 4.75 with 0.1M acetic acid / sodium acetate.

The response of the CMEs with respect to AA was studied by Differential Pulse Voltammetry, by using different values for the time and potential parameters defining the waveform, in order to seek for the set of values leading to best results.

The multiple regression analysis for the response functions of the experimental design as well all other calculations, have been performed by SPSS 13.0 software (SPSS Inc. Chicago, Illinois).

2.5 References

1. A. Malinauskas, *Synth. Met.*, **1999**, 107, 75. M. Petersson, *Anal. Chim. Acta*, **1986**, 187, 333.
3. M.C.Morvant, J.R.Reynolds, *Synth. Met*. **1998**, 92, 57; M. Łapkowski, A. Proń, Synth. Met. **2000**, 110, 79.
4. M. Dietrich, J. Heinze, G. Heywang, F. Jonas, *J. Electroanal. Chem*, **1994**, 369, 87.
5. H. Yamato, M. Ohwa, W. Wernet, *J. Electroanal. Chem*, **1995**, 397, 163.
6. H. Randriamahazaka, V. Noël, C. Chevrot, *J. Electroanal. Chem,* **1999**, 472, 103.
7. H.JAhonen, J.Lukkari, J.Kankare, *Macromol.* **2000** , 33, 6787N. Sakmeche, J.J.Aaron, M.Fall, S. Aeiyach, M. Jouini, J.C.Lacroix, P.C.Lacze, *Chem. Commun*. **1996**, 2723.
9. T. El. Moustafid, R. V. Gregory, K. R. Brenneman, P. M. Lessner, *Synth. Met.* **2003,** 435, 135.
10. N. Sakmeche, S. Aeiyach, J. J. Aaron, M. Jouini, J. C. Lacroix, P.C. Lacaze, *Langmuir,* **1999**, 15, 2566.
11. J. Bobacka, A. Lewenstam, A. Ivaska, *J. Electroanal. Chem*. **2000**, 489, 17.
12. N. Sakmeche, E. A. Bazzaoui, M. Fall, S. Aeiyach, M. Jouini, J. C. Lacroix, J. J. Aaron, P.C. Lacaze, *Synth. Met*. **1997**, 84, 191.
13. A.Lima, P. Shottland, S. Sadki, C. Chevrot, *Synth. Met*. **1998**, 93, 33
14. H. Yamato, M. Ohwa, W. Wernet, *J. Electroanal. Chem*, **1995**, 397, 163.
15. M. A. De Paoli, S. Panero, P. Prosperi, B. Scrosati, *Electrochim. Acta*, **1990**, 35, 145.
16. G. E. Barr, C. N. Sayre, D. M. Connor, D. M. Collard, *Langmuir*, **1996,** 12, 1395
17. H.K. Naoi, Y. Oura, M. Maeda, S. Nakamura, *J. Elecrochem. Soc.*, **1995**, 142, 417.
18. E.A. Bazzaoui, S. Aeiyach, P.C. Lacaze, *Synth. Met*. **1996**, 83, 159.

19. N. Sakmeche, E. A. Bazzaoui, M. Fall, S. Aeiyach, M. Jouini, J. C. Lacroix, J. J. Aaron, P.C. Lacaze, *Synth. Met*. **1997**, 84, 191.
20. H. J. Ahonen, J. Lukkari, T. Hellström, J. Mattila, J. Kankare, *Synth. Met.,* **2001**, 119, 119.
21. X. Du, Z. Wang, *Electrochim. Acta,* **2003**, 48,1713; L. Pigani, A. Heras, A. Colina, R. Seeber, J. López-Palcios*, Electrochem. Commun*. **2004**, 6, 1192.
22. S. Biallozor, A. Kupniewska, *Electrochem. Commun*. **2000**, 2, 480.
23. A. Heras, S. Lupu, L. Pigani, C. Pirvu, R. Seeber, F. Terzi, C. Zanardi, *Electrochim. Acta* **2005**, 50, 1685.
24. P. Manisankar, S. Viswanathan, A. Mercy, Pusphalatha, C. Rani, *Anal. Chim. Acta*, **2005**, 528,157.
25. W.-M. Yeh K.-C. Ho, *Anal. Chim. Acta*, **2005**, 542, 76.
26. S. P. Arya, M. Mahajan, P. Jain, *Anal. Sci*. **1998**,14, 889.
27. S. P. Arya, M. Mahajan, P. Jain, *Anal. Chim. Acta*, **2000**, 417,1.
28. M. C. Yebre-Biurrun, *Talanta* **2000**, 52, 367.
29. P. Karabinas, D. Jannakoudakis, *J. Electroanal. Chem.*, **1984**, 160, 159.
30. J.L. Goupy, *Methods for Experimental Design*, Elsevier, Amsterdam, **1993.**
31. M. Careri, A. Mangia, G. Mori, M. Musci, *Anal. Chim. Acta*, **1999**, 386,169.
32. D.L. Massart, B.G.M. Vandeginste, L.M.C. Buydens, S. De Jong, P.J. Lewi and J.P. Smeyers-Verbeke, *Handbook of Chemometrics and Qualimetrics: Part A*, Elsevier, Amsterdam (**1997**) pp. 100-102 (Chapter 5).
33. P. Rani Roy, M. Sudan Saha, T. Okajima, T. Ohsaka*, Electrooxidation and Electroanalysis,* **2004**, 16, 289.

3. New Membrane Electrodes Based on a Functionalized Tetraphenylborate Covalently Bound to the Polymeric Backbone

3.1 Intrduction

Liquid membrane Ion Selective Electrodes (ISEs) provide a fast, cheap and relatively versatile analytical approach to samples of environmental, clinical and food processing interest. ISEs can be used very rapidly and easily, under favourable conditions, when measuring ions in relatively dilute aqueous solutions [1,2]. Furthermore, they are unaffected by sample colour or turbidity and are suitable for on-line continuous analysis. In the last decades the mistrust of analysts with respect to such devices was almost completely overcome thanks to the advances achieved in the field of materials and ionophores employed for realization of the membranes, leading to a dramatic increase of the commercial diffusion of ISEs.[3,4] Conversely, some limit of potentiometric sensors does persist, like relatively short lifetime of the membrane.

Performance of ISE is in fact strongly affected by leaching phenomena of the ionic exchanger and the ionophore from the membrane. Ionic fluxes occurring across the membrane also affect the performance of the sensor in terms of lower detection limit.[5,6] Several strategies have been tested to limit such phenomena: different researchers reported about ISEs based on ionophores covalently bound to the membrane polymeric matrix, with the aim to reduce ion fluxes [7-9]. Much lower attention has been paid to the improvement of the lifetime. Moreover, a negative effects on the selectivity was sometimes observed as consequence of the immobilization of the active components on the membrane matrix by covalent linking. A considerable amount of studies have been also conducted about innovative materials for realization of the membranes: in 1997 Kim et al [10] reported about new chloride-selective electrodes based on membranes prepared by Sol-Gel method. This approach evidenced that the experimental conditions under

which the gelation of the starting siloxanes is carried out (acid catalysis and high temperatures) often are incompatible with the ionophores, that undergo chemical decomposition.

The use of acrylonitrile-butadiene copolymers**,** also known with the commercial name KRYNAC®, was proposed by Ebdon and co-workers [11,12], that reported about realization of nitrate selective electrodes based on tetraalkylammonium exchanger units bound to the copolymer by means of radicalic linking.

In this paper is reported the realization of new membrane ISEs with limited leaching of the lypophilic ionic exchanger. For this purpose KRYNAC® was employed as membrane matrix, in order to suit its reactivity for the linking of properly designed and synthesized tetraphenylborates, derivatized with allylic functionalities. The study involved the synthesis of the suitable tetraphenylborate, the radicalic linking of the exchanger to the polymeric matrix and the potentiometric characterization of the functionalized membranes.

3.2 Results and discussions

Tetraphenylborates and their derivatives are the typical ion exchangers for cation-Selective Electrodes. Their chemical stability and analytical performances are influenced by the functional groups present on the aromatic rings [13].

In order to obtain membranes with reduced leaching of ionic exchanger we projected a new tetraphenylborate derivative carrying allylic functionalities, suitable for the linking to the acrylonitrile-butadiene polymeric matrix.

The linking reaction takes place by radicalic mechanism and is promoted by dicumyl peroxide (DCP) as a starter. Scheme 1 shows two possible mechanisms [14] for the radicalic functionalization of the polymeric network with a generic derivatizing unit carrying the allylic functionality.

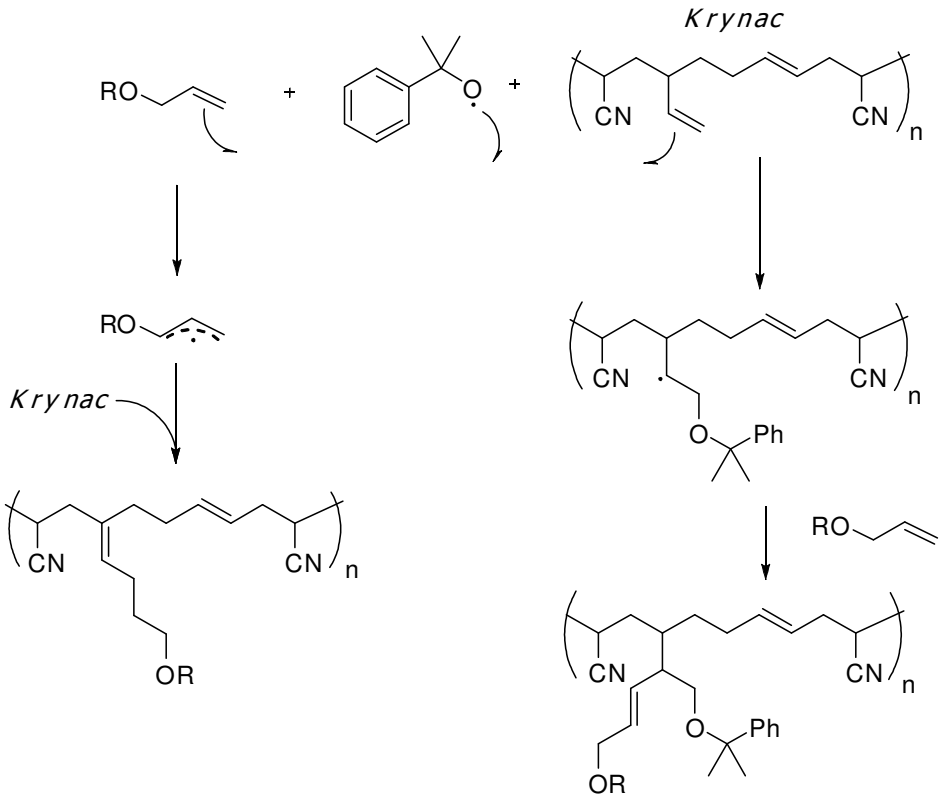

FIGURE 3.1. Possible mechanisms for the radicalic fictionalization of polymeric network with a generic derivatising unit carrying one allyl-functionality

Since direct functionalization of tetraphenylborates it is not possible, the direct sythesis of functionalised tetraphenylborate had to be performed. 1-allyloxy-4-bromobenzene was chosen as starting molecule for the synthetic pathway. For the synthesis of the tetrasubstituted derivative, 1-allyloxy-4-bromobenzene was converted in to the respective Grignard reagent, that was subsequently reacted with boron trifluoride. After the formation of the new tetraphenylborate ion, the counterion can be chosen and inserted during the treatment of the reaction crude, using a solution of the proper alkali-metal carbonate for the quenching, in order to obtain tetrakis[(4-allyloxy)phenyl]borate salts. (Figure 3.2).

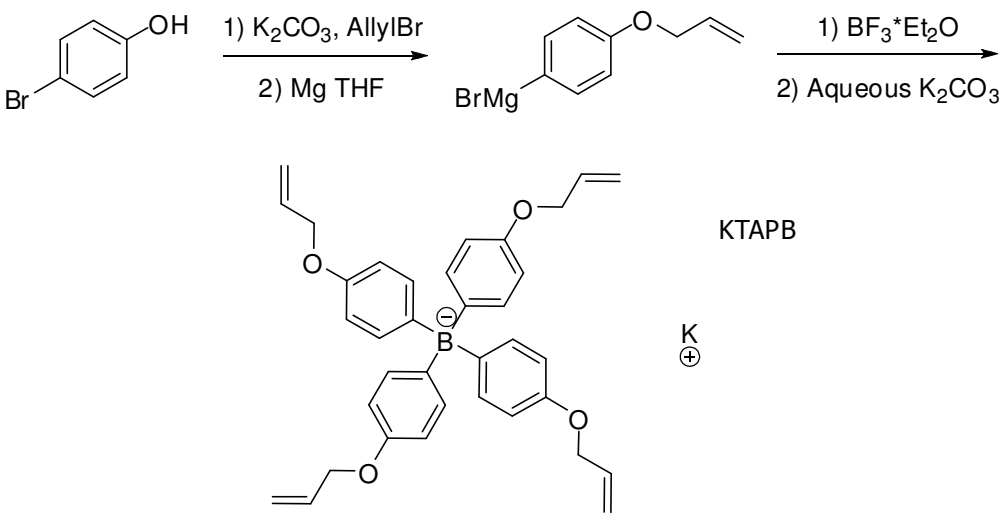

FIGURE 3.2 Synthetic pathway for the preparation of the tetrafunctionalized derivative potassium tetrakis[(4-allyloxy)phenyl]borate (KTAPB)

Both sodium and potassium salts were prepared, but conductivity measurements in THF solution of sodium salt evidenced the formation of a strong ion pair. Then such salt it is unsuitable as an ionic exchanger. Analogous experiments carried out with potassium tetrakis[(4-allyloxy)phenyl]borate (KTAPB) did not evidence formation of ion pairs, as confirmed by good results obtained through potentiometric

measurements carried out with membranes containing the still unbound potassium salt.

The experimental procedure for the synthesis of the potassium salt reached a 40% yield, expressed as purified product. Potassium tetrakis[(4-allyloxy)phenyl]borate was fully characterized by means of ESI-MS, ^{1}H NMR, UV-VIS, FT-IR..

The procedure suggested by literature [11,12] for linking of the tetraphenylborate derivatives to the polymeric network, consisted in pressing the membranes at high temperature. This method, as we verified, presents however difficulties due to formation of bubbles encapsulated in the polymeric matrix that can be limited varying gradually the temperature of the press, but the so treated membranes often resulted sticky. Better outcomes were obtained using a 1:1 mixture of Krynac® and PVC as polymeric matrix, but the hot pressing procedure was not suitable for membranes containing ionophores, because these undergo thermal decomposition. A new procedure for the linking of the ionic exchanger was then set up: the radicalic linking reaction was carried out in dry THF solution, before casting the membrane. For this purpose the THF solution containing Krynac®, the catalyst (dicumylperoxyde, DCP) and the derivatized tetraphenylborate was stirred under reflux for 8 hours while PVC, plasticizer solvent and ionophore were added after cooling down the starting solution. After removing the THF excess by a nitrogen stream, the membrane cocktail was normally cast on glass rings, so obtaining membrane with suitable mechanic characteristics.

In order to evaluate the effectiveness of the linking reaction of KTAPB, dynamic extraction experiments were carried out under conditions of continuous high flows. Krynac/PVC membranes with bound KTAPB showed a leaching of 13% of the original amount of the tetraphenylborate, while when analogous experiments were carried out with PVC membranes containing unbound KTAPB the leaching extent raised to 28%. In order to obtain more detailed information about the leaching of KTAPB simply dissolved or grafted on the polymeric matrix, further extraction experiments were carried out. These measurements were conducted with materials different with respect to those employed for the preparation of the membranes, in order to obtain information about the effectiveness of the leaching unbiased by other factors. For

this purpose, the extent of the KTAPB leaching was compared for two Krynac/PVC membranes without plasticizer solvent, containing the same amount (%) of the functionalized tetraphenylborate simply dissolved (Membrane A) or linked before the membrane casting by stirring a mixture of Krynac®, PVC, DCP and KATPB in THF under reflux for 8 hours (Membrane B). After casting and THF evaporation the membranes were subjected to extraction with deionised water carried out under the same experimental conditions reported for the above discussed analogous experiments. In order to avoid data biasing ascribable to decomposition of KTAPB, the evaluation of the extent of leached tetraphenylborate was performed by determination of total boron by ICP-MS in the aqueous solutions resulting from the extraction. The results of these experiments showed that Membrane A leached the 4.7±0.3 % of the total amount of dissolved KTPAB, while the leaching extent for Membrane B decreased to 1,4±0.1 %, so evidencing a significantly lower release of the linked tetraphenylborate with respect to the same salt simply dispersed in the same matrix. A second extraction was carried out on the membranes recovered from the first treatment, but no further leaching was noticed for both membranes.

The behaviour of the new derivatized membranes was studied and compared with the response of the membranes containing unbound KTAPB and commercially available potassium tetrakis(4-chlorophenylborate) (KTpClPB) by potentiometric characterization of two electrodes for each of six typologies. Particularly, the comparative study was carried out on ISEs containing: *i)* KTAPB bound to the polymeric network, with and without valinomycin as potassium-selective ionophore (ISEs 1 and 2), *ii)* KTAPB not bound to the polymeric network, with and without ionophore (ISEs 3 and 4), *iii)* commercially available potassium tetrakis(4-chlorophenylborate) (KTpClPB), with and without ionophore (ISEs 5 and 6). The composition of the studied membranes is reported in table 3.1.

Component	***ISE1***	***ISE2***	***ISE3***	***ISE4***	***ISE5***	***ISE6***
Ion Exchanger	KTAPB (1.5%)	KTAPB (1.5%)	KTAPB (1.5%)	KTAPB (1.5%)	KTpClPB (1.5%)	KTpClPB (1.5%)
Ionophore (Valinomycin)	7.5 %	-	7.5%	-	7,5%	-
Polymeric Matrix (Krynac/PVC 1:1)	70 %	74%	73%	80%	73%	79%
Plasticizer DOS	17.5%	19.7%	18%	18.5%	18%	19.5%
DCP	3.5%	3.8%	-	-	-	-

TABLE 3.1 Composition of the membranes employed for the preparation of the studied ISEs

The performance of the electrodes was monitored for 37 days, recording 9 calibration curves with K^+ ions over the ageing time .

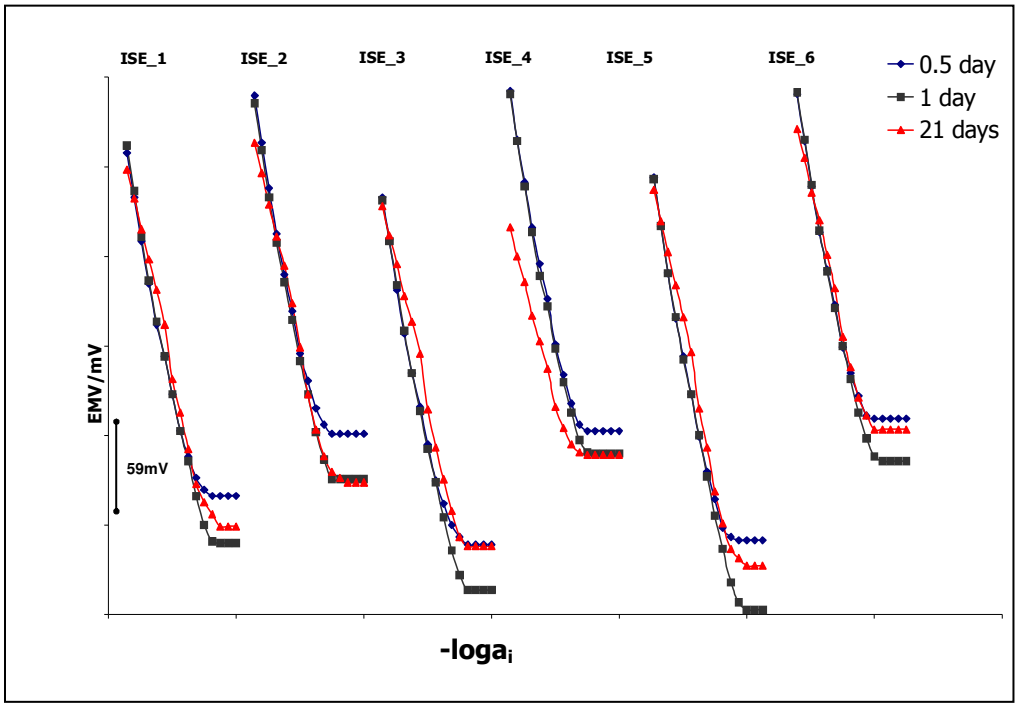

FIGURE 3.3 Calibration curves recorded for each ISE typology after different aging times (0.5 day, 1 day and 21 days).

EMF measurements were carried out increasing KCl concentration, ranging from 10^{-8}M to 10^{-1}M.

K^+ over Na^+ selectivity measurements were also carried out with freshly prepared ISEs, showing a not significant (*p>0.05*) effect of the binding of the ionic exchanger on the selectivity of the ionophore. Selectivity measurements were carried out by separate solution method (calibration ranging from 10^{-8}M to 10^{-1}M) and selectivity coefficient $K_{K,Na}$ was calculated according to Jupac recommendations (pKsel K/Na = 3.84±0.07 for ISE 1)

LDL (Lower Detection Limit) and sensitivity were calculated according to Jupac recommendations (slope of the calibration line were determined in concentration range comprised between 10^{-4}M and 10^{-1}M KCl)

The comparison of the performance of the electrodes, evaluated in terms of LDL and sensitivity (Slope of the calibration line) over the time, was carried out by means of 2-ways Analysis of Variance (ANOVA) with interactions, the two classification factors being *i*) the ISE typology and *ii*) the ageing time.

Two ways ANOVA showed that the ageing time was a significant classification factor on the LDL due to the initial improvement of the performance (conditioning effect) as well as the ISE typology . The interaction effect between the factors resulted also significant. (*p<0.01*) mainly due to the different conditioning effect of the three typologies of the electrodes.

Although the presence of the valinomycin resulted to be the main effect influencing the LDL values of the ISEs, the *Bonferroni's* post-hoc test evidenced a significant difference between the responses of ISEs 1 and 3, containing the ionophore and bound and unbound KTAPB, respectively. The trend lines of LDL versus time, shown in figure 1, evidence better performance of the ISE based on bound KTAPB and valinomycin, with respect to the parent electrode containing unbound KTAPB.

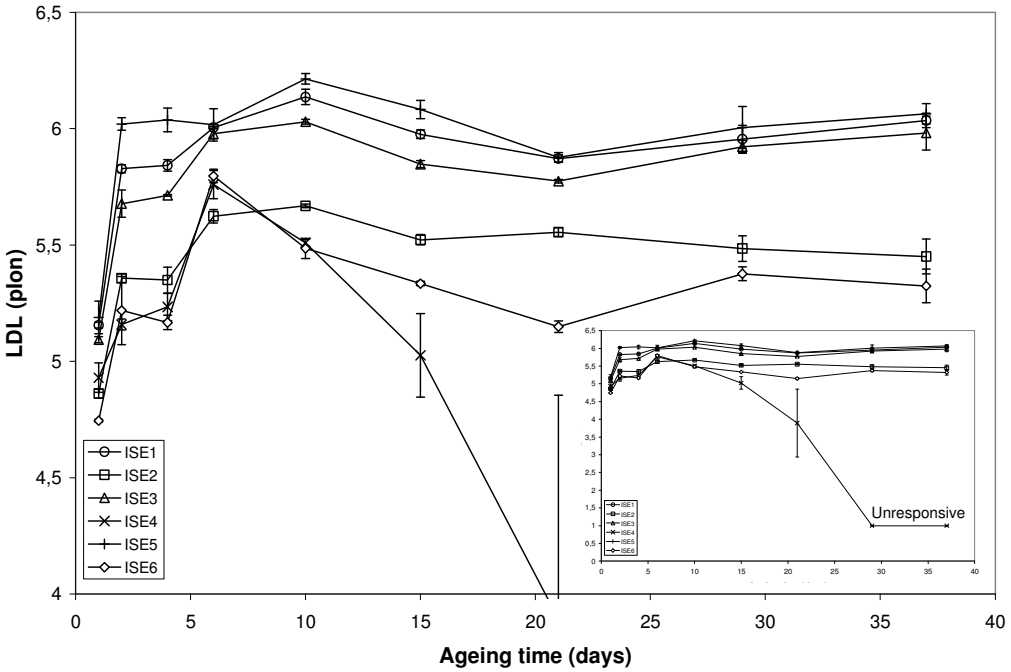

FIGURE 3.4 Trend of LDL recorded over the time for the studied ISEs. Values are expressed as mean and standard deviation of two ISEs for each typology.

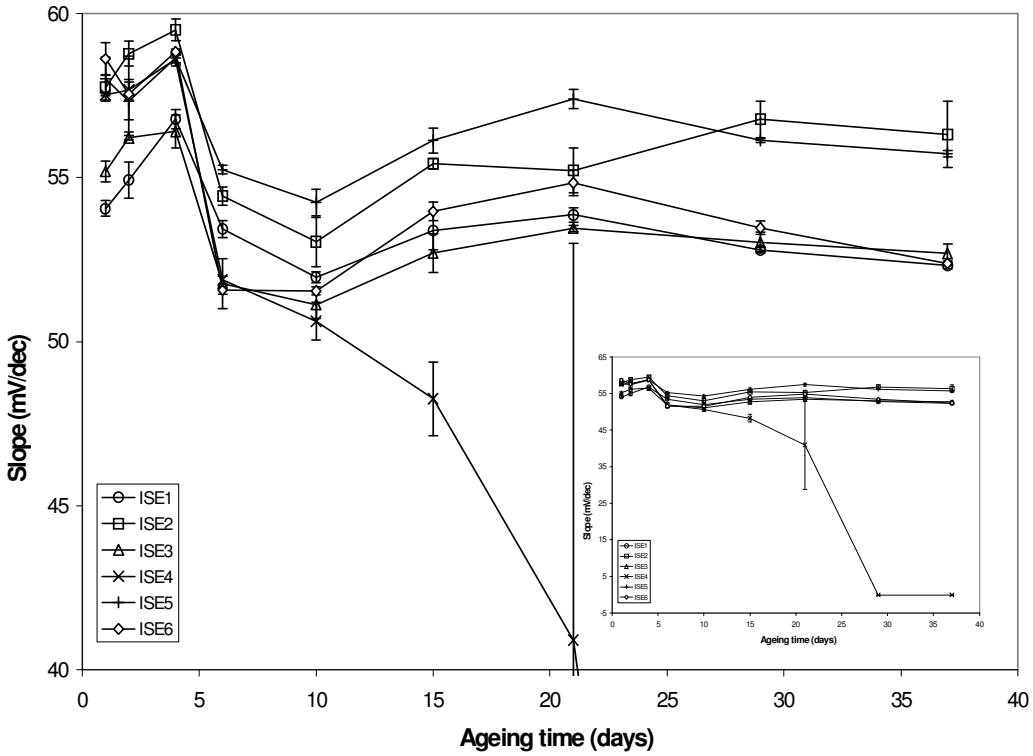

FIGURE 3.5 Trend of LDL recorded over the time for the studied ISEs. Values are expressed as mean and standard deviation of two ISEs for each typology

On the other hand, the presence of valinomycin in the membranes reduces the effect of binding the exchanger, improving the performance of all the ISEs and leading to comparable performance of ISEs 1 and 5. Moreover ISE 2 does show a much more constant performance than ISE 6 whose LDL apparently worsens with time.

The ANOVA applied to the slope values, ranging from 50 to 58 mV/dec did not result in significant effects, apart of a not significant positive correlation with the LDLs (p=0.08).

A crucial aspect that has to be discussed is the behaviour of the membranes containing the new functionalized tetraphenylborate not bound to the polymeric network (ISE 4): ageing experiments showed a dramatic worsening of the performance of the electrodes based on such membranes, that became unresponsive after about 25 days. This datum is probably due to the low chemical stability of KTAPB in membrane but, on the other hand, do confirm the effectiveness of the linking of KTAPB to the polymeric matrix.

3.3 Conclusions

A new tetraphenylborate ion exchanger functionalized with allylic moieties, synthesized and linked to a copolymer acrylonitrile-butadiene, provided ISEs with interesting performances and lifetimes. Reduced leaching of the ion exchanger was demonstrated by means of dynamic extraction experiments simulating the continuous monitoring of high flows, while ANOVA confirmed the better performances of the new ISEs, with respect to membrane electrodes with unbound lipophylic exchangers. The obtained results are encouraging for the perspective aimed to extend the study to the synthesis of other linkable exchangers carrying activating functional groups, like trifluoromethyl units

3.4 Experimental

Reagents and general procedures

Reagents were purchased from Aldrich (Milan, Italy) and used without further purification. The starting reagent 1-allyloxy-4-bromobenzene was prepared according to literature procedure. The syntheses of the tetraphenylborate derivatives were conducted under nitrogen atmosphere, using dried glassware. UV-VIS measurements were performed using a Perkin Elmer Lambda 25 spectropohotometer, FT-IR spectra were recorded with a Thermo Nicolet Nexus line spectrophotometer.

Synthesis of potassium tetrakis[(4-allyloxy)phenyl]borate (KTAPB)

A suspension of Mg (0.8 g, 0.033 mol) in dry THF (5 ml) was stirred in a three-necked round bottomed flask, equipped with a refrigerant, the nitrogen inlet and a dropping funnel. The mixture was heated until reflux and a solution of 1-allyloxy-4-bromobenzene (7 g, 0.033 mol) in 12,5 ml of THF was added drop by drop. When the reaction started, the mixture was cooled and kept at room temperature by refrigeration. The complete Mg consumption, occurred after 30 minutes, was evidence of the formation of the Grignard reagent. 1,54 ml of a 48% solution of BF_3 in ethylic ether (1,741 g, 0,006 mol) were carefully added to the Grignard solution from the dropping funnel. (CAUTION!). The stirred reaction mixture was then refluxed for 12 h.

The reaction crude was evaporated to dryness under reduced pressure and the residue oil was taken up with ethyl acetate and saturated aqueous solution of K_2CO_3. The separated organic phase was dried over solid K_2CO_3 and evaporated to dryness under reduced pressure. Purification of the residue by precipitation from cold ethylic ether afforded 1,3 g of KTAPB (40%) as a white solid.

^{1}H NMR (300 MHz, DMSO *d_6*) δ: 4,5 (dt, 2H), 5,25-5,29 (dd, 1H), 5,37-5,44 (dd, 1H), 5,99-6,12 (m, 1H), 6,99 (d, 2H), 7,52 (d, 2H). ESI-MS(-) *m/z*: 543 [M^-].

UV-VIS and FT-IR .

Membranes

The membranes were prepared according to the different procedures reported in the results and discussion section. The composition of the studied membranes is reported in table 1. Linking procedure performed after the membrane casting was carried out by dissolving membrane components in THF, pouring the cocktail into glass rings, allowing the THF to evaporate and finally pressing (100kPa) the resulting membrane between two hot (100°C) steel plates for 10 minutes. Conversely, the linking procedure performed before the membrane casting was carried out in THF solution, as described in the result and discussion section.

Dynamic Extraction Experiments

In order to evaluate the effectiveness of the linking reaction of KTAPB, dynamic extraction experiments were carried out under high flows of analyte solutions. For this purpose a weighted portion (0,3g) of the membrane was exposed for 12 h to a continuous flow of a 10^{-3} M aqueous solution of KCl (1000 ml), driven by a peristaltic pump. The whole aqueous solution were then extracted, in 10 portions of 100 ml, with ethyl acetate (3x 50 ml). The organic layers were combined and the amount of extracted KTAPB was determined spectrophotometrically (UV-VIS, λ=290 nm).

A second experiment was carried out by the same extraction procedure on weighted portion (0,3g) of two free plasticized Krynac/PVC containing the same amount (%) of the functionalized tetraphenylborate simply dissolved (Membrane A) or linked before the membrane casting by stirring a mixture of Krynac, PVC, DCP and KATPB in THF under reflux for 8 hours (Membrane B)**.** The amount of boron present in sample resulting by the extraction was detemined by ICP-MS ("X-SERIES^{II}",Thermo-Electron-Corporation, Winsford, UK).

3.5 References

1. E. Bakker and E. Pretsch, *Angew. Chem. Int. Ed.*, **2007**, 46, 5660-5668.
2. E. Pretsch, *TrAC Trends in Analytical Chemistry*, **2007**,26, 46-51.
3. A. Ceresa, E. Bakker, B. Hattendorf, D. Günther, E. Pretsch, *Anal. Chem*. 2001, 73, 343-351.
4. Zs. Szigeti, I. Bitter, K. Tóth, C. Latkoczy, D.J. Fliegel, D. Günther, E. Pretsch, *Anal. Chim. Acta*, **2005**, 532,129-136.
5. T. Sokalski, A. Ceresa, T. Zwickl, E. Pretsch, *J. Amer. Chem. Soc.*, **1997,** 119, 11347 – 1134
6. Zs. Szigeti, T. Vigassy, E. Bakker, E. Pretsch, *Electroanalysis,* **2006**, 18, 1254–1265.
7. S. Daunert and L.G. Bachas, *Anal. Chem.,* **1990**, 62, 1428 – 1431
8. D.N. Reinhoudt, J.F.J. Engbersen, Z.Brzozka, H.H. van der Vlekkert, G.W.N. Honig, H.A.J. Holterman, U.H. Verkerk, *Anal Chem.*, 1994, 66, 3618–3623.
9. M. Püntener, T. Vigassy, E. Baier, A. Ceresa, E. Pretsch, *Anal. Chim.Acta.*, 2004, 503, 187-194.
10. W. Kim, S. Chung, S.B. Park, S.C. Lee, C. Kim, D.D. Sung, *Anal. Chem.*, **1997**, 69, 95–98.
11. L. Ebdon, J. Braven, N.C. Frampton, *Analyst,* **1991**,116, 1005-1010.
12. J.Braven, L.Ebdon, N.C.Frampton, T. Le Goff, D. Scholefield, P.G. Sutton, Analyst, **2003,** 128, 1067-1072.
13. M.T. Diaz, E. Bakker, *Anal. Chem.*, **2001**, 73, 5582-5589.
14. J.L. Valentìn, A. Rodriguez, A.m. Fernandez, L. Gonzales, J*. Appl. Polym. Sci.*, **2005**, 96,1-5.

4.Solid contact-based ISEs: a preliminary study

4.1 Introduction

In the last years ISEs achieved very good analytical performances comparable with those of the most sensitive analitycal techniques. Very lower detection limits and high selectivities are obtained from both liquid and solid inner contact ISEs.

Inner filling solution in liquid-contact ISEs induces in fact fluxes of ions through the membrane. That causes biased potentiometric responses. Reducing or compensating this effect [1] low limit of detection (LOD) combined with high selectivity coefficients were obtained.

In the solid contact ISEs, originally known as coated wire ISEs, the use of the inner filling solution is avoided; in this way bias sources are reduced in lower detection limits (LDL) and selectivity coefficient measurements. The first version of SC-ISE consisted in a Pt wire coated with a traditional PVC-based ion selective membrane. Due to the ill-defined redox couple between membrane and solid contact, drifting potentials were obtained. The membrane, in fact, is assumed to be permeable to both oxygen and water.

The group of Pretsch found a spontaneously formation of a water layer (WL) between the membrane and contact surface of the electrode as source of potential instability, correlated to worse lower detection limit. [2] This water layer acts as non optimized inner solution and it is re-equilibrated after every change in sample solution.

Recently de Marco et alt. demonstrated the very first direct structural evidence for the formation of a water layer on coated-wire polymeric-membrane ion-selective electrodes (ISEs) [3].

Introducing a lipophylic redox-active layer between the ion selective membrane and the electrode surface, the formation of the water layer as well as the CO_2 and oxygen interferences were eliminated [4,5,6,7] It was found that membranes placed on electrochemically deposited conducting polymer (e.g., 3-polyoctylthiophene

(P3OT), polyethylendioxythiophene (PEDOT), polypyrrole (PP), [8,9,10]) showed promising LDL.
Applying the same concepts , improvements were also achieved for both potentiometric sensor whit traditional PVC membrane and for plasticizer free polyacrylate membranes [11] .

4.1.1 Solid State ISEs

CPs impart the lipophylicity to the solid contact and avoid the presence of the water layer. CPs are also useful as ion-to electron trasducers in solid-state ISEs for several reasons: i) CPs can be easily deposited on the electronic conductors, ii) CPs are electronically conducting materials, iii) CPs are electroactive materials with mixed ionic and electronic conductivity, in fact CPs. in absence of the WL, maintain the redox active behaviour with a well-defined pathway for the ion-to-electrode transfer process [12]. Therefore the high redox capacitance of CPs minimize the polarizabilty of the solid contact.

In this work, poly(2,2'-bithiophene) (PBT) is investigated as inner solid contact in selective potentiometric sensor, and the results are compared to the those obtained with a POT based analogue.
The poly(2,2'-bithiophene) (PBT) is really similar to PP and to other thiophenic polymers in terms of lipophilicity and redox behaviour, furthermore is more easily electropolymerizable [13]
In a previous work J.Sutter and E. Pretsch have shown that the potentiometric response behaviour of poly(vinyl chloride) (PVC) and polyurethane (PU) Ca^{2+}-selective membrane with different inner contact are significantly different[14]. The best results were obtained with solvent cast P3OT as the internal contacting layer. They showed that different conditions of electro-polymerization can influence the potentiometric responses.
Here, we have investigated the possibility to employ PBT as inner contac in SC-ISEs.

Moreover the photooxidation on CPs was investigated to reduce the potential drift under condition of variable exposition to light.
The presence of WL in electromodiefied solid contact coated with PVC selective membrane. P3OT and PBT electrosynthetized are compared with P3OT drop cast on Au electrode.
The π-conjugated system typical of the organic CPs makes them strongly sensible to the light. In several work was discovered drifting EMFs due to light effect over all in SC-ISEs with inner contact based on lipophilic self assembling monolayer (SAM) or CP films. Although potentiometric values light-dependency was described as this phenomenon on CPs has never completely investigated..
SC ISE based on acrylic ion selective membrane are also characterized. Thereby CP based SC-ISEs with one-pot polymerized acrylic solvent free membrane are also prepared.

4.2 Results and discussion

4.2.1. Light effect on EMF potentiometric measurements.

The π-conjugated system typical of the organic CPs makes them strongly sensible to the light.
Electromagnetic radiation adsorbed by the polymer generates an electron transfer along the conjugated system.
Several studies were carried out on conducting polymeric, materials commonly employed in solar cells [15] or optical sensors, in order to amplify the photo-induced currents.
The degradation products of conducting polymer related with UV irradiation were also charecterized. Poly-3alkyl thiophenes showed as the photo-oxydation involves the polymer backbone degradation and the chain scission[16].
In contrast, the effect of photo-induced current on potentiometric behaviour of solid contact electrode was never investigated.
In this work, the photo-sensitivity of screen printed gold electrodes modified with P3OT was investigated by potentiometric experiments.

For this purpose, three different types of potentiometric sensors have been fabricated by modifying the electrodic surface whit P3OT layers obtained by different procedures

P3OT was chosen as polymer model since this derivative presents a thiophenic ring functionalized whit a relatively long alkylic chain that increases its lipophilicity and makes it particularly suitable as inner contact for SC-ISEs.

The EMF responses of the P3OT gold modified electrodes were recorded over time and switching light on and off alternatively.

The coating procedures of the screen printed gold electrodes were *i)* the drop casting of the CH_2Cl_2 P3OT solution or *ii)* the electropolymerization of 3OT. Electrosynthesized P3OT CMEs were prepared under different experimental conditions. Polymeric films were in fact obtained by galvanostatic or potentiodynamic (CV) way. Drop casting coating procedure was chosen because it allowed to obtain undoped P3OT layers. On the other hand, electrosynthesis allowed to make polymers with different oxidation level.

It is a well known fact that CPs change the wavelength of adsorption by changing the conjugation level. In fact, undoped CPs show light absorption at wavelengths higher with respect to π-doped polymers (less conjugated) that are able to adsorb only electromagnetic radiation of higher energy (lower wavelengths).

Our experiments have been carried out simulating a common potentiometric measurement.

A remarkable EMF drift was observed for SC_ISEs kept in uncontrolled conditions commonly employed in laboratory during the characterization of potentiometric sensors, *while* the same sensors kept in a dark box showed more stable potentials.

Such experiments were conducted by keeping potentiometric cell in a dark box and subsequently irradiating the polymer with a 60 W common incandescence lamp mounted at a distance of 10 cm from the cell. The EMF was continuously recorded and related to the on-off switching of the lamp.

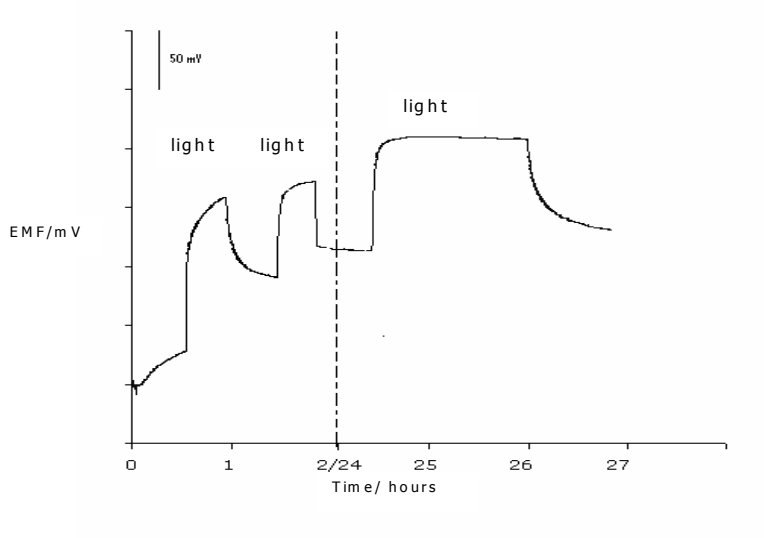

FIGURE 4.1. EMF time trace of drop-cast P3OT Ca-PVC ISE recorded switching light on of. EMF change is ascribable to light sensitivity of the polymer

When the electromagnetic radiation interact with the polymer, the associated electronic transitions are documented by EMF changes, strictly ascribable to the modification of the polymer structure and conjugation.

It is also well known that in SC potentiometric sensors (with and without ion-selective membrane) electron transfer phenomena from the polymer to the circuit and vice versa, is accompanied by corresponding transfer of analyte ions form the sample to keep the electroneutrality of the system. Under electromagnetic influenced effect EMF change is caused by the shift in the redox equilibrium in the conducting polymer.

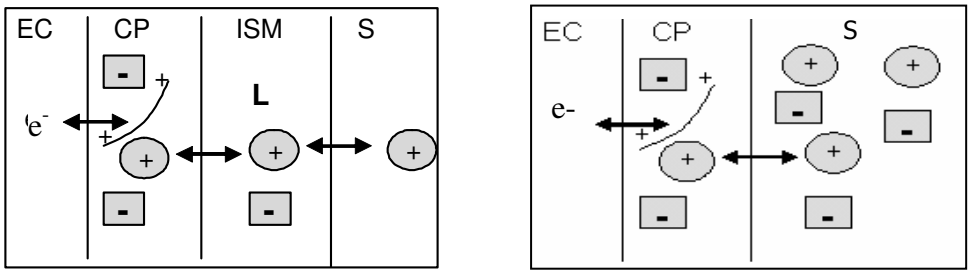

FIGURE 3.2 .operanting principle of solid-contact ISEs based on an oxidized (π-doped) conducting polymer as ion-electron transducer

EC Electronic Contact; **CP** Conducting Polymer; **ISM** Ion Selective Membrane; **S** sample solution , **L** Ion recognition site, "**+**"doped CP *(Bobaka, Electroanalysis **2006** (18) 7)*

In the absence of light, no ion movements are required to explain the EMF change: that is just a change in the phase-boundary potential.

The topic of this work was to find the experimental conditions (film thickness, deposition mode, and electro-induced doping) that minimize the EMF drift associated to on-off switching of the light.

In fact, it was found that light sensibility is strictly depending by thickness of the film and by the doping grade of the polymer. In thin and un-doped CP films the evidence of the light effect arises quickly and the EMF changes are more pronounced, while higher starting potential and lower photosensitivity have been observed for thicker and oxidized P3OT CMEs

Photoexcitation is also a reversible process as shown in figure 4.1

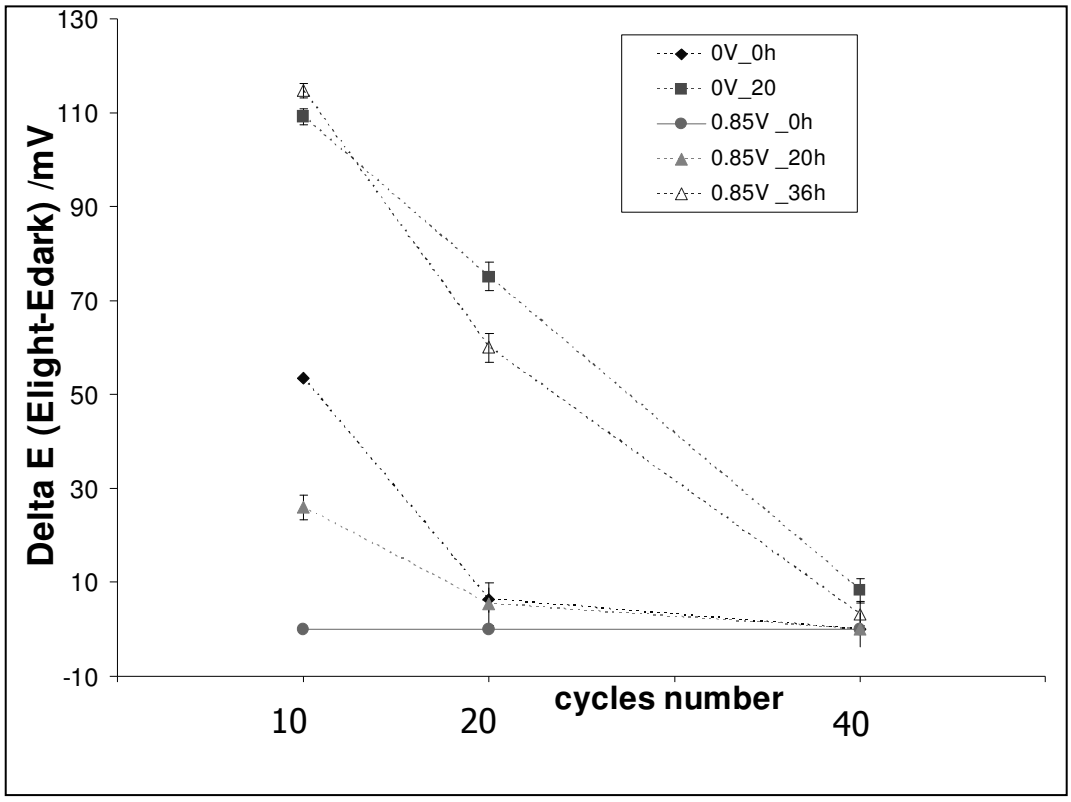

FIGURE 4.3 EMFs were recorded switching light on and off, EMF changes were calculated as $\Delta EMF = (E_{light} - E_{dark})$ and graphed with respect to polymer thickness.

Light was switched on and EMF light are measured after 15 minutes. Conversely EMF dark is measured just before switching on the electromagnetic radiation.

ΔEMFs were considerate over aging time of the doped and undoped P3OTs.

The photoinduced EMF drift vary inversely with the film thickness since the interaction with light involves only the surface of the cast polymer, while the transduction phenomena are ascribable to the "bulk" polymer. For this reason, the EMF variation induced by the light for a very thick film is observed after much longer times than the drift for thinner films.

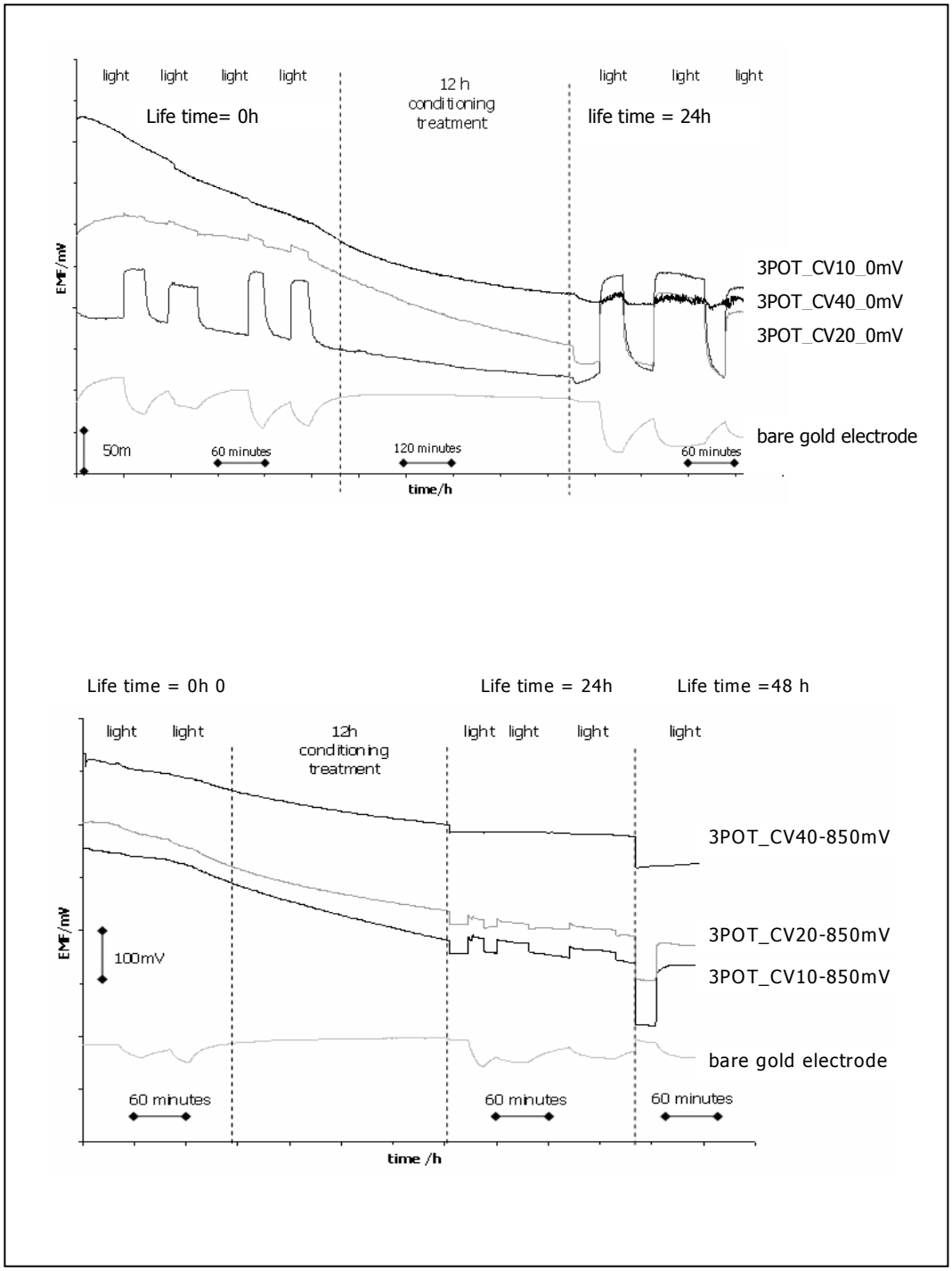

Figure 4.4. Light dependence of the EMF recorded over time for undoped 3POT (top) and of π-doped P3OT (bottom) CV10,CV20, CV40 indicate the cyclic voltammetric scans, 0 mV-850 mV are the applied potentials for electrodoping the polymers.

These qualitative results indicate that CME obtained with thicker and doped polymers show less light dependence of the EMF values. The results obtained with POT electrosynthesized by 80 CV scans and doped at three potential levels (0 V, 0.85 V and 1.2 V) support these conclusions. However, a too strong electrochemical doping treatment lead to irreversible polymer degradation, as evidenced by the behaviour of P3OT doped for long times. (see figure 4.5)

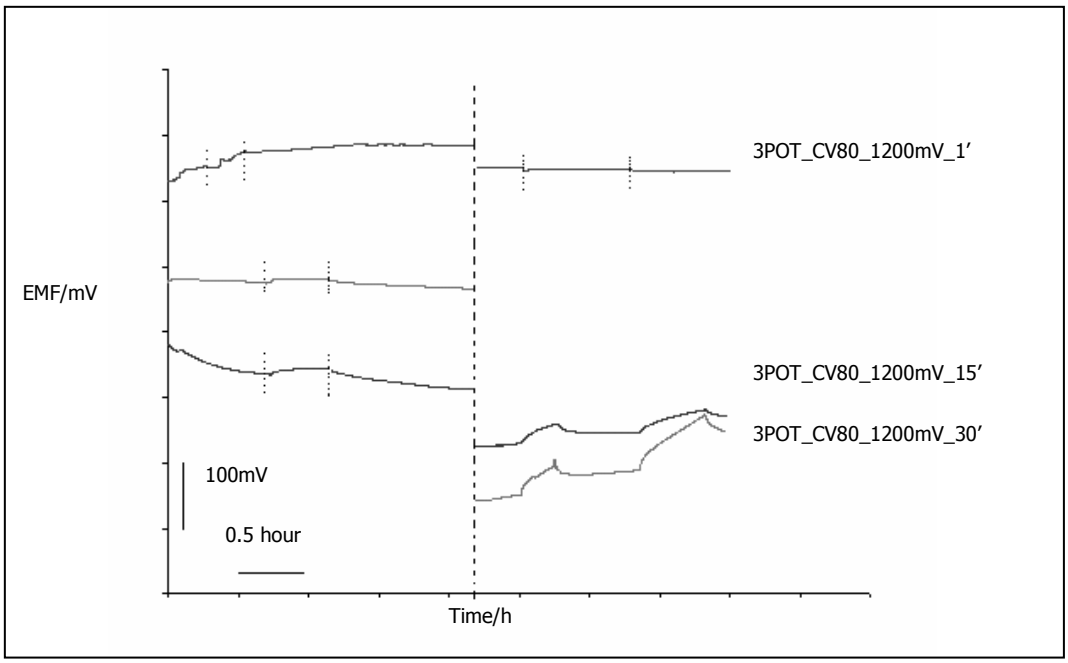

FIGURE 4.5. EMF of three different doped P3OT. Doped polymer for longer time showed after 12 hours aging time higher photosensitivity than P3OT doped for 1 minute.

The effect of ion-selective membrane coating was also investigated for the thickest P3OT doped under different experimental conditions (0 V for 1 minute, 1.2 V for 1 minute and 30 minutes). Corresponding EMFs time trace recorded switching light on-off are shown in Figure 4.6

In the following, EMF measurements with a Na-selective PVC membrane drop cast on P3OT modified electrodes and CMEs with and without PVC membrane were compared.

ELECTRODE	Doping treatment	NaPVCM
E1	1.2V for 30 min	Yes
E2	1.2V for 30 min	No
E3	1.2V for 1 min	Yes
E4	1.2V for 1 min	No
E5	0 for 30min	Yes
E6	0 foer 30 min	No

TABLE 4.2 electrode table lists doping treatment of P3OT and if the electrodes is coated with Na PVC selective membrane

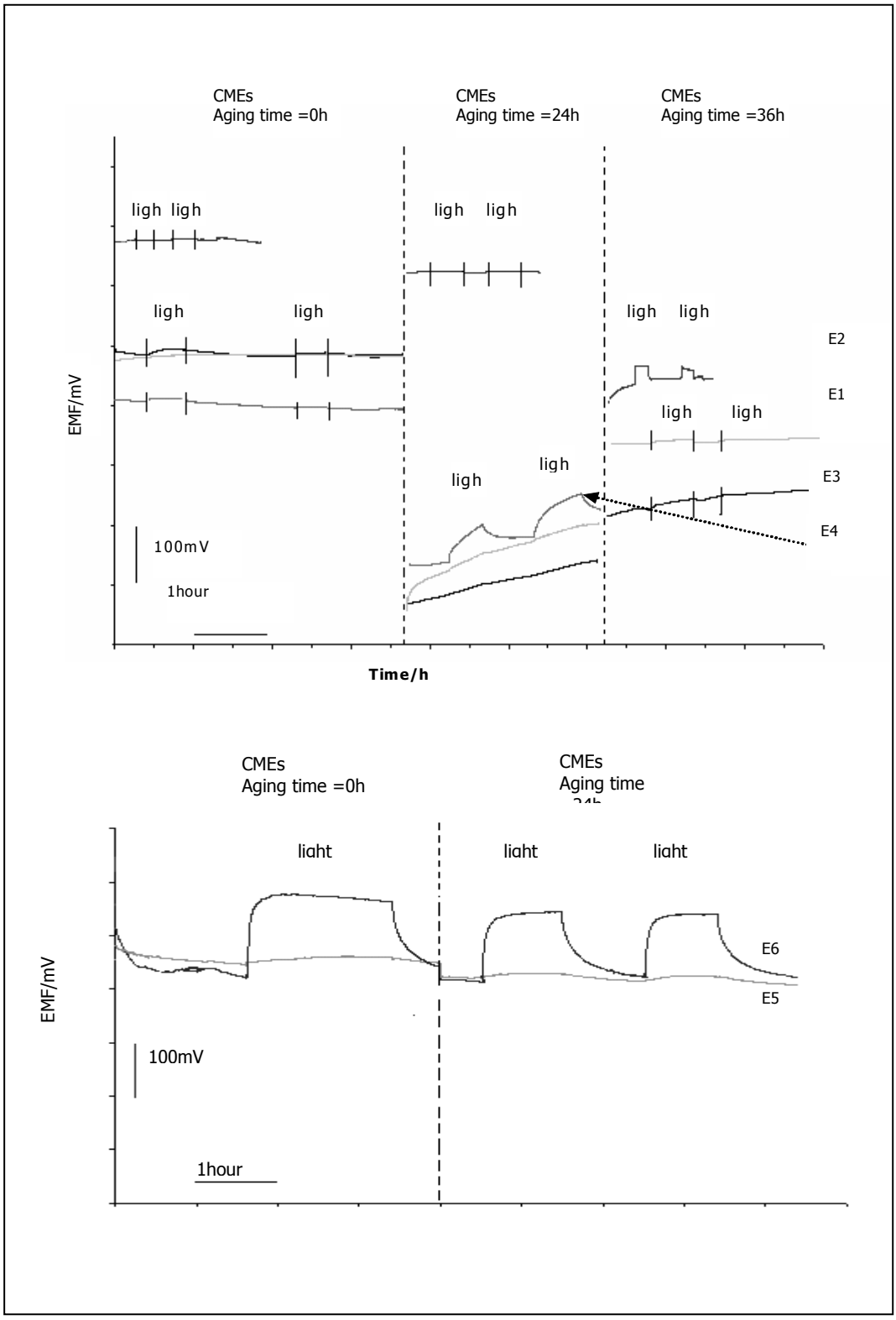

FIGURE 4.6. Effect of the light on π-doped P3OT with and without PVC Na-selective membrane (top) and on undoped P3OT(botton) with and without PVC membrane. EMF were recorded over time switching light on-of.

The obtained results show that the presence of the PVC membrane reduces the photosensitivity of the films although the relationship between the light response and the doping degree was maintained. Moreover, the casting of PVC membrane probably modifies the interaction between the polymer and electromagnetic radiation that will be partially absorbed by the PVC membrane.

4.2.2 Solid Contact Ca ISEs with Conducting Polymers

Electropolymerization procedure of PBT results faster and more reproducible responses with respect to 3-octhylthiophene (P3OT), due to higher reactivity of the monomer in which the aromatic rings are activated by a mesomeric effect.

Several studies rely on the potentiometric behaviour of solid-contact ISEs that are strongly influenced by the nature of inner contact. The sensors with a cast lipophilic layer between the membrane and the electrode showed better performances whit respect to SC-ISEs in which the polymeric membrane is directly deposited on the electrode contact.

P3OT was selected as inner layer, in several works for its lypophilicity, stability and redox behaviour.

However it was found that inadequate casting procedures have dramatic effects on the sensor response (less good lower detection limit and biased selectivity[17-18]

Since the conducting polymer-based ISEs, as previously demonstrated, are sensitive to photo-induced doping all measurement were carried out in a dark cell.

SC Ca-selective electrodes obtained by drop-casting P3OT, and by electrosynthesized P3OT and PBT were prepared and compared by means of potentiometric characterization (LDL and selectivity).

Electrosyntesized P3OT resulted to be more suitable with respect to the drop-cast parent material because of the high solubility of the latter in the solvent employed for the dissolution of the membrane components (THF).

Both Au-modified electrodes obtained by deposition of P3OT, tested in combination with PVC Ca-selective membranes, were submitted to a specific experiment called "Water Layer Test" (WLT).

WLT evidences the presence of a undesired solution layer interposed between the membrane and the inner contact and consist in EMF measurements carried out in a solution of primary ion replaced with a concentrated solution of an interfering ion. Stable EMF values (absence of time-EMF drift) are associated to the absence of such layer (FIG).

WLT test carried out on Au-modified electrodes obtained by deposition of P3OT did not evidence the formation of the water layer. This behaviour is ascribable to the lipophilicity of such polymeric coatings.

On the other hand, PBT SC-ISEs showed different responses depending on the experimental conditions employed for the electrodeposition of the polymer, as shown in table 3.3

Sensor	Solid contact (CP)	Monomer concentration (M)	Potential Scan rate (mVs^{-1})	Number of cycles	WLT
E1	PBT	0.02	100	3	Yes
E2	PBT	0.02	100	10	Yes
E3	PBT	0.001	200	20	No

TABLE 4.3 Experimental condition of CV electrosynthesis of PBTs . The results of Water Layer Test (WLT) are reported . Yes indicates water presence, No indicates close ideal behaviour of EMF time-traces.

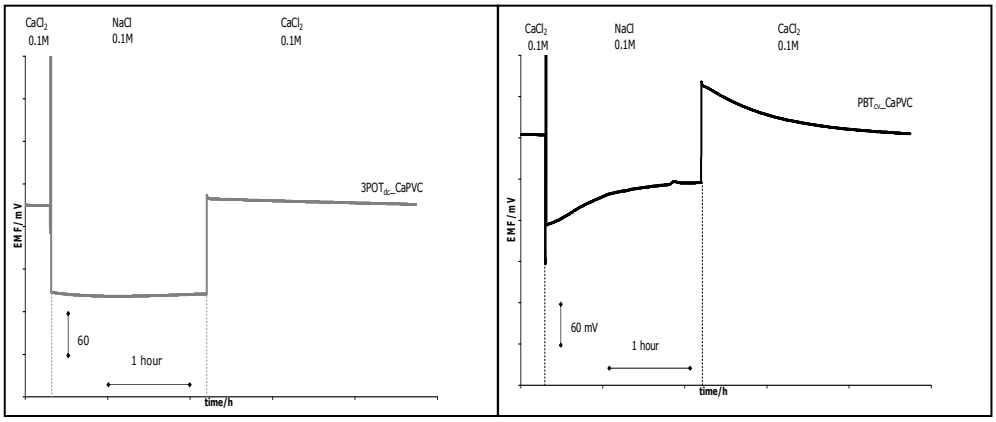

FIGURE 4.7. Water layer test of SC-ISEs . The inner contacts are : electropolymerized P3OT (left) and PBT (right). P3OT SC ISE shows stable EMF, conversely drifting EMF recorded for PBT SC ISEs (E2) indicates the presence of WL .

On the basis of these evaluations, the electropolymerization conditions (monomer concentration, potential scan rate and number of cycles) were chosen in order to avoid the WL in PBT SC ISEs.

The best response was obtained with PBT electropolymerized by CV from a 10^{-3} M monomer solution in a potential window ranging from 0.0 V to 1.4 V, with a scan rate of 200 mV/s and 20 cycles.

PBT_CaPVC so prepared minimizes WL and the EMFs measured are not affected by oxygen and CO_2.(Figures 4.8 and 4. 9)

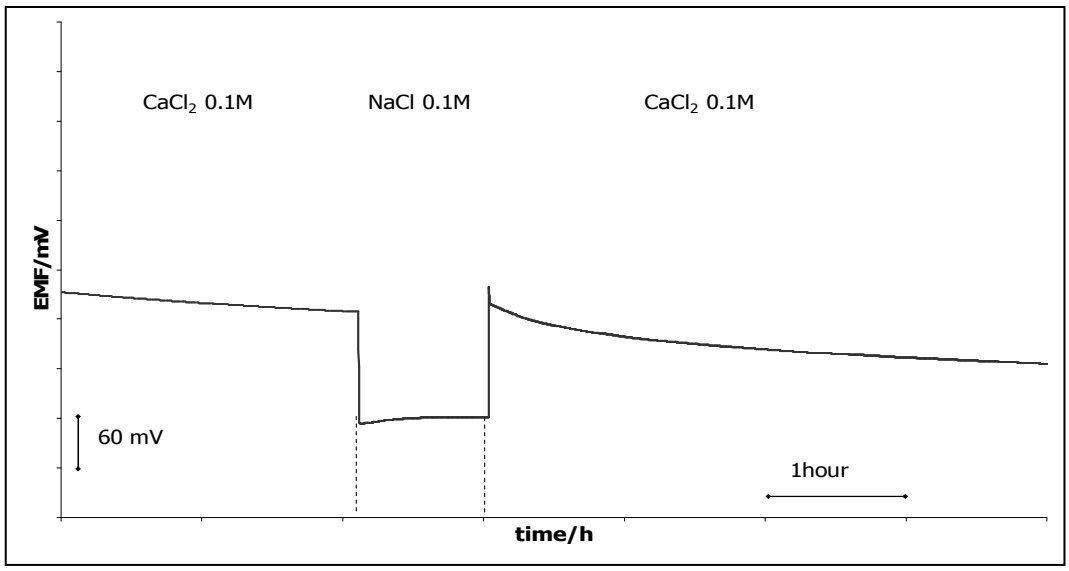

FIGURE 4.8 Water layer test carried out to test E3 (PBT SC-ISE)

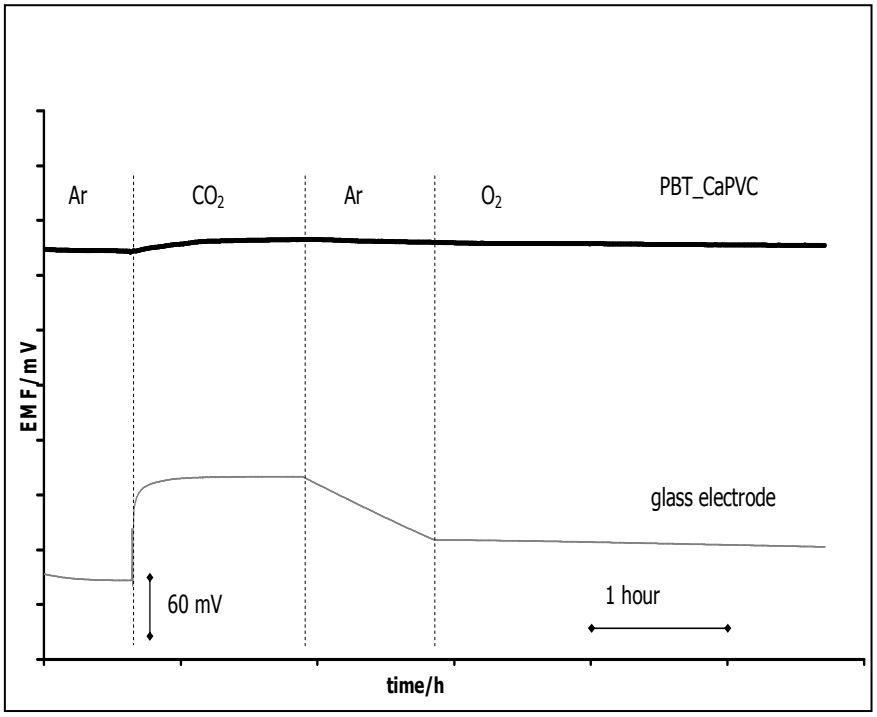

FIGURE 4.9 EMF time trace of PBT (E3) based SC Ca-selective electrode, recorded in 10^{-3}M $CaCl_2$ solution bubbling inside Argon, CO_2 and O2 . EMF time trace of a glass electrode was also recorded.

LDL and selectivity coefficients for each kind of sensor were also determined.

Selectivity coefficients were determined for four interfering ions (Mg^{2+}, K^+, Na^+, H^+) by the separate standard solution method(SSM) [15]. LDL was obtained according to IUPAC recommendation by decreasing $CaCl_2$ concentration in a solution containing NaCl 10^{-4} M as background.

Selectivity coefficients and LDL values observed for the studied electrodes are reported in Figure 4.11.

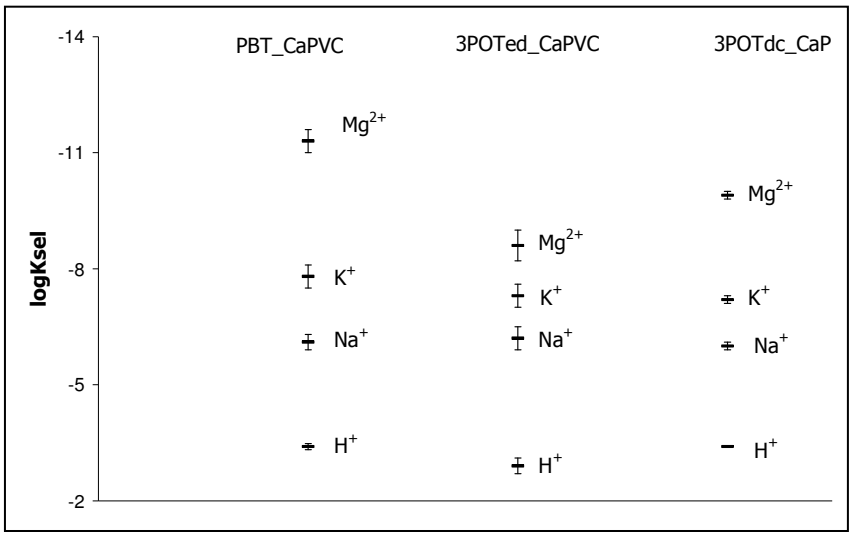

FIGURE 4.10 . Potentiometric selectivity coefficients , logKi.j obtained with separated standard solutions for measuring range of 10^{-2} to 10^{-4} M for solid contact electrodes based on electropolymerized PBT electrodeposited (ed) 3POT and drop-cast (dc) 3POT

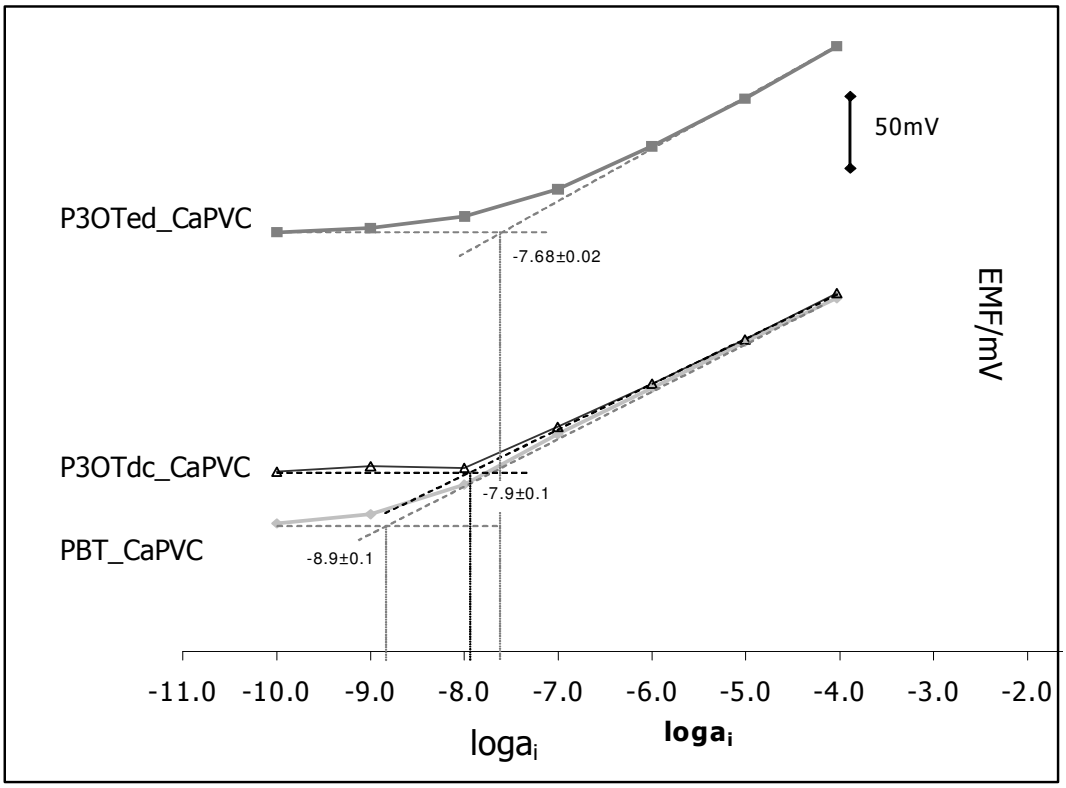

FIGURE 4.10. Calibration curves obtained with PBT_CaPVC , P3OTed_CaPVC, and 3POTdc_CaPVC in $CaCl_2$ with a background of 10^{-4} M NaCl.

Selectivity coefficients and LDLs obtained for PBT_CaPVC, P3OTdc_CaPVC and P3OTed_CaPVC were compared.
These results provide an encouraging outlook about the potentialities of CP modified SC ISEs

4.2.3 SC-ISE based on self-plasticized polymer (PEHDM)

As previously discussed, PBT modified electrodes are suitable as inner contact for SC-ISE .
In this part of the work electrosynthesized PBTed and P3OTed and drop cast P3OTdc were compared as solid contacts for new ISEs.

It is well known that ion fluxes can be reduced by using self–plasticized polyacrylates as ion-selective membrane. Good results were obtained in previous works, with drop-cast poly(methymethacrylate-decymethymethacrylate) solvent free membranes [20]

Poly EHMM-HDMM (**PEHDM)** membranes were obtained by in–situ polymerization reaction of a EHDM membrane cocktail. Lithium selective cocktail contains EHMM as monomer, HDMA as cross-linker and AIBN as radical starter. LiVIII and NATPFB are the ionophore and ion exchanger respectively **(Li-PEHMD).**
The reaction takes place by a radical mechanism induced photochemically or thermally. Conventional Lithium PCV membrane (Li-PVC) was also prepared by common procedure.

ISE	MEMBRANE	POLYMERIZATION	ELECTRODIC CONTACT
ISE_a	Li-PVC	-	Liquid contact [a,b]
ISE_b	Li-PEHDM	Thermo induced	Liquid contact [a]
ISE_c	Li-PEHDM	Photo induced	Liquid contact [a]
ISE_d	Li-PEHDM	Photo induced	PBT
ISE_e	Li-PEHDM	Photo induced	P3OTed

TABLE 4.6 Membranes, and electrode contacts used. [a] and [b] indicate the inner filling solution composition :10^{-3} M KCl and 10^{-3} M LiCl , respectively

Polymerization conditions of the selective membrane influence dramatically the potentiometric behaviour of the sensor; in fact the ionophores can be differently degraded either from UV light or from warming.

The polymerization procedure is, from this point of view, crucial for the performance of the electrodes.

Liquid contact (LC) ISEs with photo- and thermopolymerized Li-PEHDM membrane (ISE_b and ISE_c), and with Li- PVC membrane (ISE_a) were prepared.

At least 3 electrodes were prepared for each typology. Photo and thermo-polymerization of acrylic membranes were carried out directly within plastic pipette-tips, that constitute the end of the electrode bodies.

Polymerization procedures were evaluated in terms of the selectivity coefficients obtained by potentiometric experiments. The selectivity of the LI_PEHDM was investigated for Ca^{2+}, K^+ and Na^+ by separate solutions method (SSM).

IonJ	Li PVC (ISE_a)	Li PEHDM (ISE_b)	Li PEHDM (ISE_c)	Li PEHDM (ISE_d)	Li PEHDM (ISE_e)
Ca^{2+}	-1.6±0.2 (27)	-1.15± 0.05 (29)	-1.34± 0.05 (15)	-2.053±0.007 (30)	-1.467±0.004 (31)
Na^+	-2.03± 0.05 (54)	-2.2± 0.1 (34)	-2.17±0.05 (53)	-2.08±0.03 (36)	-1.905±0.005 (49)
K^+	-4.3± 0.2 (32)	-2.17± 0.07 (9)	-2.04±0.08 (16)	-2.8±0.1 (37)	-2.443±0.004 (30)

TABLE 5.7 Potentiometric selectivity coefficients, log $K_{i,j}$ obtained by the separate solution method (SSM), PVC and PEHDM Li selective membranes for ISE_a, ISE_b, ISE_C, ISED_d and ISE_e, standard deviations are calculated for n = 3. The slopes for the concentration range 10^{-2} to 10^{-4} M are given in parentheses.

Photo-polymerized LiPEHDM and LiPVC membranes showed comparable results, while thermo-polymerized membrane showed non-Nernstian behaviour for the primary ion.

LC LiPVC electrodes exhibit best selectivity for K^+ than Li-PEHDM; this fact could be ascribed to the polymeric matrix effect.

PBT and P3OTed solid contact electrodes coated with photo-polymerized LiPEHDM were characterized by potentiometric measurements. LDL and selectivity were calculated and compared with those of LC Li PVC electrodes.

Selectivity coefficients followed the trend of liquid contact electrodes.

LDL values of PBT-LiPEHDM and LC-LiPVC, expressed as log of the ion activity, were -5.9 (0.2) and -6.9 (0.2), respectively.

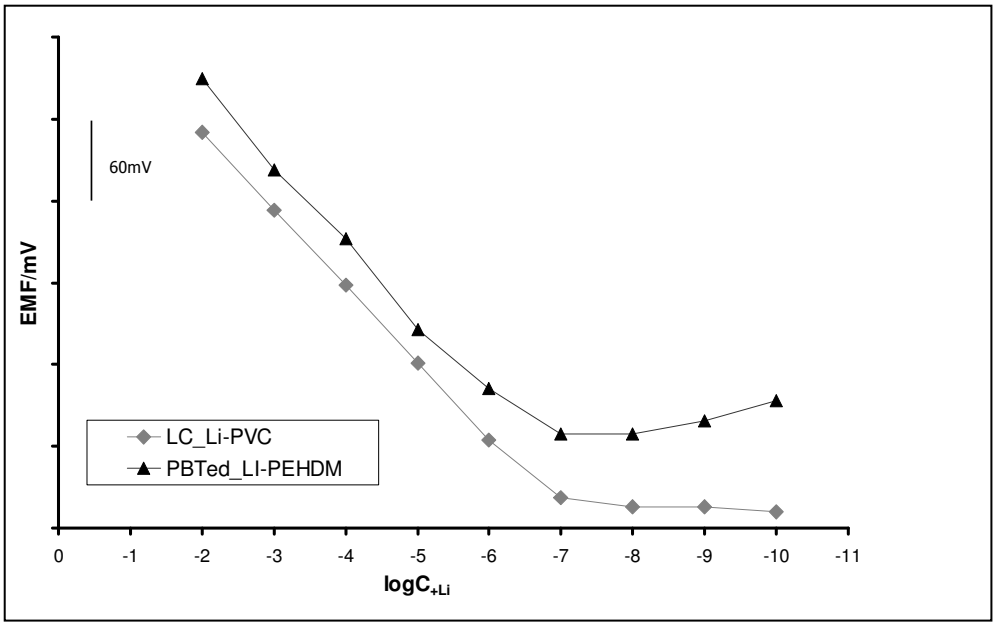

FIGURE 4.12 calibration curves obtained whit ISE_a (LC_Li-PVC) and ISE_d (PBT_Li-PEHDM) by decreasing concentration of LiCl solution (from 10^{-2} to 10^{-10} M)

This difference could be ascribable to unbuffered ionic strength or to unconsidered proton interference.

However if the first results were promising this technique must be standardised. More factors (cleaning grade of electrode, impurity in the membrane reagent, amount of cocktail volumes, photo and thermo stability of the active component of the membrane and of the conducting polymers) play an important role on the final result and should be carefully controlled and evaluated in the future.

4.3 Conclusions

Photosensitivity of P3OTs by potentiometric measurement was investigated. EMFs recorded by switching light on of evidence a relationship between the light-sensitivity and polymers typology. Particularly thin and undoped films showed highest EMF changes when the cell was irradiated with electromagnetic radiations. On the other hand, thicker and π-doped P3OT exhibited over time more stable EMF values. PVC

membrane, adsorbing part of the radiation, reduces the light sensitivity of the P3OT films.

Potentiometric performance of Solid Contact ISEs based on different conducting polymers as ion-to electron transducers were investigated. Responses of PBT SC CaPVC ISEs were compared with those obtained with drop cast and electropolymerized P3OTs. All typologies of the electrodes showed negative responses to the WLTs and the corresponding EMFs recorded, bubbling CO_2 and O_2 into 10^{-3} M $CaCl_2$ solution, were stable over time.

LDL and potentiometric selectivity obtained for PBT and for drop cast P3OT based Ca selective electrodes were comparable.

New ways to prepared solid contact ISEs based on self-plasticized selective membrane were investigated. In situ thermally and photochemically induced polymerization of Li-EHDM were carried out to prepared liquid and solid contact lithium selective electrodes. Encouraging results were obtained with photopolymerized membranes.

4.4 Experimental.

Reagents

Chemically synthesized poly(3-octythiophene) (P3OT) was obtained from Applications Chemistry&Technologies (AC&T, Saint Egrève, France). 3-octylthiophene (3OT) (Aldrich, 97%) and 2-2'bithiophene (BT) (Fluka, 97%) and $LiBF_4$ (Aldrich, 98%) were used as received. Chloroform was p.a. grade from Merck, acrylonitrile (ACN, fluka) was distilled over CaH_2 before use.

NaCl, KCl, $CaCl_2$, $MgCl_2$, LiCl were Suprapur® from Merck, HCl Hydrochloric acid (1 mol L^{-1}) was Titrisol® from Merck. Deionized water (specific resistance 18,2MΩ, NANOpure; Barnstead, Basel, Switzerland) was used to prepare all solutions.

N,N-Dicyclohexyl-N',N'-dioctadecyl-diglycolic diamide (CaIV),

4-*tert*-Butylcalix[4]arene-tetraacetic acid tetraethyl ester (NaX),

N,N,N',N',N'',N''-Hexacyclohexyl-4,4',4''-propylidynetris(3-oxabutyramide) **(**LiVIII),

sodium tetrakis[3,5-*bis*(trifluoromethyl)phenyl]borate (NaTFPB), bis(ethyl exhylsebacate) (DOS) and tetrahydrofuran (THF) were Selectophore® from Fluka.

Electrochemical polymerizations

Electrochemical syntheses of 3OT and BT were carried out by using an μAutolab Type II potentiostat/galvanostat (EcoChemie, Utrecht, Neerland) connected to a conventional one compartment three electrode electrochemical cell. Gold tips for rotating disk electrode (GDE) (Au disk: 3 mm; tip: 10 mm; type 6.1204.020, Metrohm AG, Herisau, Switzerland) , Gold printed electrodes (GPE surface 0.04 cm^2) and glassy carbon (GC) tips for rotating electrodes (GC disk 2mm, 6.1204.110 Metrohm.) were used as working electrodes (WE).
As counter electrode (CE) and as reference electrode (RE) a GC disk electrode and a home made Ag/AgCl, KCl 3M (agar-agar bridge) were employed respectively.
Before use each WE electrode was polished with 0.3μm alumina and rinsed with water and acetone

EMF measurement

Potentials were measured whit a custom-made 14-channel electrode monitoring system at room temperature. A double-junction Ag/AgCl/1M KCl containing 1M NH_4NO_3 (type 6.0729.100, Metrohm) was used as reference electrode.
All EMF values were corrected for liquid-junction potentials according to the Henderson equation. Activity coefficients were calculated by the Debye–Huckel approximation.

Conducting polymer modified electrodes: light dependency EMF

Electrodes Modification

P3OT film were deposited on GPE surface by galvanostatic (GS) or potentiodinamic (Cyclic voltammetry, CV) electrochemical polymerizations from a solution of 3OT 0.1M and supporting electrolyte (LiF_4B 0.1M in dry ACN) previously purged whit A.

GS polymerization was carried out applying a constant density of current of 1.43 mA/cm^2 for different times in order to produce polymeric layers of different thickness (60, 80, 120, 240, 360 s).

CV polymerizations were carried out in a window potential ranging from 0 V to 1.5 V (potential scan rate 0.1 V/s; step potential 0.025 V). polymer with different thickness were obtained changing the number of the CV scans (10, 20, 40, 80).

Experimental condition of electropolymerization procedures were listed in Table 4.7

	GS						CV **Cycles(n°)**			
Time(s)	60	80	120	240	360	**Cycles(n°)**	10	20	40	80
Doping	0.0 V	0.0 V	0.0 V	0.0 V	0.0V	Doping	0.0 V	0.0 V	0.0 V	0.0 V
	0.85 V	0.85 V	0.85 V	0.85 V	0.85V		0.85 V	0.85 V	0.85 V	0.85 V
	1.00 V	1.00 V	1.00 V	1.00 V	1.00V		1.00 V	1.00 V	1.00 V	1.00 V

TABLE 4.7 Experimental conditions of electrochemical polymerizations

Both CV and GS polymerized polymers were prepared in different π-doping grade (0 V,0.85 V,1.0 V and 1.2 V).

After the electrosynthesis, all polymers were undoped in the polymerization solution at 0 V for 60 s, then electrocharacterized by three CV scans (window potential ranging from 0 V to 1.4 V; scan rate 100 mv/s) in a ACN solution containing only $LiBF_4$ (0.1 M), before potentiometric experiment the electrodeposited polymers were polarized at different potentials and for different times: i) un-doped P3OT (0 V; for 60, 1000, 2000 s), ii) partially π-doped P3OT (0.85 V, 60 s) and π-doped P3OT (1 V-1.2 V; 60, 1000, 2000 s).

P3OT was applied on the gold print electrode by drop-casting 10 µL of a 0.25 mM solution (respective monomer) in chloroform. After 2 minutes the films were dry.

Two replicates for all typology of CMEs were prepared.

ISEs electrodes

The Na-selective membrane for solid-contact ISEs contained 0.98 wt.% (9.87 mmol kg^{-1}) NaX ionophore (4-*tert*-butylcalix[4]arene-tetraacetic acid tetraethyl ester), 0.52 wt.% (5.75 mmol kg^{-1}) NaTFPB (sodium tetrakis[3,5-bis(trifluoromethyl)phenyl]borate, and 32.97 wt.% PVC, 65.59% of DOS. 20 mg of the membrane was prepared in 0.2 mL of THF. 2 µL of such membrane cocktail were drop cast, for two times (waiting solvent evaporation) on the P3OT modified electrodes.

EMF Measurement: light –darkness experiments

Potentiometric measurement have been carried out in a glass beaker containing 200 mL of a solution of 10^{-3}M NaCl.

EMFs were recorded over time switching the light on-off.

Electromagnetic radiation source was common lamp (Philips 60W)

Conducting polymer as solid contact for conventional PVC Ca-selective membrane

Ion selective membrane and solid contact electrodes

The Ca-selective membrane for solid-contact ISEs contained 0.99 wt.% (12.40 mmol kg^{-1}) Ca ionophore(N,N-dicyclohexyl-N',N'-dioctadecyl-diglycolic diamide), 0.5 wt.% (5.49 mmol kg^{-1}) NaTFPB, and 32.51 wt.% poly(vinylchloride) (PVC); 66.01% of bis(2-ethylhexyl)sebacate (DOS); 203 mg of the membrane were dissolved in 2 mL of THF.

50 µL of membrane cocktail were drop cast on the CMEs. The membrane thickness was 100 µm.

P3OT were deposed on the gold electrode by drop-casting procedure or electrosynthesized by 80 CV scans (window potential ranging from 0 V to 1.5 V, potential scan rate 0.1mV/s, doping potential 1.2 V).

Poly-2-2'bithiophene (PBT) films were electropolymerized on GDE by CV way changing: i) monomer concentration (0.02 M or 0.001 M), ii) number of scans (3, 10,

20) and iii) potential scan rate (0.05 Vs^{-1}, 0.1 Vs^{-1}, 0.2 Vs^{-1}). $LiBF_4$ was the supporting electrolyte (0.1M in ACN dry).

Before being electrocharacterized all polymers were kept at 0 V for 60 s in the polymerization solution. P3OTand PBT CMEs were characterized, in a solution of ACN containing only the supporting electrolyte (0.1 M $LiBF_4$), by three CV scans in a window potential ranging from 0 V to 1.4 V for and from 0 V to 1.3 V respectively.

SC ISEs were constructed as described in [18].

For selectivity measurements, the solid-contact ISEs were conditioned in a 10^{-2}M solution of $MgCl_2$ at least for 2 h. For the measurements in dilute solutions the electrodes were conditioned at least 2 days in a 10^{-4}M of $CaCl_2$ and then over night in 10^{-6}M CaCl2, NaCl 10^{-4}M as background, the sample solutions had the same background.

Self-plasticized membranes in situ polymerized

PVC Li- selective membrane (Li-PVC) contains containing 1.03 w.t% (12.94mmolKg-1) of LiVIII ionophore,0.61 w.t.%(6.8394mmolKg-1) of NaTFPB, 29.83 w.t% of PVD and 68.84w.Y % of DOS, was dissolved in THF (2 mL) during ca. 4 h and poured into a glass ring(d=22mm) on a glass plate and covered whit an other glass plate. After overnight evaporation of the solvent at room temperature, disks of 5 mm in diameter were punched from the master membrane (thickness 100 µm) and glued with a PVC/THF slurry to a plasticized PVC tubing mechanically fixed on to a 1000 µL pipette-tip. The inner filling solution consisted of 10-2M KCl for selectivity measurements and 10-3M LiCl for low concentration measurements. The Ag/AgCl inner reference electrode in 10-2M NaCl electrolyte, was separated from the internal solution by a diaphragm.

Solution, containing of 98.61 wt % (2001.3mg) ethylhexymethylmethacrylate (EHMA), 0.84 wt % (17.17 mg) 1,6-hexyl dihydroxymethacrylate (HDMM) as cross linking agent, and 0.54 wt% AIBN (azobisisobutyronitrile) as radical starter, is the polymerizing polyacrylic membrane (EHDM).

Liquid and solid contact PEHDM Li selective electrodes

Self-plasticized Li-selective membrane (Li-EHDM) contains 1.26 wt.% (15.84 mmol kg^{-1}) LiVIII ionophore (N,N,N',N',N'',N''-hexacyclohexyl-4,4',4''-propylidynetris(3-oxabutyramide)), 0.51. wt.% (5.79 mmol kg^{-1}) NaTFPB, and 98.22 wt% EHDM, was dissolved in THF for 4h. THF was removed under argon stream. When THF was completely evaporated, the solution was degassed by ultrasonic treatment.
Liquid contact PEHMD Li-selective electrodes were prepared by in-situ (pipette tip) polymerization of the membranes. 10 µL of membrane cocktail were putted into the 100 µL pipette tips. Membranes polymerization were obtained by heatingt (themopolymerization) or by UV radiation (photopolymerization) directly inside the pipette tips

Thermally induced polymerization was carried out keeping the pipette tips, containing 10 µL of Li-EHDM, over night within an oven at 80 °C under Ar atmosphere.
Photopolymerization was carried out by placing the pipette tips under the UV lamp and switching light on-off every five minutes , for three times. The Membranes were ready after twelve hours. UV lamp used for photopolymerization was (Ultramed 400W/FDA R7S, Osram, Germany), UVA (315-400 nm) 82W and UVB (280-315 nm) 10Watt.
After polymerization, the pipette tips containing Li-PEHDM were mounted onto a 1000 µL pipette tip. The inner filling solution consisted in 10^{-2}M KCl for selectivity measurements and 10^{-3} M LiCl for low concentration measurements. The Ag/AgCl inner reference electrode in10^{-2} M NaCl electrolyte, was separated from the internal solution by a diaphragm.

Solid-contact Li-selective electrodes were prepared by in situ (disk glassy carbon chemically modified electrode) polymerization of EHDM membrane.
Thermopolimerization was carried out by heating in a glass bottle 100 µL of ion selective solution (80 °C for 4 min. under Argon stream). 10 µL of this solutions

were drop cast on conducting polymer modified electrode. The membrane polymerization is done after 36 hours.

Photopolymerization is carried out exposing 5 μL of Li-EHDM (previously put inner a 10 μL pipette tip) for 5 min at the UV radiation. Then the solution was drop cast onto CME and placed under the UV light lamp. The electrodes were irradiated three times for five (sliping time five minutes).

3OT (0.1M) and BT(0.01M) were electropolymerized on GC tips rotating disk electrodes by CV procedures (40 cycles and 3 cycles respectively, potential scan rate 0.1mV/s, doping potential 1.0 V).

Electrosynthesized conducting polymesr were characterized in a LiBF4 0.1M ACN solution by 3 CV scans in a window potential ranging from 0.1 V to 1.3 V or to 1.4 V for PBT and P3OT, respectively.

Potentiometric experiments

Before selectivity measurements all Li-selective electrodes were conditioned in 10^{-2}M KCl solution at least 12 h. For measurements in dilute solutions the electrodes were conditioned at least 2 days in a 10^{-4}M of LiCl and then over night in 10^{-6}M LiCl.

4.5 References

1. Z. Szigeti, T. Vigassy, E. Bakker, E. Pretsch *Electroanalysis*, **2006**,18,1254.
2. Fibbioli, M.; Morf, W. E.; Badertscher, M.; de Rooij, N. F.; Pretsch, E. *Electroanalysis* **2000**,12,1286.
3. Roland De Marco, Jean-Pierre Veder, Graeme Clarke, Andrew Nelson, Kathryn Prince, Erno Pretschc and Eric Bakker *Phys.Chem.Chem.Phys*. **2008,** 10, 73.
4. Fibbioli, M.; Bandyopadhyay, K.; Liu, S.-G.; Echegoyen, L.; Enger, O.; Diederich, F.; Bühlmann, P.; Pretsch, E. *Chem. Commun.* **2000**, 339.
5. O. Enger, F. Nüesch, M. Fibbioli, L. Echegoyen, E. Pretsch, F. Diederich J. *Mater. Chem.* **2000**, 10, 2231
6. J. Bobacka. *Anal. Chem*. **1999**, 71, 4932.
7. M. Velazquez, J. Bobacka, A.Ivaska, A. Lewenstam *Sensors and Actuators B* **2002**, 82 ,7.
8. A. Cadogan, Z.Gao, A. Lewenstam, A. Ivaska, and D. Diamond *Anal. Chem.* **1992**, *64*, 2496.
9. R. E. Gyurcsányi, A.S. Nybäck, K. Tóth , G. Nagy and A. Ivaska A*nalyst,* **1998,** 123 1339.
10. J. Bobacka. *Electroanalysis* **2006**, 18, 7.
11. E. Bakker, D. Günther, E. Pretsch . *Trends. Anal. Chem.* **2005**, 24, 1.
12. J.Bobaka, A. Ivaska, A. Lewenstam *Electroanalisys* **2003**, 15, 366.
13. Gary.P.Evans "The electrochemistry on Conducting Polymers" Advances in Electrochemical Science and Engineering (VCH),**1990** Vol.1, 51-55
14. J. Sutter, E. Pretsch *Electroanalysis*, **2006**, 18, 19.
15. G. Tsekouras, C.O. Too and G.G. Wallace. *Synthetic Metals* **2007**, 157, 441.
16. N. Ljungqvist and T.Hjertberg *Macromolecules* **1995**, 28, 5993.
17. K. Y. Chumbimuni-Torres, N. Rubinova, A. Radu, L. T. Kubota, and E. Bakker. *Anal. Chem*. **2006**, 78, 1318.
18. J. Sutter, A. Radu, S. Peper, E. Bakker, E. Pretsch*, Analytica Chimica Acta* **2004,** 523, 53.
19. E.Bakker *Anal.Chem*. **1997** 69, 1061.
20. Qin Y, Peper S, Bakker E. Electroanalysis, **2002**,14 19.

5.Potentialities of a modified QCM sensor for the detection of analytes interacting via H-bonding and application to the determination of ethanol in bread

5.1 Introduction

Piezoelectric quartz crystals are widely used for controlling frequency in communication equipment and have long been used as frequency and time standards. These stable devices become selective gas detectors when coated with suitable materials[1] and [2]. In the last year The interest on piezoelectric gas sensors based on frequencymetric transduction is rapidly growing, both in the aspects of new sensing materials and of their applications.

One of the first applications of such sensors derived from the deposition of a gaschromatographic stationary phase on the surface of PQC unit [3]. The interactions between the sensing coating and the detected analytes are usually aspecific, [4] involving bulk dissolution of organic molecules in polymeric layers, dispersion interactions, polarizability, dipolarity, etc.

Nowadays, electronic noses, olfactory systems based on QCM sensor, are widely employed for volatile compounds analysis in food and environmental chemistry

The operating principle of QCM sensors is based on the interaction between the surface of a quartz crystal coated with the sensing layer and the analytes. If a rigid layer behaviour is assumed for the crystal, the change in resonant frequency is a function of the mass changes on the surface of the PQC, according to the Sauerbrey equation [5]: Usually, the sensing films employed as coatings for QCM sensors are empirically chosen and their deposition is classically carried out by casting techniques like Spin Coating [6], Ion Plasma [7] and Langmuir–Blodgett (LB) [8]. Although the LB is one of the most promising techniques among the above cited, this casting method requires dedicated and expensive equipment. The chemical nature of the

organic sensing coatings employed for the realization of QCM sensors is very heterogeneous; metal oxide thin film, zeolites, electrodeposed phospholipide and conducting polymer (CP) films.

These polymers include polythiophenes [9], polypyrroles [10] and polyanilines [11] and [12]. Functionalised polythiophenes have been found to be versatile materials with interesting electrochemical properties suitable for sensor application [13] and [14]. The synthesis of a customized monomer, obtained by functionalization of a molecular receptor with an electropolymerizable 2,2'-bithiophene-3-yl-hexylene unit was design to realized a selective layer , by electropolymerization , onto the surface of a gold-coated piezoelectric quartz crystal (PQC). The so obtained QCM sensor showed binding properties for organic volatile compounds containing electronegative atoms. The aim of the present study, was to investigate on the potential of the sensor for quantitative analysis focused on volatile compounds like ethanol, ethyl acetate, chloroform, dichloromethane, tetrachloroethylene, acetone, acetonitrile, toluene, in order to develop reliable and simple methods of analysis for these compounds. First, the characterization of this sensor was performed as detection unit for gas chromatography (GC), that allowed to determine the detection limits of the QCM sensor for the analytes.

The sensor selectivity was established as sensitivity of the method for each analytes. On the basis of the findings concerning ethanol and of the interest towards this compound in foods, the study was then focused on the development of a novel method based on the application of the sensor in the determination of ethanol in industrially packed bread. This type of analysis is of concern in food analysis since ethanol is a common ingredient in formulated foods, naturally present or added in liquid form, and carries out important technological function, i.e. it extends their shelf-life owing to its capacity to inhibit or reduce the rate of microbial growth. In Europe there is no restriction about the use of ethanol in foods as a preservative, except in Italy, where current regulations allow its addition as an anti-moulding agent in pre-packed bread, at a maximum concentration of 2% on a dry weight basis

[16]. The long lifetime of the sensor previously demonstrated [15] was the main feature of the device exploited in this work for the proposal of a system for on-line measurements of ethanol in bakery products. Another advantage of the proposed device, consists in its cheapness with respect to amperometric ethanol biosensors [17], [28] and [19], requiring the use of immobilized enzymes. The Italian official method for the quantification of ethanol in bread is based on static headspace followed by gas chromatography with a flame ionization detector (GC-FID) [20]. With reference to other studies dealing with the development of reliable methods for the analysis of volatile components in food and environmental samples[21-23], in the present study we demonstrate that the direct injection of the headspace of a vial containing the sample in a stream of carrier gas, without chromatographic system, directed to the detection QCM cell allows to quantify ethanol in a simpler way and in shorter times. The device proposed was proved promising as "on-line sensor" for quality control during bakery production.

5.2. Results and discussion

Synthesisi of electropolymerisable molecular receptor

The development of our sensor was focused on the design and synthesis of an electropolymerisable molecule carrying the receptorial moiety[15], see Figure5.1. The working mechanism of the moiety is known to be based on the formation of hydrogen bonds with the analytes[27]. Electropolymerisation processes employed for the deposition of sensing coatings on PQC units, with respect to other techniques like "spin coating" or direct spraying of solutions, allow to control and standardise the deposition process. Previous literature studies referring about QCM sensors realised by electropolymerisation processes concerning unfunctionalised monomers like derivatives of thiophene, pyrrole and aniline, empirically chosen and not capable of specific interaction with analytes[27].The monomeric receptor synthesized and studied in this work undergoes conformational variations as a consequence of coordination, and is suitable to selectively interact with neutral molecules like halogenated or oxygenated solvents.

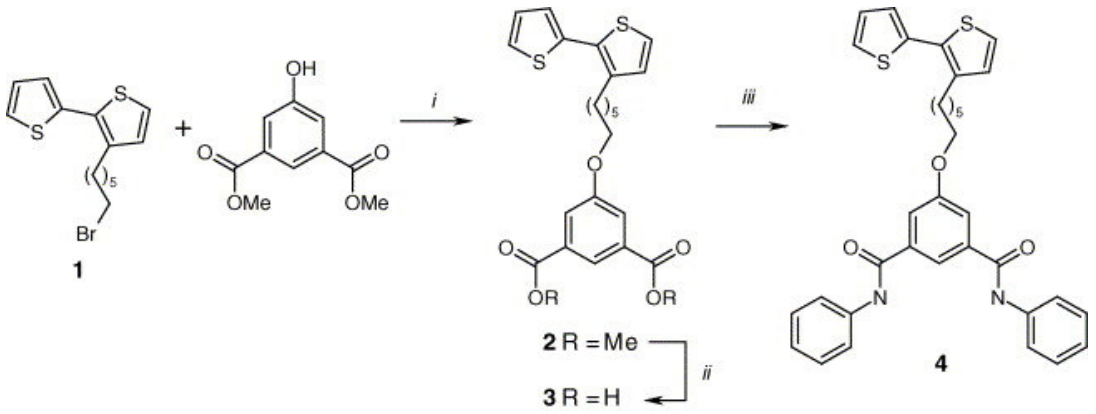

FIGURE. 5.1. Synthetic pathway and structure of the electropolymerisable molecular receptor. (i) NaH, DMF, *T* = 80 °C; (ii) KOH, H_2O/THF, reflux; (iii) 1,3-diisopropylcarbodiimide, aniline, DMF.

On the basis of our previous studies [13] regarding the realization of chemically modified electrodes with calixarene units as sensing agents, 2,2'-bithiophene was chosen as monomeric unit and a saturated hexyl chain was inserted as a spacer arm between the monomer and the receptor. The hexyldithienyl building block (**1**) was synthesized as first step and the synthetic pathway leading to the electropolymerizable receptor is shown in figure 5.1. 3-(6-Bromohexyl)-2,2'-bithiophene **1** was reacted with dimethyl 5-hydroxyisophtalate, to obtain the derivative **2** that was hydrolysed to **3**. The so obtained acid derivative was finally converted in the receptor **4** by reaction with aniline, in the presence of 1,3-diisopropylcarbodiimide

Electrodeposition

A generic electrosynthesis of a polymeric film can be carried out by means of potential-controlling techniques like constant potential chronoamperometry (potentiostatic growth) and cyclic voltammetry (potentiodynamic growth) or by current-controlling techniques like galvanostatic growth. Our findings evidenced that cyclic voltammetry is the most suitable technique in order to obtain a homogeneous and well anchored coating. Furthermore, cyclic voltammetry

performed in EQCM mode in 1:5 dichloromethane/acetonitrile solutions of monomer (5×10^{-4} M) and TBAHFP 0.1 M as supporting electrolyte, allowed us to control at every cycle the mass of the deposed film. The regularity of the deposition is well documented by voltammograms and frequencygrams simultaneously recorded during the growth of the polymeric

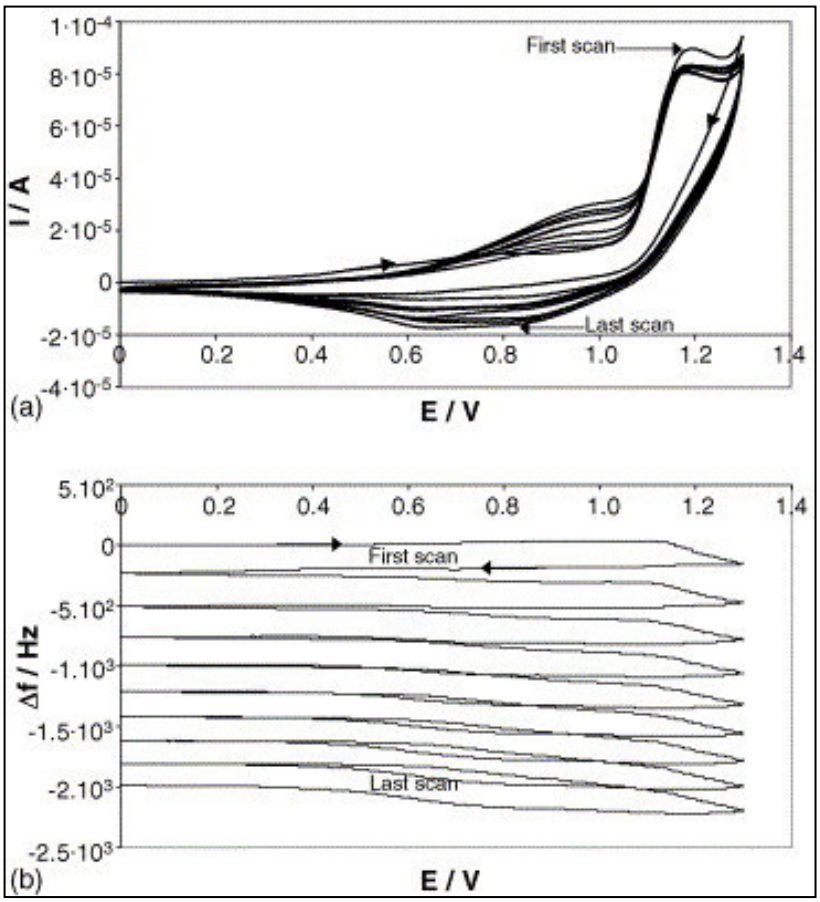

FIGURE 5.2. Frequency–CV trend recorded during potenziodinamic polymerization of molecular receptor. Δf= $-2e^{-3}$ Hz was the cut off value

It was found that he electropolymerisation procedure influenced the QCM sensitivity, best results were obtained for coating layer obtained by controlled electrodeposition in order to have a mass of $3 \times 10{-}6$ g of polymer on the sensor. [15]

The capabilities of the modified QCM were preliminary evaluated using the sensor as detection unit for gas chromatography by connecting the GC column to the QCM cell. First application in this field was reported by Wohltjen and Dessy [29] and based on the GC piezoelectric response demonstrated by King [30], but many other studies were subsequently published on the argument [31] and [32].

In this way the detection and quantitation limits with respect the analytes (reported in table 5.1) chosen on the basis of the binding properties of the receptor were calculated. As expected from the preliminary studies [15], the lowest LOD and LOQ values were obtained in the case of ethanol, whereas the highest one was obtained for toluene (Table 5.1). The observed behaviour could be ascribed to the different kinds of interactions between the analytes and the receptor moiety: in particular, ethanol is able to interact with the receptor layer by means of strong hydrogen bonds, whereas weaker π-π inter actions are responsible for toluene retention.

Analyte	slope	LOD		LOQ	
		mg/kg	µg	mg/kg	µg
Ethyl acetate	0.00107 (5e-5)	1370	8.22 e^{-2}	3690	2.21 e^{-1}
Acetone	0.00076 (4e-5)	1300	7.81 e^{-2}	2010	1.20 e^{-1}
Chloroform	0.0021 (1e-4)	2000	1.20 e^{-1}	3400	2.04 e^{-1}
Dichloromethane	0.000677 (9e-6)	2490	1.49 e^{-1}	3050	1.83 e^{-1}
Ethanol	0.006 (9e-4)	290	1.73 e^{-2}	620	3.69 e^{-2}
Tetrachloroethylene	0.000736 (7e-6)	2620	1.57 e^{-1}	3340	2.00 e^{-1}
Toluene	0.00085 (3e-5)	2740	1.64 e^{-1}	7610	4.57 e^{-1}
Acetonitrile	0.0008 (1e-4)	400	2.37 e^{-2}	800	4.79 e^{-2}

Table 5.1. LOD and LOQ of the sensor for the selected analytes, expressed as concentration of the injected solutions and as absolute detected mass. Sensitivity expressed as slope is also reported, SD in parenthesis

On the basis of these findings, the study was then aimed to the development of a novel reliable method for the detection of ethanol in food with focus on bakery products.

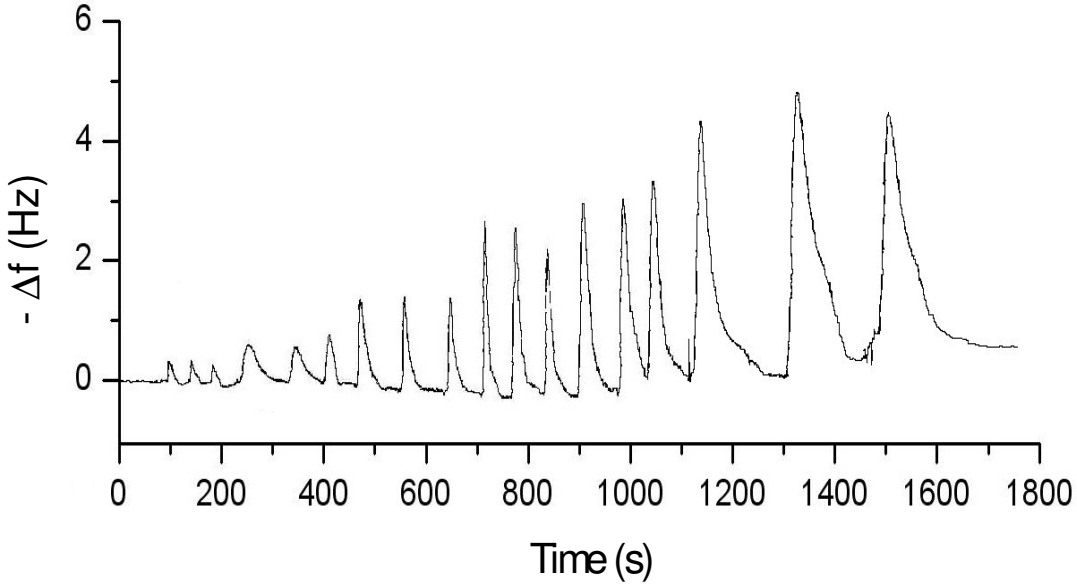

FIGURE. 5.2. Frequencygram recorded during progressive injections of headspace volume (100 µl) from whole-meal bread samples with different ethanol concentration (three replicate injections for each level).

The GC-FID based official method was used as reference technique in order to quantify the ethanol content in the bread samples industrially produced on purpose. The regression lines obtained for the whole-meal bread ($y = 0.1163(\pm0.0013)x$, $r^2 = 0.999$ ($n = 12$)) and durum-wheat bread ($y = 0.1168(\pm0.0008)x$, $r^2 = 0.998$ ($n = 12$)) allowed to calculate the real concentration of ethanol in the analysed samples. The true concentrations were: 1.70%, 1.43%, 1.29%, 0.92%, 0.80%, 0.26% (w/w) for the whole-meal bread and 2.06%, 1.68%, 1.56%, 1.34% 1.02%, 0.68% (w/w) for the durum-wheat bread. These values were finally used to calibrate the response of the sensor. Three replicate measurements were carried out for each concentration level. The frequencygram recorded by multiple headspace injections of the considered samples indicates a good repeatability of the signal (Figure.5. 2).QCM

calibration lines were obtained by plotting the areas of the peaks recorded with the QCM sensor *versus* the ethanol percentage determined by the classical GC-FID method, as shown in Figure. 5.3 and Figure. 4.4.

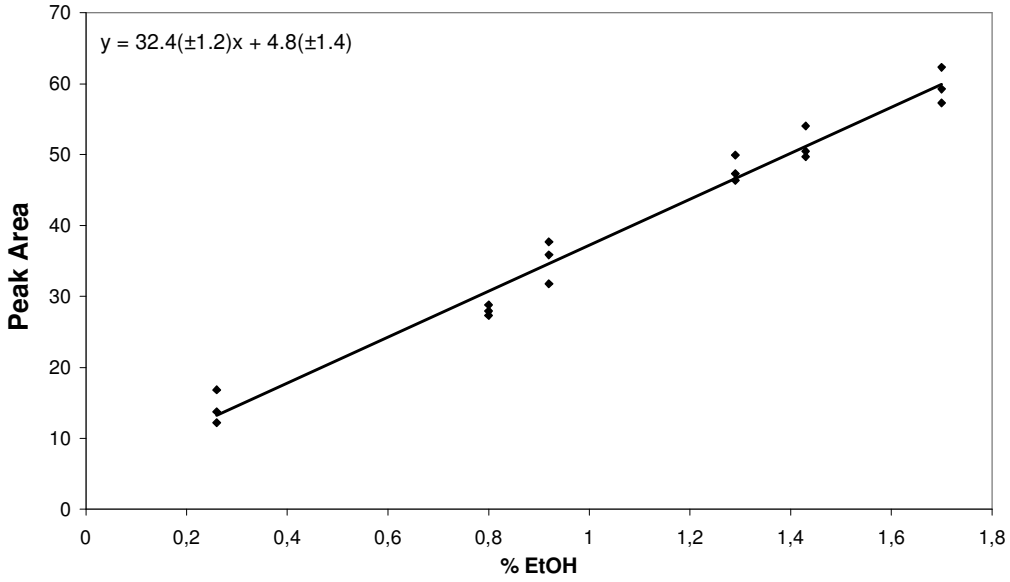

FIGURE 5.3. Calibration line and calculated function for whole-meal bread with ethanol concentration ranging from 0.26% to 1.70% (w/w).

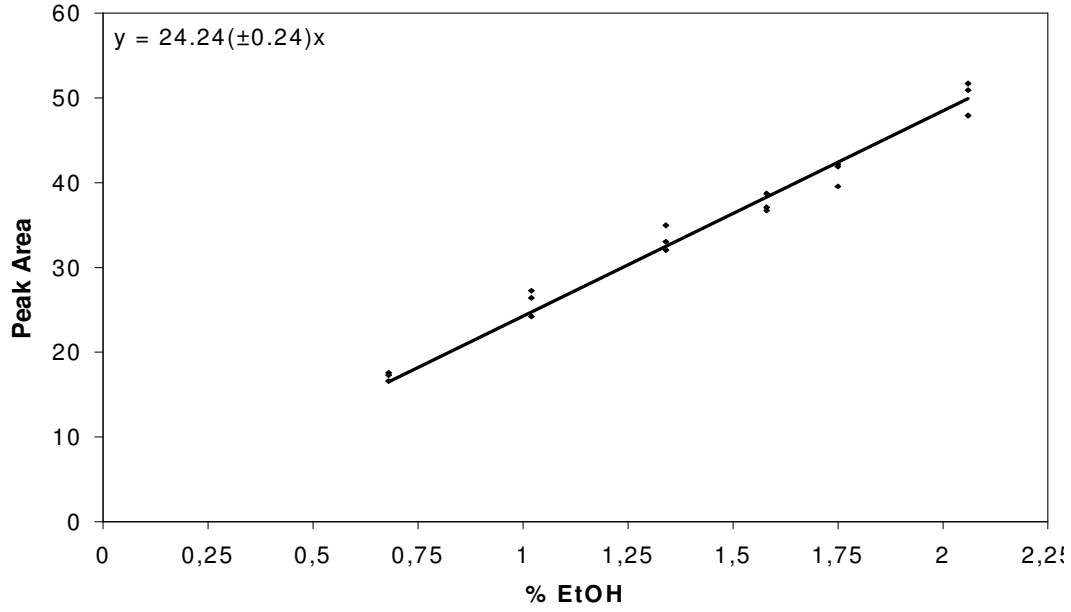

FIGURE 5. 4. Calibration line and calculated function for durum-wheat bread with ethanol concentration ranging from 0.68% to 2.06% (w/w).

Homoscedasticity of data was checked before the calculation of the calibration functions. For both the bread typologies, linearity was demonstrated in the ranges of interest applying Mandel's fitting test. The quadratic term resulted to be not significant both for the whole-meal bread (F_{calc} = 6.28; $F_{tab(1,15,\alpha=0.01)}$ = 8.68), and for the durum-wheat bread (F_{calc} = 3.95; $F_{tab(1,16,\alpha=0.01)}$ = 8.53).

The calibration on durum-wheat bread and on whole-meal bread were carried out using two different QCM units, with different coatings deposed under the same experimental conditions. Sensitivities resulted to be significantly ($p < 0.01$) different, as evaluated by an appropriate Student's *t*-test [33]. The slight difference between the slope values is explainable with the tolerance arising from the frequencymetric control of the mass of the polymerised coating, and is comparable with the standard error of the method obtained with the official GC-FID method. The slight difference was also proved by comparison of the values of s_{x0} (process standard deviation) [34]calculated for each calibration line (s_{x0} = 0.06 for durum-wheat bread *versus* 0.07 for whole-meal bread).

As reported in the experimental part potassium carbonate was used as moisture trap inserted between the injector and the QCM device. The choice of the drying agent was evaluated considering different salts: calcium chloride was not useful for our purposes since showed a strong retention of ethanol, whereas potassium carbonate allowed to obtain best results. Although K_2CO_3 could also partially retain small amounts of the analyte, this phenomenon was compensated by the calibration function, constructed using the GC-FID reference method. The signal of ethanol was not interfered by water in this official chromatographic method.

In order to calculate the ethanol concentrations on a dry matter basis, the determination of percent moisture was carried out according to the official method of analysis[26]. The so corrected ethanol concentrations were in the 0.4–2.6% (w/w) range for the whole-meal bread and in the 0.6–3.2% (w/w) range for the durum-wheat bread.

5..3 Conclusions

The use of the QCM sensor developed as detection system for GC allowed to evaluate its response in terms of sensitivity and detection limit with respect to a pool of compounds selected on the basis of the properties of the immobilized receptor. The results obtained, show that the performances of the sensor are suitable for the development of a novel and cost-effective method for ethanol determination in on-line quality control of bakery products. The procedure presents the advantage of the direct injection of headspace in the QCM detection cell without any separation system, which was avoided exploiting the selective binding properties of the electropolymerised coating.

5.4. Experimental

Reagents

The commercially available reagents were used without any further purification. Acetonitrile was dried over molecular sieves and preserved under nitrogen

Ethanol, *tert*-butanol, toluene, ethyl acetate, acetone, chloroform, dichloromethane, tetrachloroethylene, acetonitrile, methanol, hexane with a purity grade in the 95–99.9% range were purchased from Sigma–Aldrich (Milan, Italy).

Bread samples

Durum-wheat bread and whole-meal bread were prepared by a bakery factory with different amounts of ethanol added for purpose at the end of the bread-making process. The samples as provided by the factory were prepared with ethanol concentrations approximatively in the range 0.4–2.1% (w/w). After the ethanol addition, all the samples were hermetically sealed into polypropylene bags. Before the analysis, samples were minced, frozen under liquid nitrogen and maintained at −20 C.

Static headspace sampling

0.5 g of bread were put in a 10-ml vial filled with 2 ml of water and maintained at the temperature of 80 °C for 30 min under constant magnetic stirring. One hundred microliters of the headspace were then injected by using a gas-tight syringe into the injection port of the gas chromatograph.

Bread samples in which ethanol was removed under vacuum (until no ethanol GC signal was detected) were considered as blank samples and used for validation purposes.

Tert-butanol was used as internal standard for ethanol quantitation at the final concentration of 0.6% (w/w). Four concentration levels of ethanol in the 0.5–2.5% (w/w) range were analyzed by performing a spiking procedure. Three replicated measurements at each concentration level were carried out. Statistical analyses (Bartlett, lack-of-fit and Mandel test) were performed to check the goodness of fit and linearity [24] and [25]. The significance of the intercept (significance level 5%) was established running a *t*-test.

GC-FID analysis

A HP 5890 Series II Plus gas chromatograph (Agilent Technologies, Milan, Italy) equipped with a FID was used. Carrier gas was helium at a flow-rate of 1 ml min^{-1}. The gas chromatograph was operated in splitless mode with the injector and the detector maintained at the temperature of 220 °C and 200 °C, respectively. Chromatographic separation was performed on a 60 m × 0.25 mm, d_f 0.5 μm HP-INNOWAX capillary column (Agilent Technologies). The following GC oven temperature program was applied: 50 °C for 10 min, 30 °C min^{-1} to 200 °C for 1 min. Signal acquisition and treatment were performed using the Turbochrom software v.4.04 (PE Nelson, Milan, Italy).

Dry matter

Dry matter was determined following the procedure reported on the Gazzetta Ufficiale della Repubblica Italiana[26].

Sensor preparation

Synthesis of electropolymerizable receptor was carried according to procedures reported in literature [15]

Polymeric film production

The electropolymerizations and the characterization of the sensor were carried out using a potentiostat CHI 430 (CH Instrument, Texas) supplied with QCM unit, managed by dedicated software. The electropolymerizations were performed in a Teflon cell (5 ml) using QCM devices as working electrodes, a silver–silver chloride pseudoreference (with respect to which the ferrocene system showed an $E_{1/2}$ = 0.402 V, calculated as mean value of cathodic and anodic peak potentials in cyclic voltammograms) as reference electrode and a platinum rod as counter electrode; quartz/chrome/gold QCM devices with a fundamental frequency of 7.98 ± 0.005 MHz were used.

Tetrabutylammonium hexafluorophosphate (TBAHFP, Fluka, >99%) 0.1 M was employed as supporting electrolyte.

The receptor was electropolymerized on the surface of the QCM units by cyclic voltammetry using 5×10^{-4} solutions of the monomer, prepared in a mixture of dry acetonitrile and dichloromethane (1:5) and supporting electrolyte. The polymeric film was produced through 16–25 scans in a potential window ranging from 0 to 1.3 V and at a scan rate of 0.08 V/s.

The growth of the polymer was monitored by means of the frequency signal, acquired simultaneously to the current signal, in the electrochemical quartz crystal microbalance (EQCM) mode on the same instrument. In this way, it has been

possible to obtain a standard thickness constant in every electropolymerization by stopping it at the frequency shift of −2 kHz, corresponding to about 3×10^{-6} g of a polymer. An halved thickness polymer has been deposited at a frequency shift of −1 kHz.

The obtained polymers were potentiostatically reduced at a potential of 0 V for about two minutes in a 0.1 M solution of the supporting electrolyte in acetonitrile, then washed with dry acetonitrile and dried under nitrogen.

Unfunctionalised poly(2,2′-bithiophene) was prepared starting from a 10^{-3} M solution of 2,2′-bithiophene and TBAHFP (0.1 M) in dry acetonitrile, under the same experimental conditions employed for the electropolymerization of the receptor.

Detection and quantitation limits of the QCM sensor

The same bread samples analysed by GC-FID were submitted to analysis using QCM detection system. The equipment consisted of an injection septum connected to the detection cell through a moisture trap and a steel-made tube. The moisture trap was realised with a glass cylinder filled with potassium carbonate dispersed on glass spheres. Nitrogen was used as carrier gas with a flow of 20 ml min^{-1}. QCM signal was acquired by using a computerised integrated potentiostat/EQCM CHI 430 (CH Instruments, Texas).

Sensor detection and quantitation limits

Limit of detection (LOD) and limit of quantitation (LOQ) of the sensor for acetone, ethanol, tetrachloroethylene, dichloromethane, chloroform, acetonitrile, ethyl acetate and toluene were calculated following Eurachem guidelines [24] by constructing appropriate calibration curves.

All the working solutions were prepared by a proper dilution of the pure standards in hexane.

All statistical analyses were carried out by using the statistical package SPSS 14.0 for Windows (SPSS, Chicago, IL, USA).

5.5 References

1. J. Janata, M. Josowicz and D.M. De Vaney, Chemical sensors, *Anal. Chem.* **1994**, **66** 207R.
2. R.L. Bunde, E.J. Jarvi and J.J. Rosentreter, Piezoelectric quartz crystal biosensors, *Talanta* **1998**,**46** ,1223.
3. H. King, Piezoelectric sorption detector, *Anal. Chem.* **1964**, 36, 1735.
4. Zhang, Z.K. Chen, G.W. Bao and Sam F.Y. Li, *Talanta* **1998**, 45, 727.
5. Sauerbery, *Z. Phys.* **1959**, **155** ,206.
6. Haug, K.D. Schierbaum, G. Gauglitz and W. Göpel, *Sens. Actuators B, Chem.* **1993**, **11**, 383.
7. E. Dominguez, L. Jun, R.L. Curiale and E.J. Poziomek, *Anal. Lett.* **1995**, 28, 945.
8. V. Tsionsky and E. Gileadi, , *Langmuir* ,**1994**,10, 2830.
9. Roncali *Chem. Rev.* **1992**, 711.
10. Syritski, J. Reut, A. Öpik and K. Idla, *Synt. Met.* **1999**, 102, 1326
11. .M. Bruti, M. Giannetto, G. Mori and R. Seeber, *Electroanalysis* **1999**, 11,565.
12. E. Agbor and M.C. Monkman, *Sens. Actuators B, Chem.* **1995**, 28, 173.
13. Giannetto, G. Mori, A. Notti, S. Pappalardo and M.F. Parisi, *Chem. Eur. J.* **2001,** 715, 3354.
14. Bello, M. Giannetto and G. Mori, *J. Electroanal. Chem.* **2005**. **575** 257.
15. Giannetto, V. Mastria, G. Mori, A. Arduini and A. Secchi, *Sens. Actuators B: Chem.* **2006**,115, 62.
16. 31213/07/1998, Regolamento recante norme per il trattamento con alcool etilico del pane speciale preconfezionato. Gazzetta Ufficiale della Repubblica Italiana no. 200 28/08/1998.
17. H. Liao, J.-C. Guo and W.-C. Chen, *J. Magn. Magn. Mater.* **2006,** 304, 421.
18. S. Alpeeva, A. Vilkanauskyte, B. Ngounou, E. Csoeregi, I.Y. Sakharov, M. Gonchar and W. Schuhmann. *Microchim. Acta* **2005,**152, 21.

19. A.M. Azevedo, D.M.F. Prazeres, J.M.S. Cabral and L.P. Fonseca, *Biosens. Bioelectr.* **2005**, 21, 235.
20. Istituto Superiore di Sanità, Metodi di analisi utilizzati per il controllo chimico degli alimenti Rapporti ISTISAN 96/34, 1996.
21. M. Careri, G. Mori, M. Musci and P. Viaroli, *J. Chromatogr. A,* **1999**, **848**, 327.
22. F. Bianchi, M. Careri, C. Mucchino and M. Musci, *Chromatographia* **2002, 55,** 595.
23. F. Bianchi, M. Careri, C. Corradini, M. Musci and A. Mangia, *Curr. Anal. Chem.* **2005, 1**, 129.
24. The Fitness for Purpose of Analytical Methods: A Laboratory Guide to Method Validation and Related Topics, EURACHEM Guide, 1st English Edition 1.0-1998, LGC (Teddington) Ltd.
25. N. Draper and H. Smith, Applied Regression Analysis, Wiley, New York, **1981.**
26. DM 27/05/1985, Approvazione dei 'Metodi ufficiali di analisi dei cereali'— supplemento n. 3, Gazzetta Ufficiale della Repubblica Italiana n° 145 del 21/06/1985.
27. J. Janata and M. Josowicz, Chemical Sensors, *Anal. Chem.* **1998**, 70, 179R.
28. S. Steiner, *Angew. Chem. Int. Ed.* 2002, 41, 48.
29. H. Wohltjen and R. Dessy, *Anal. Chem.* **1979**, 51, 1458.
30. W.H. King Jr., *Anal. Chem.* **1964** ,36, 1735.
31. G. Watson, W. Horton and E. Staples, *Proceedings of the Ultrasonic Symposium* 1991,305–309.
32. W.H. Steinecker, M. Rowe, A. Matzger and E.T. Zellers, *Proceedings of the 12th International Conference on Solid State Sensor, Actuators and Microsystems* Boston, June 8–12 (2003), 1343.
33. D.L. Massart, B.G.M. Vandeginste, L.M.C. Buydens, S. De Jong, P.J. Lewi and J.P. Smeyers-Verbeke, *Handbook of Chemometrics and Qualimetrics: Part A*, Elsevier, Amsterdam, **1997**, (Chapter 8), 208.

34. W. Funk, V. Dammann and G. Donnevert, Quality Assurance in Analytical Chemistry, VCH, Weinheim, **1995** (Chapter 1) 25.

6. Conclusions

Chemical sensor are suitable devices in Analytical chemistry.

The possibility to realize small devices with high selectivity, low limit of detection and long life time makes the sensors interesting alternatives to the traditional analytical techniques.

Selectivity of the chemical sensor is based on molecular recognition obtained by suitable ionic or molecular receptor

Moreover, low limits of detection and long life time are achieved reducing leaching phenomena from the sensor-sample interface.

In this view we have realized chemical sensors based on sensing moieties bound to electrodic surface.

We have realized new CME with the aim to improve selectivity, lower detection limit, and increase the shelf life of these devices.

In chapter 2 we have realized Pt-PEDOT modified eelctrodes suitable as redox-mediator sensors for the determination of ascorbic acid by DPV. Galvanostatically electropolytmerized PEDOT showed reproducible and stable amperometric responses. The cheapness of the monomer (EDOT) allows the realization of "disposable" electrodes whit good potentialities for determination of AA concentration in food samples (fruit juices, preserved foods etc.)

New ISEs with interesting lifetime were realised. A new tetraphenylborate ion exchanger functionalized with allylic moieties was synthesized and linked to an acrylonitrile-butadiene copolymer.

Linking procedure involved only the polymeric backbone and ion exchanger, avoiding a possible degradation of the ionophore.

New potassium-selective electrodes were prepared coupling PVC with functionalized acrylonitrile-butadiene.

Six different typologies of ISEs were prepared in order to evaluate the effect of the bound ion exchanger on the performances of the sensors

Reduced leaching of the ion exchanger was demonstrated by means of potentiometric measurement and continuous flux extraction experiments, simulating the most critical working conditions of the potentiometric sensors.

The behaviour of P3OT and PBT as ion to electron transducers in ISEs was also investigated:
It is kwon that both CP light-sensitivity and water layer presence lead to not stable EMF responses.
Electropolymerization procedures were tuned in order to obtain stable EMF values.
Since CP light-sensitivity in potentiometric sensor has never completely investigated, we have rationalized the light-depending responses of 3POT-based potentiometric sensors.
Thick and π-doped conducting polymer are less light sensitive over time, while PCV membrane improve the stability for these kind of polymer in the presence of light.
PBT was employed for the first time as ion to electron transducer in Ca-PVC selective solid contact electrode and potentiometric performances agreed with those previously obtained by drop cast P3OT solid contact.
PEHDM selective membrane was obtained by thermo and photo induced in situ-polymerization. The so obtained self-plasticized membranes showed reduced ion fluxes and active component leaching.
First encouraging results were achieved for PBT Li selective electrode based on this technology .
Concerning the realization of piezoelectric sensors, we have designed and developed a new sensor obtained by electroplymerization of a selective molecular receptor on the gold surface of a PQC unit. The sensor was successfully employed for the development af a new rapid method for the quantification of ethanol in industrial bakery products.

7. Molecular structures

Chapter 2

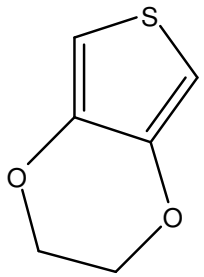

2,3-Dihydrothieno[3,4-b]-1,4-dioxin (EDOT)
Molecular Formula $C_6H_6O_2S$
Molecular Weight142.18

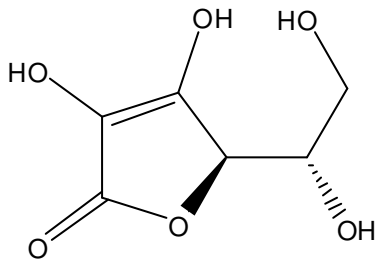

L-Ascorbic acid
Molecular Formula: $C_6H_8O_6$,
Molecular Weight: 176.12

Chapter 3

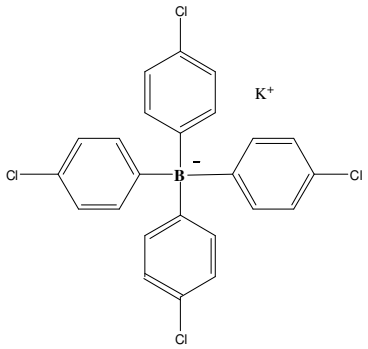

Potassium tetrakis(4-chlorophenyl)borate (KTAPB)
Molecular Formula: $(ClC_6H_4)_4BK$,
Molecular Weight: 496.11

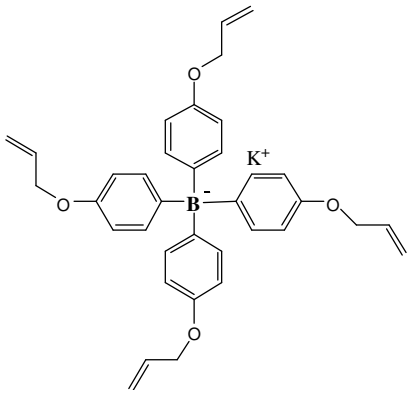

Potassium tetrakis(4(allyloxy)phenyl)borate KTAPB
Molecula formula C36H36BK
Molecular waight 582

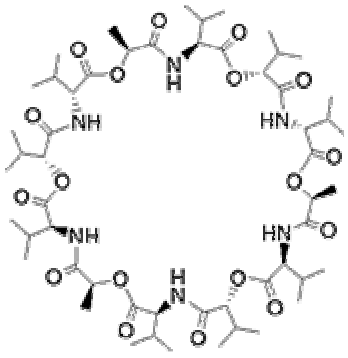

Valinomycin
Molecular Formula: $C_{54}H_{90}N_6O_{18}$
Molecular Weight: 1111. 32

Chapter 4

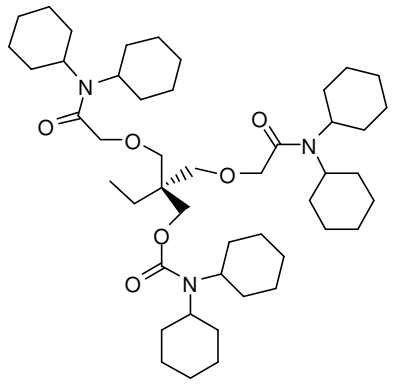

LiVIII Lithium Ionophore
N,N,N',N',N'',N''-Hexacyclohexyl-4,4',4''-propylidynetris(3-oxabutyramide)
Molecular Formula:$C_{48}H_{83}N_3O_6$
Molecular Weight:798.19

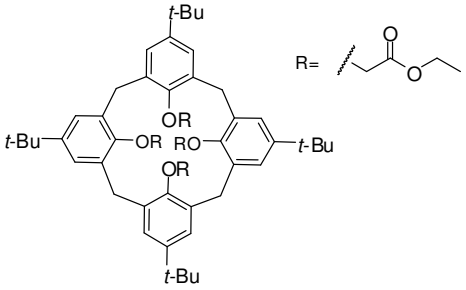

NaX Sodium ionophore
4-*tert*-Butylcalix[4]arene-tetraacetic acid tetraethyl ester
Molecular Fformula: $C_{60}H_{80}O_{12}$
Molecular Weight: 993.27

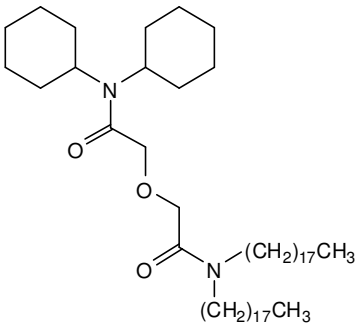

CaIV Calcium ionophore (ETH 5234)
N,N-Dicyclohexyl-N′,N′-dioctadecyl-diglycolic diamide
Molecular Formula:$C_{52}H_{100}N_2O_3$
Molecular Weight:801.36

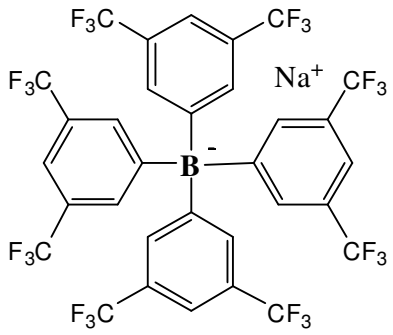

Tetrakis[3,5-bis(trifluoromethyl)phenyl]boron sodium
Molecular Formula: $C_{32}H_{12}BF_{24}Na$
Molecular Weight :886.20

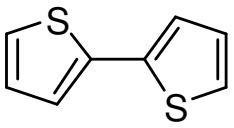

2-2′ bithiophene
Molecular Formula $C_8H_6S_2$
Molecular Weight: 166.26

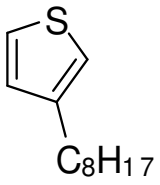

3-octylthiophene
Molecular Formula $C_{12}H_{20}$
Molecular Weight 196.35

Chapter 5

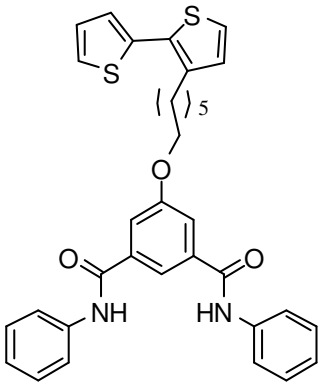

5-[(6-[2,2′]-bithiophenil-3-yl–hexyloxy)-N,N′-diphenyl-isophtalammide
Molecular formula $C_{34}H_{34}N_2O_3S_2$
Molecular weight 580

Acknowledgments

I would like to thank:

Prof. Giovanni Mori for having supervised my work.

Dr Marco Giannetto for the scientific help during these years

Prof. Dr. Ernö Pretsch for having hosted in his group me at the ETH in Zürich *(while we all became world champions. Gol di Grosso.)*

All the students who participated the experimental work described in this thesis.

E ora due parole informali per ringraziare tutte le persone che volontariamente o no mi hanno permesso di realizzare tutto questo.

Un grazie di cuore va ai "tecnici" (Giuseppe, Marco e Marinella) per la loro disponibilità a realizzare i "miei desideri" ….

Come non ricordare i ragazzi del "dipartimento e dintorni": Marcello, Massimiliano, Michela, Elisa, Tiziana, Luciano e Laura , Matteo e Daniele, per i pranzi, le cene e gli "happy hours"…la vetreria imprestata i consigli chimici e non…Grazie!!!!

(grazie agli *ex-laboratorio* **21**: Valentina Enrica e Alessandro, non solo colleghi, per fortuna).

Un grazie speciale alle mie amiche, senza di loro questi anni non sarebbero stati così belli: Laura S., Elena, Barbara, Laura B., Lucia, Paola. Grazie mille ragazze!

Grazie Silvia, Leni, Raffaella e Roberto per esserci, punto!

Grazie ad Attilio, Raffaella (e Famiglia Manghi), Alessandro, Simone, Daniele, e ai "miei ragazzi" di Langhirano! *Grazie!!! Grazie!!! Grazie!!! Grazissime!!!*

Grazie alla mia famiglia. Mamma-Papà mi avete sempre sostenuto senza influenzare le mie scelte; gioendo di ogni mio successo e "sorridendo" di ogni mio insuccesso. Grazie !

Grazie, ma forse non basta, a Riccardo il Chimico più bravo del mondo…nonché il mio Amore!

E infine un bel grazie va a me stessa, (la persona che ha reso davvero possibile tutto questo)